Genome analyses reveal the hybrid origin of the staple food crop white Guinea yam

Yu Sugihara[1], Kwabena Darkwa[2], Hiroki Yaegashi[3], Satoshi Natsume[3], Motoki Shimizu[3], Akira Abe[3], Akiko Hirabuchi[3], Kazue Ito[3], Kaori Oikawa[3], Muluneh Tamiru-Oli[34], Atsushi Ohta[1], Ryo Matsumoto[2], Agre Paterne[2], David De Koeyer[25], Babil Pachakkil[67], Shinsuke Yamanaka[6], Satoru Muranaka[6], Hiroko Takagi[6], Ben White[8], Robert Asiedu[2], Hideki Innan[9], Asrat Asfaw[2*], Patrick Adebola[2*], Ryohei Terauchi[13*]

[1] Laboratory of Crop Evolution, Graduate School of Agriculture, Kyoto University, Kyoto, Japan

[2] International Institute of Tropical Agriculture (IITA), Ibadan, Nigeria

[3] Iwate Biotechnology Research Center, Kitakami, Iwate, Japan

[4] Department of Animal, Plant and Soil Sciences, School of Life Sciences, AgriBio Building, La Trobe University, Melbourne, Australia

[5] Fredericton Research and Development Centre, Agriculture and Agri-Food Canada, Fredericton, New Brunswick, Canada

[6] Japan International Research Center for Agricultural Sciences, Tsukuba, Japan

[7] Department of International Agricultural Development, Tokyo University of Agriculture, Tokyo, Japan.

[8] Earlham Institute, Norwich, UK

[9] Laboratory of Population Genetics and Genome Evolution, The Graduate University for Advanced Studies, Hayama, Japan

* Co-corresponding authors:

Asrat Asfaw: A.Amele@cgiar.org

Patrick Adebola: P.Adebola@cgiar.org

Ryohei Terauchi: terauchi@ibrc.or.jp

Abstract

White Guinea yam (*Dioscorea rotundata*) is an important staple tuber crop of West Africa. However, its origin remains unclear. In this study, we re-sequenced 336 accessions of white Guinea yam and compared them with the sequences of the wild *Dioscorea* species using an improved reference genome sequence of *D. rotundata*. Our results suggest a hybrid origin of white Guinea yam from crosses between the rainforest wild species *D. praehensilis* and the savannah-adapted *D. abyssinica*. We identified a higher genomic contribution from *D. abyssinica* in the sex chromosome of Guinea yam and an extensive introgression around the *SWEETIE* gene. Our findings point to a complex domestication scenario for Guinea yam and highlight the importance of wild species as gene donors for improvement of this crop through molecular breeding.

Introduction

Yams (*Dioscorea* spp.) are major starchy tuber crops in the tropics. Overall, ten yam species are cultivated around the world, including *D. alata* in Southeast Asia, *D. trifida* in South America, and *D. rotundata* in West and Central Africa (*1*). *D. rotundata* also known as white Guinea yam is the most important species in West and Central Africa, an area accounting for 92.5% of the global yam production in 2018 (http://www.fao.org/statistics). Beyond its nutritional and food values, Guinea yam is also important for the culture of West African people (*2*). Recently, a whole genome sequence of Guinea yam was reported (*3*).

Despite the considerable importance of Guinea yam, its origin has been elusive. Two types of Guinea yams are known; white Guinea yam (*D. rotundata*) and yellow Guinea yam (*D. cayenensis*). *D. cayenensis* was proposed to be a triploid species of hybrid origin with *D. rotundata* and *D. burkilliana* as the maternal and paternal parent, respectively (*4*, *5*). It was also suggested that the

triploid *D. rotundata* is a hybrid between *D. rotundata* and *D. togoensis* (*5*). However, the origin of diploid *D. rotundata*, which represents the majority of Guinea yam, has been ambiguous. There are two candidate wild species as the progenitors of diploid *D. rotundata*; a savannah-adapted wild species *D. abyssinica* and a rainforest-adapted wild species *D. praehensilis*. A recent genome study involving 86 *D. rotundata*, 47 *D. praehensilis* and 34 *D. abyssinica* accessions proposed that diploid *D. rotundata* was domesticated from *D. praehensilis* (*6*). Here, we address this hypothesis using an expanded set of wild and cultivated *Dioscorea* genomes.

In this study, we generated an improved version of the Guinea yam reference genome, and used it to analyze the genomes of 336 accessions of *D. rotundata* and its wild relatives. Based on these analyses, we attempted to reveal the history of Guinea yam domestication. Our results suggest that diploid *D. rotundata* was most likely derived from homoploid hybridization between *D. abyssinica* and *D. praehensilis*. By evaluating the genomic contributions of each parental species to *D. rotundata*, we revealed a higher representation of *D. abyssinica* genome in the sex chromosome and a signature of extensive introgression in *SWEETIE* gene on chromosome 17.

Genetic diversity of Guinea yam

We obtained DNA samples of 336 accessions of *D. rotundata* maintained at IITA, Nigeria, representing the genetic diversity of Guinea yam landraces and improved lines of West Africa. These samples were subjected to whole genome resequencing by illumina sequencing platform. The resulting short reads were aligned to the newly assembled reference genome (supplementary text S1 and S2) and SNP information was extracted to use for genetic diversity studies (supplementary text S3). Based on admixture analysis by sNMF (*7*), we defined five major clusters (Fig. 1A). When *K* is 2, cluster 1 was clearly separated from the other accessions. Principal Component Analysis (PCA) also separated cluster 1 from the rest (Fig. 1B). Accessions in cluster 1 had a higher heterozygosity and ~10 times larger number of unique alleles than those in the remaining four clusters (Fig. S1 and

Fig. S2). Because flow cytometry analysis confirmed that all 10 accessions analyzed in cluster 1 were triploids (Table S1), we hypothesized that cluster 1 represents triploid *D. rotundata* that was reported as a hybrid between *D. rotundata* and *D. togoensis* (*5*). After removing the cluster 1 accessions, nucleotide diversity of *D. rotundata* was estimated to be 14.83 x 10^{-4} (Table S2), which is approximately 1.5 times larger than that reported previously (*6*).

Phylogenomic analysis of African yam

Using the SNP information, we constructed a rooted Neighbor-joining (NJ) tree (*8*) based on 308 Guinea yam accessions sequenced in the present study excluding cluster 1 triploid accessions, as well as 80 *D. rotundata*, 29 *D. abyssinica*, 21 Western *D. praehensilis*, and 18 Cameroonian *D. praehensilis* as sequenced in the previous study (*6*) using two accessions of Asian species *D. alata* as an outgroup (Fig. 1C). According to this NJ tree, *D. rotundata* accessions sequenced in this study were genetically close to the *D. rotundata* accessions reported in the previous study (*6*) (Fig. 1C). However, the NJ tree showed that *D. rotundata* was more closely related to *D. abyssinica* than to Western D. *praehensilis* (Fig. 1C), which is inconsistent with the previous report (*6*) showing that *D. rotundata* was most closely related to Western *D. praehensilis*.

To elucidate the evolutionary relationships of the three wild *Dioscorea* species, *D. abyssinica* (indicated as A), Western *D. praehensilis* (P). Cameroonian *D. praehensilis* (C) that are closely related to *D. rotundata*, we adopted the ∂a∂i analysis (*9*), which allows estimating demographic parameters from an unfolded site frequency spectrum. First, three phylogenetic models, {{A, P}, C}, {{C, P}, A}, {{C, A}, P} were tested using 17,532 SNPs that were polarized using an outgroup *D. alata* without considering migration among the species. Out of the three models, {{A, P}, C} had the highest likelihood (Table. S3). This result is not consistent with the previous study (*6*) where {{P, C}, A} had the highest likelihood as studied by a different method with fastsimcoal2 (*10*). To exactly repeat the previous analysis, we tested these three models with fastsimcoal2 (*10*) on the previous

reference genome (*3*), resulting in {{A, P}, C} with the highest likelihood (Table S4). Taken together, our result is not consistent with the previous report (*6*). However, it is consistent with the PCA result of the same report, where Cameroonian *D. praehensilis* is separated from the other African yams in the PC1 (Fig. 2A of (*6*)). Based on the assumption that {{A, P}, C} is the true evolutionary relationship among the three wild *Dioscorea* species, the evolutionary parameters were re-estimated by ∂a∂i allowing symmetric migration among the species (Fig. 1D). Since our result shows that Cameroonian *D. praehensilis* is distantly related to *D. rotundata* and is unlikely involved in genetic exchange with *D. rotundata* (Fig. 1C), we hereafter focus on Western *D. praehensislis* and designate it as *D. praehensilis* for brevity.

Hybrid origin of Guinea yam

Three hypotheses of the origin of Guinea yam (*D. rotundata*) can be proposed from the results of NJ tree (Fig. 1C) and ∂a∂i (*9*) (Fig. 1D). The first is that *D. rotundata* was derived from *D. abyssinica* (Hypothesis 1 in Fig. 2A). The second is that *D. rotundata* was derived from *D. praehensilis* (Hypothesis 2 in Fig. 2A). However, in Hypotheses 1 and 2, the divergent time of *D. rotundata* from the wild species may not be sufficient to separate the three lineages and there is incomplete lineage sorting among them. The third hypothesis is that *D. rotundata* was originated as an admixture between *D. abyssinica* and *D. praehensilis* (Hypothesis 3 in Fig. 2A).

Before estimating the evolutionary parameters for the three hypotheses, we studied the allele frequencies of 388 *D. rotundata* sequences including 80 in the previous study (*6*) focusing on 144 SNPs that are positioned over the entire genome and are oppositely fixed in the two candidate progenitors (Fig. 2B). If Hypothesis 1 or 2 is correct, allele frequencies in these 144 SNPs should be highly skewed to either of the progenitors. However, the patterns of allele contribution from the two candidate species to *D. rotundata* is almost same. This result suggests that the admixture origin of Guinea yam (Hypothesis 3) is most likely.

136 The three hypotheses were tested by ∂a∂i (*9*) with symmetric migration rates, using 15,461 SNPs
137 polarized by *D. alata* (Fig. 2A), which showed that Hypothesis 3 had the highest likelihood and the
138 lowest Akaike information criterion (AIC) (Fig. 2A and Table. S3). This result is in support of the
139 admixture hypothesis that *D. rotundata* was derived from crosses between *D. abyssinica* and *D.*
140 *praehensilis*. The estimated parameters by ∂a∂i indicates that the hybridization between *D. abyssinica*
141 and *D. praehensilis* was relatively recent in relation to the divergence between the two wild species,
142 and it also indicates that the genomic contribution from *D. abyssinica* and that from *D. praehensilis*
143 were approximately 68% and 32%, respectively. Introgression generally results in highly asymmetric
144 genomic contributions from the parental species, whereas hybridization shows symmetric genomic
145 contributions (*11*). The observed intermediate genomic contributions support the hybridization rather
146 than the introgression hypothesis.

147 To evaluate the genetic distances of *D. rotundata* from the two parental species for each
148 chromosome, F_{ST} (*12*) was calculated (Fig. 2D). We observed varying genetic distances from the two
149 parents across the different chromosomes, while the overall genetic distance of *D. rotundata* from *D.*
150 *abyssinica* was smaller than that from *D. praehensilis* (Fig. 2D). Intriguingly, chromosome 11, to
151 which we previously mapped the candidate locus for sex determination (*3*), had the shortest genetic
152 distance from *D. abyssinica* and the longest genetic distance from *D. praehensilis* among the all
153 chromosomes, indicating that chromosome 11 of *D. rotundata* is highly skewed to *D. abyssinica* (Fig.
154 2D). This observation mirrors the case of the X chromosome in *Anopheles gambiae* complex (African
155 mosquito) (*13*).

156

157 **Evolutionary history of Guinea yam**

158

159 To infer the maternal history of Guinea yam, a haplotype network of the whole plastid genome was
160 constructed using all samples used in the NJ tree (Fig. 1C) as well as the triploid accessions in cluster
161 1 (Fig. 3A and supplementary text S6). According to this haplotype network, Cameroonian *D.*

praehensilis has the largest genetic distance from *D. rotundata*. This result is in line with the phylogenomic trees of African yam (Fig. 1C and Fig. 1D). Strikingly, plastid genomes of diploid and triploid *D. rotundata* are uniform, and are very similar to that of Nigerian or Beninese *D. abyssinica*. Plastid genomes of *D. praehensilis* from Nigeria, Benin and Ghana seem derived from Nigerian or Beninese *D. abyssinica*. These results indicate that *D. abyssinica* is an older lineage than *D. praehensilis* and that the place of origins of *D. rotundata* and *D. praehensilis* is probably around Nigeria or Benin. Using whole genome diversity of *D. rotundata*, a recent study (*6*) has hypothesized that the origin of *D. rotundata* was around north Benin, and our result supports this. Plastid genomes of some wild species are identical to those of cultivated Guinea yams. Gene flow from cultivated yams to wild yams may account for this observation (*14*).

The results of nuclear genome admixture (Fig. 2) and plastid haplotype network (Fig. 3A) indicate that the maternal origin of diploid *D. rotundata* was *D. abyssinica* and its paternal origin was *D. praehensilis* (Fig. 3B). Hybridization between *D. abyssinica* and *D. praehensilis* has been reported to be rare (*15*), but such rare hybrids seem to have been domesticated by humans. The triploid *D. rotundata* shared the plastid haplotype with diploid *D. rotundata*, therefore diploid *D. rotundata* served as the maternal parent and *D. togoensis* as the paternal parent. *D. cayenensis* is reported to have *D. rotundata* as the maternal parent and *D. burkilliana* as the paternal parent (*4*, *5*). All cultivated Guinea yams are hybrids with *D. abyssinica* plastid genomes.

To understand the change of population sizes, demographic history of African yam was re-inferred by ∂a∂i (*9*) allowing migration (Fig. 3C and supplementary text S7). The same dataset to Fig. 2C was used for this analysis. By fixing the parameters predicted in Fig. 2C except for the population sizes, we re-estimated each population size at the start and end points after the emergence of those species assuming an exponential increase/decrease of the population sizes. According to this analysis, after the emergence of the wild progenitors of Guinea yam, the population size of *D. abyssinica* is decreasing, while that of *D. praehensilis* is increasing (Fig. 3C). This finding may indicate *D.*

187 *praehensilis* population was possibly derived from *D. abyssinica*, which is consistent with the result
188 of the haplotype network (Fig. 3A).
189
190 **Extensive introgression at the *SWEETIE* locus**
191 To explore multiple introgression to *D. rotundata* from the two wild species, the f_4 statistic (*16*) was
192 analyzed using the four groups: a) *D. rotundata* cluster 2 and 5, b) *D. rotundata* cluster 4 and c) *D.*
193 *abyssinica* and d) *D. praehensilis* (supplementary text S8). f_4 statistic reveals the representation of
194 two alternative discordant genealogies (Fig. 4A). Basically, f_4 value is close to zero if the two groups
195 (group a and b) of *D. rotundata* show a concordant genealogy in relation to *D. abyssinica* and *D.*
196 *praehensilis*. On the other hand, if the two groups of *D. rotundata* exhibit discordant genealogy and
197 a large genetic distance to each other, f_4 is diverged from zero. We obtained f_4 statistic, f_4 (P_{25}, P_4, P_P,
198 P_A) for each SNP and applied a sliding window analysis (Fig. 4B). f_4 value was close to zero across
199 the genome indicating that overall we cannot decide between topology 1 and 2. However, the genomic
200 regions around the *SWEETIE* gene showed the lowest f_4 (P_{25}, P_4, P_P, P_A) [$Z(f_4)$ = -5.66], with
201 overrepresentation of topology 2 in the *SWEETIE* gene（DRNTG_01731）. To see the genealogical
202 relationships around the *SWEETIE* gene, Neighbor-Net (*17*) was constructed around that locus (4.00
203 Mbp ~ 4.15 Mbp on chromosome 17) (Fig. 4C). Neighbor-Net showed that the locus of cluster 4 was
204 close to that of *D. praehensilis*, while those of cluster 2 and 5 and some other accessions were close
205 to *D. abyssinica*. This indicates that the *SWEETIE* gene was introgressed from the wild species more
206 than one time. The *SWEETIE* gene encodes a membrane protein that is known to be involved in
207 general control of sugar flux (*18*). In *Arabidopsis*, the *sweetie* mutant shows pronounced changes in
208 the accumulation of sugar, starch and ethylene with significant growth and developmental alterations
209 (*19*). We still do not know the effect of this introgression on the phenotype of Guinea yam, but this
210 locus seems to be a target of selection.
211
212 **Homoploid hybrid speciation as the trigger of domestication**

Homoploid hybridization can contribute to increased genetic variation by recombination between distantly related species, and it often allows the hybrid to adapt to unexploited niches (*20*). In the case of Guinea yam, the savannah-adapted wild species *D. abyssinica* and the rainforest-adapted wild species *D. praehensilis* have not been suitable for agriculture; however, their hybrid *D. rotundata* could have been adopted by humans to the man-made environment. Gene combinations from different wild yams might have contributed to the Guinea yam domestication. New alleles from wild yams seems to have been introduced to cultivated Guinea yams like the *SWEETIE* gene, and it probably conferred plants with beneficial phenotypes for humans. This study highlights the need to consider how to effectively leverage gene pools of wild species from different habitat for rapid breeding of Guinea yam using genomics information.

Acknowledgements

This study has been carried out under AfricaYam Project funded by Bill and Melinda Gates Foundation (BMGF) as well as EDITS-Yam project funded by JIRCAS, Japan. The authors thank Sophien Kamoun for valuable comments in the preparation of manuscript.

Reference and Notes

1. J. F. Hancock, "Starch Staples and Sugar" in *Plant evolution and the origin of crop species* (CABI Publishing, Wallingford, UK, ed. 3, 2012).
2. J. E. Obidiegwu, E. M. Akpabio, The geography of yam cultivation in southern Nigeria: Exploring its social meanings and cultural functions. *J. Ethnic. Foods.* **4**, 28-35 (2017).
3. M. Tamiru, S. Natsume, H. Takagi, B. White, H. Yaegashi, M. Shimizu, K. Yoshida, A. Uemura, K. Oikawa, A. Abe, N. Urasaki, H. Matsumura, P. Babil, S. Yamanaka, R. Matsumoto, S. Muranaka, G. Girma, A. Lopez-Montes, M. Gedil, R. Bhattacharjee, M. Abberton, P. L. Kumar,

I. Rabbi, M. Tsujimura, T. Terachi, W. Haerty, M. Corpas, S. Kamoun, G. Kahl, H. Takagi, R. Asiedu, R. Terauchi, Genome sequencing of the staple food crop white Guinea yam enables the development of a molecular marker for sex determination. *BMC Biol.* **15**, 86 (2017).

4. R. Terauchi, V. A. Chikaleke, G. Thottappilly, S. K. Hahn, Origin and phylogeny of Guinea yams as revealed by RFLP analysis of chloroplast DNA and nuclear ribosomal DNA. *Theor. Appl. Genet*. **83**, 743–751 (1992).
5. G. Girma, K. E. Hyma, R. Asiedu, S. E. Mitchell, M. Gedil, C. Spillane, Next-generation sequencing based genotyping, cytometry and phenotyping for understanding diversity and evolution of guinea yams. *Theor. Appl. Genet*. **127**, 1783–1794 (2014).
6. N. Scarcelli, P. Cubry, R. Akakpo, A.-C. Thuillet, J. Obidiegwu, M. N. Baco, E. Otoo, B. Sonké, A. Dansi, G. Djedatin, C. Mariac, M. Couderc, S. Causse, K. Alix, H. Chaïr, O. François, Y. Vigouroux, Yam genomics supports West Africa as a major cradle of crop domestication. *Sci. Adv.* **5**, eaaw1947 (2019).
7. E. Frichot, F. Mathieu, T. Trouillon, G. Bouchard, O. François, Fast and Efficient Estimation of Individual Ancestry Coefficients. *Genetics*. **196**, 973–983 (2014).
8. N. Saitou, M Nei, The neighbor-joining method: a new method for reconstructing phylogenetic trees. *Mol. Biol. Evol.* **4**, 406–425 (1987).
9. R. N. Gutenkunst, R. D. Hernandez, S. H. Williamson, C. D. Bustamante, Inferring the Joint Demographic History of Multiple Populations from Multidimensional SNP Frequency Data. *PLoS Genet*. **5**, e1000695 (2009).
10. L. Excoffier, I. Dupanloup, E. Huerta-Sánchez, V. C. Sousa, M. Foll, Robust demographic Inference from genomic and SNP data. *PLoS Genet*. **9**, e1003905 (2013).
11. R. A. Folk, P. S. Soltis, D. E. Soltis, R. Guralnick, New prospects in the detection and comparative analysis of hybridization in the tree of life. *Am. J. Bot.* **105**, 364–375 (2018).
12. S. Wright, The genetical structure of populations. *Ann. Eugen.* **15**, 323–354 (1951).

13. M. C. Fontaine, J. B. Pease, A. Steele, R. M. Waterhouse, D. E. Neafsey, I. V. Sharakhov, X. Jiang, A. B. Hall, F. Catteruccia, E. Kakani, S. N. Mitchell, Y.-C. Wu, H. A. Smith, R. R. Love, M. K. Lawniczak, M. A. Slotman, S. J. Emrich, M. W. Hahn, N. J. Besansky. Extensive introgression in a malaria vector species complex revealed by phylogenomics. *Science.* **347**, 1258524 (2015).

14. N. Scarcelli, H. Chaïr, S. Causse, R. Vesta, T. L. Couvreur, Y. Vigouroux, Crop wild relative conservation: Wild yams are not that wild. *Biol. Conserv.* **210**, 325–333 (2017).

15. N. Scarcelli, S. Tostain, Y. Vigouroux, C. Agbangla, O. Daïnou, J.-L. Pham, Farmers' use of wild relative and sexual reproduction in a vegetatively propagated crop. The case of yam in Benin. *Mol. Ecol.* **15**, 2421–2431 (2006).

16. D. Reich, K. Thangaraj, N. Patterson, A. L. Price, L. Singh, Reconstructing Indian population history. *Nature.* **461**, 489–494 (2009).

17. D. H. Huson, D. Bryant, Application of Phylogenetic Networks in Evolutionary Studies. *Mol. Biol. Evol.* **23**, 254–267 (2006).

18. N. Veyres, M. Aono, B. S. Sangwan-Norree, R. S. Sangwan, Has Arabidopsis SWEETIE protein a role in sugar flux and utilization? *Plant Signal. Behav.* **3**, 722–725 (2008).

19. N. Veyres, A. Danon, M. Aono, S. Galliot, Y. B. Karibasappa, A. Diet, F. O. Grandmottet, M. Tamaoki, D. Lesur, S. Pilard, M. Boitel-Conti, B. S. Sangwan-Norreel, R. S. Sangwan, The Arabidopsis sweetie mutant is affected in carbohydrate metabolism and defective in the control of growth, development and senescence. *Plant J.* **55**, 665–686 (2008).

20. J. Mallet, Hybrid speciation. *Nature.* **446**, 279–283 (2007).

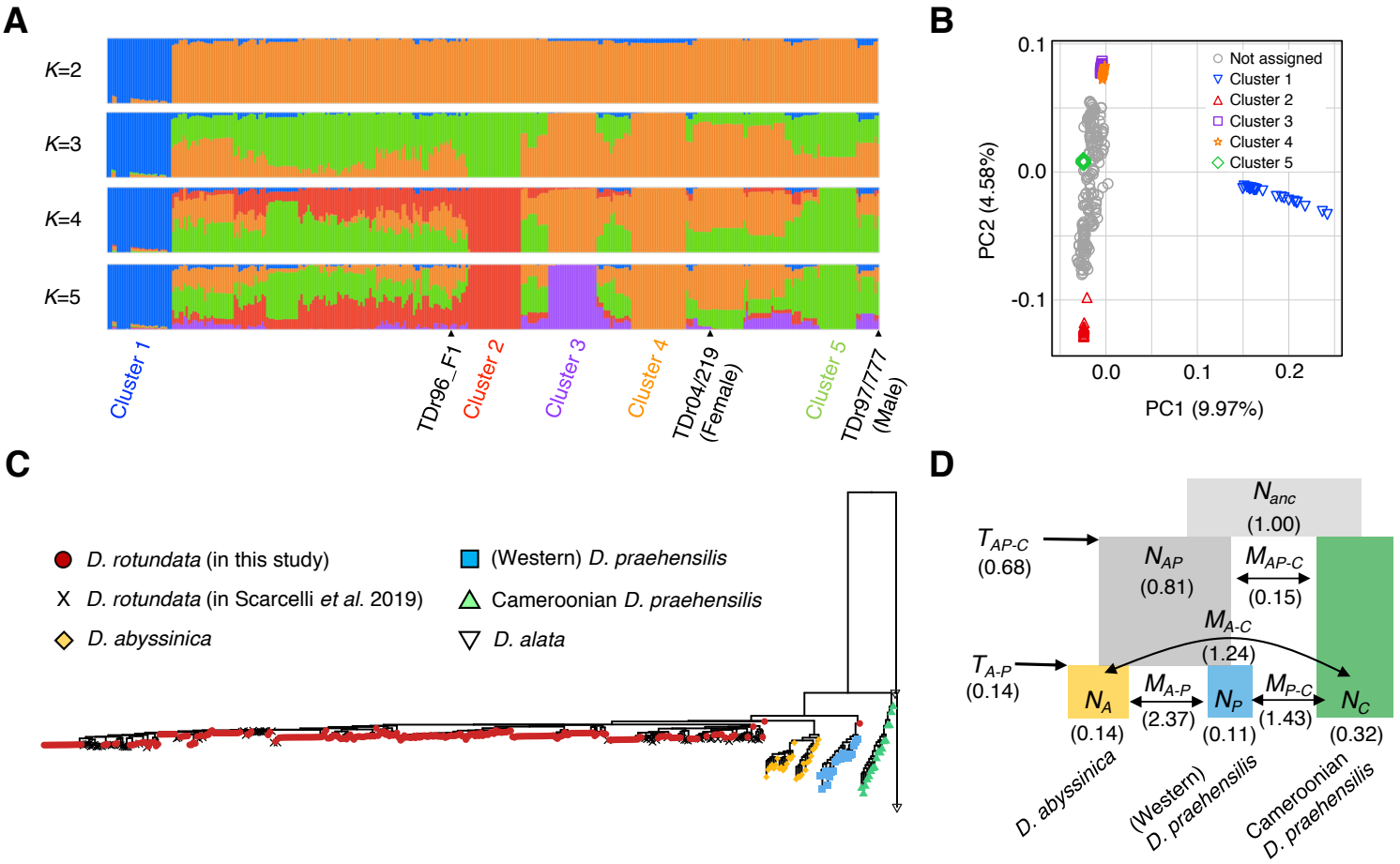

Fig. 1. Genetic diversity and phylogenomics of Guinea yam and its wild relatives. (A) Ancestry proportions of each Guinea yam accession with 6,124,093 SNPs. "TDr96_F1" is the sample used as the reference genome. **(B)** PCA result of the 336 Guinea yam accessions. **(C)** Neighbor-joining tree of four African yam lineages reconstructed using *D. alata* as an outgroup based on 463,293 SNPs. The sequences of *D. rotundata* in the previous study (*6*) were included in the tree as represented by "X". The 308 *D. rotundata* (excluding 28 accessions in cluster 1 due to the triploid accessions) analyzed in this study are close to those in the previous study (*6*). **(D)** Evolutionary relationship of three African wild yam lineages (*D. abyssinica*, Western *D. praehensilis*, Cameroonian *D. praehensilis*) as inferred by ∂a∂i (*9*) using 17,532 SNPs. *N*, *M*, and *T* represent the relative population size from N_{anc}, migration rate, and divergence time, respectively.

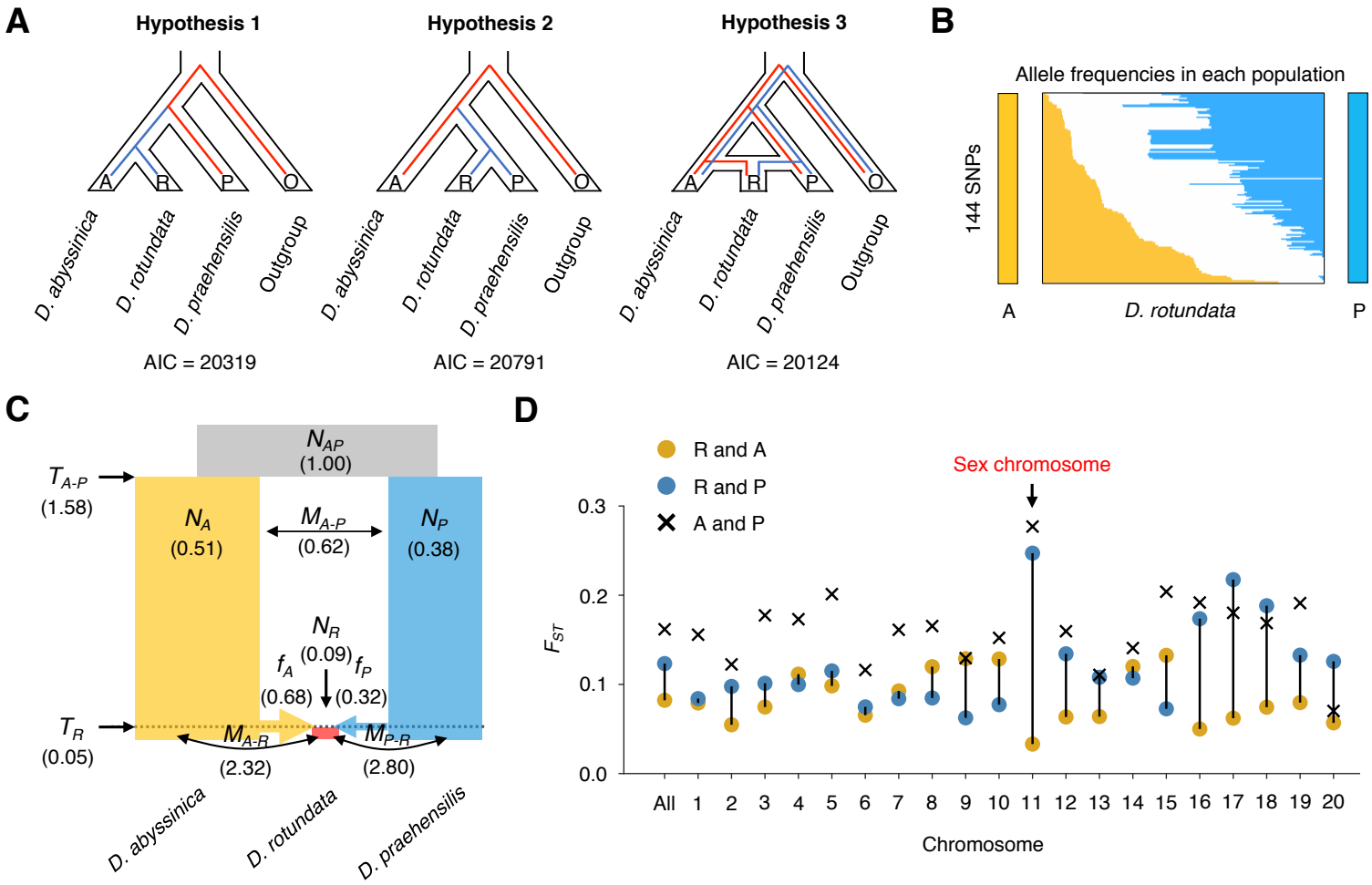

Fig. 2. Evidence for the hybrid origin of Guinea yam. (A) Hypotheses for the domestication of Guinea yam (*D. rotundata*). Hypothesis 1 assumes that *D. rotundata* was diverged from *D. abyssinica*. Hypothesis 2 assumes that *D. rotundata* was diverged from *D. praehensilis*. Hypothesis 3 assumes that *D. rotundata* was derived from the hybrid between *D. abyssinica* and *D. praehensilis*. *D. alata* was used as an outgroup. **(B)** Frequencies of fixed alleles of *D. abyssinica* (A) and *D. praehensilis* (P) among the 388 *D. rotundata* sequences including 80 in the previous study (*6*). **(C)** Evolutionary parameters related to the hybrid origin of Guinea yam as inferred by ∂a∂i (*9*) using 15,461 SNPs. **(D)** F_{ST} among the three African yams, *D. rotundata* (R), *D. abyssinica* (A) and *D. praehensilis* (P) for each chromosome. Chromosome 11 of *D. rotundata* containing sex locus shows a lower distance to that of *D. abyssinica*.

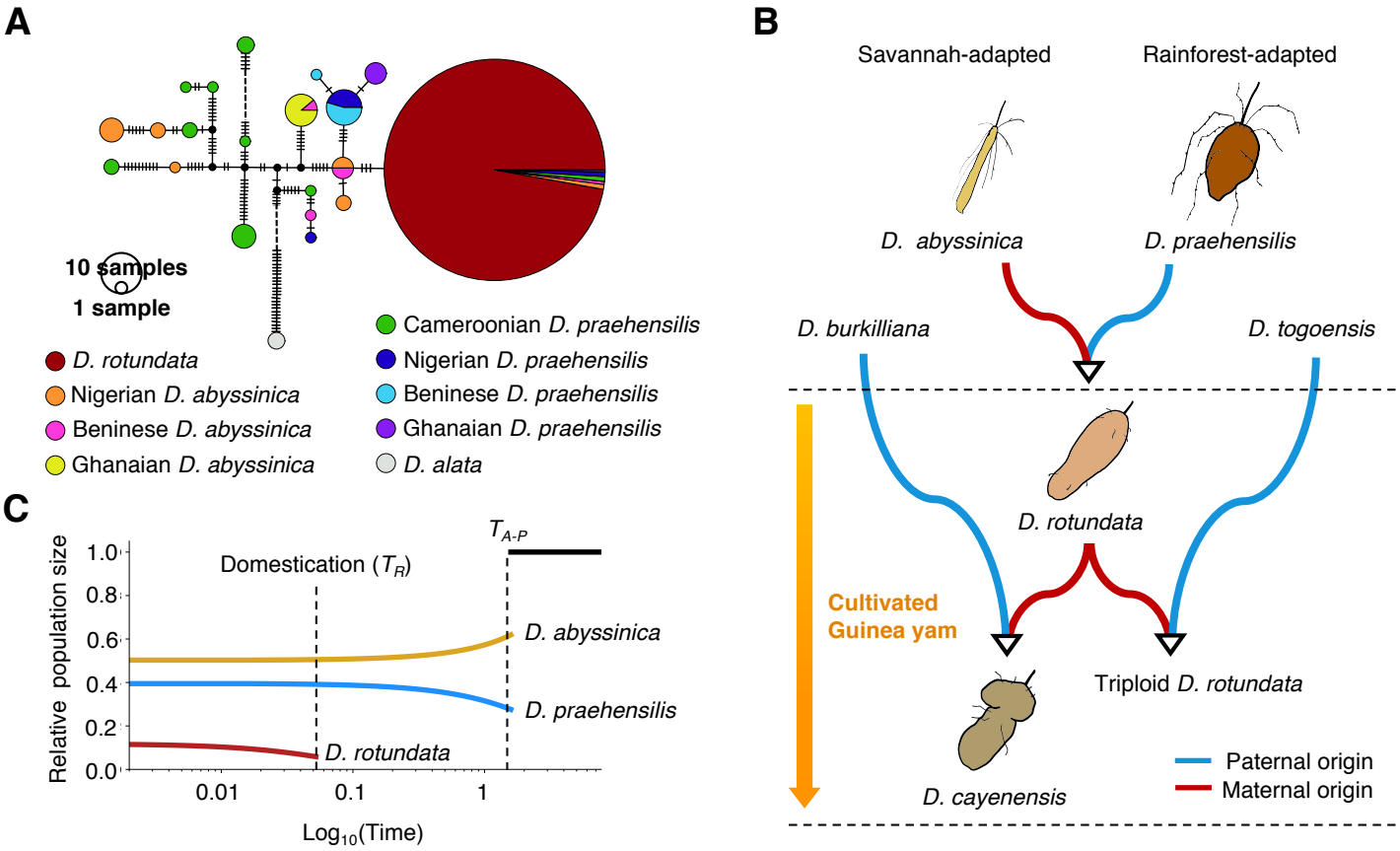

Fig. 3. Evolutionary scenario of African yam origins. **(A)** Haplotype network of the whole plastid genomes of 416 *D. rotundata* (including the triploid accessions), 68 wild relatives, and two *D. alata* used as the outgroup. The number of vertical dashes represent the number of mutations. Western (Nigerian, Beninese, and Ghanaian) *D. praehensilis* and *D. rotundata* seem diverged from Nigerian and Beninese *D. abyssinica*. **(B)** Domestication process of Guinea yam. The blue line represents the paternal origin, and the red line represents the maternal origin. **(C)** Changes of population sizes of *D. rotundata* and its wild relatives as inferred by ∂a∂i (*9*). The parameters except for that of population size were identical to those used in Fig. 2C. After the domestication of *D. rotundata*, the population size of *D. rotundata* has been increasing with the migration from the wild progenitors.

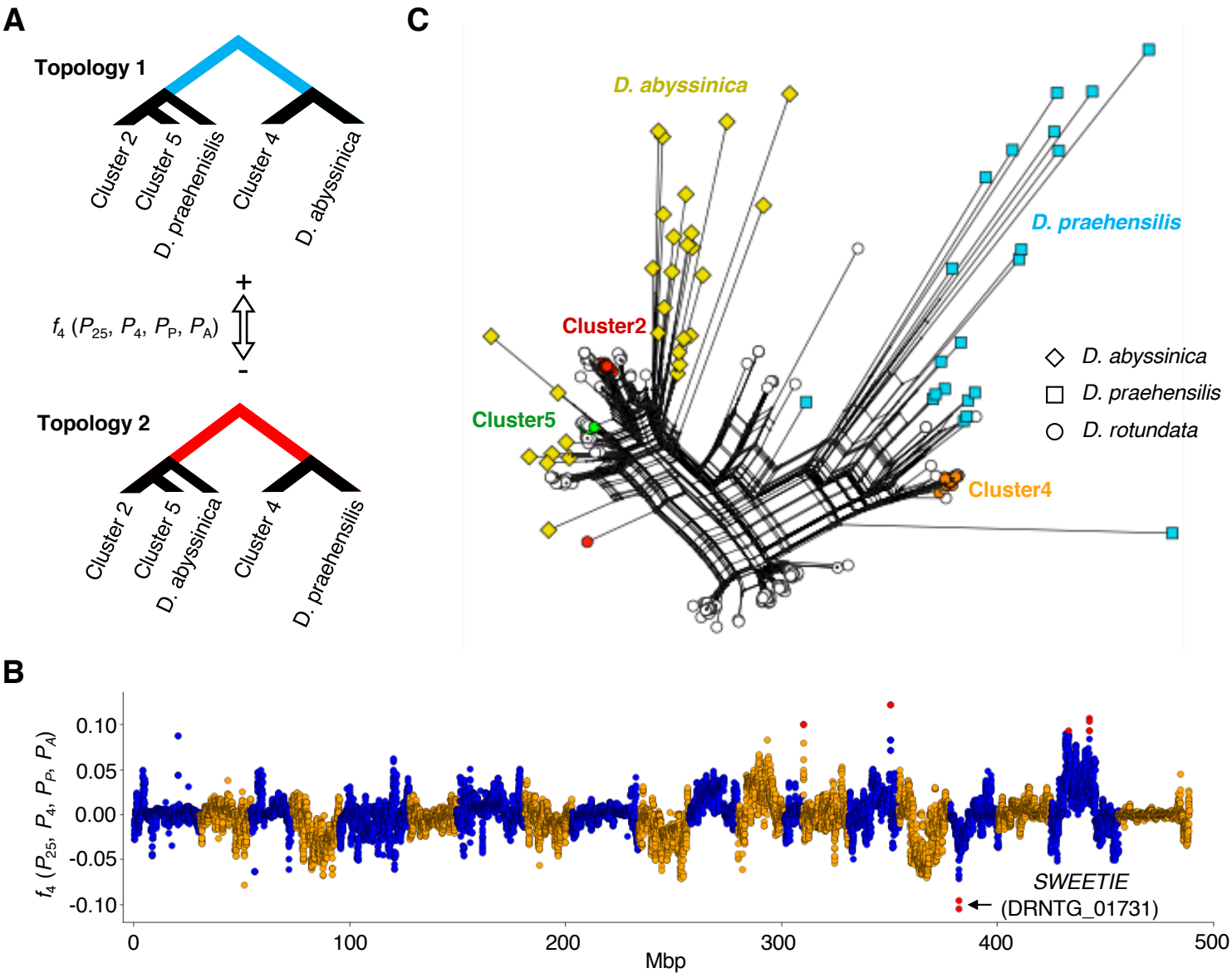

Fig. 4. Signature of extensive introgression around the *SWEETIE* gene. (A) Topology of f_4 (P_{25}, P_4, P_P, P_A) in cluster 2, 4, 5 and wild yams. Positive f_4 values represent the long internal branch of the upper tree (Topology 1). Negative f_4 values represent the long internal branch of the bottom tree (Topology 2). **(B)** f_4 values across the genome. This was conducted with 250 Kb window and 25 Kb step. Red dots indicates outliers of the sliding window which have $|Z(f_4)| > 5$.The locus around the *SWEETIE* gene shows extraordinarily negative f_4 values. **(C)** Neighbor-Net around the *SWEETIE* gene (4Mbp ~ 4.15Mbp on chromosome 17). This was constructed by SplitsTree (*17*) using 458 variants.

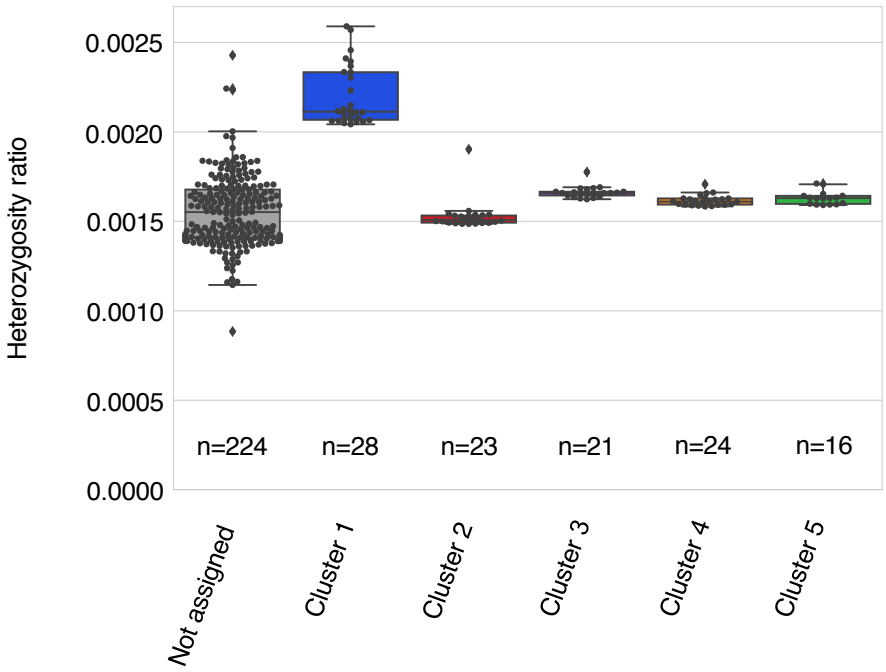

Fig. S1. Heterozygosity ratio in five clusters of *D. rotundata*.

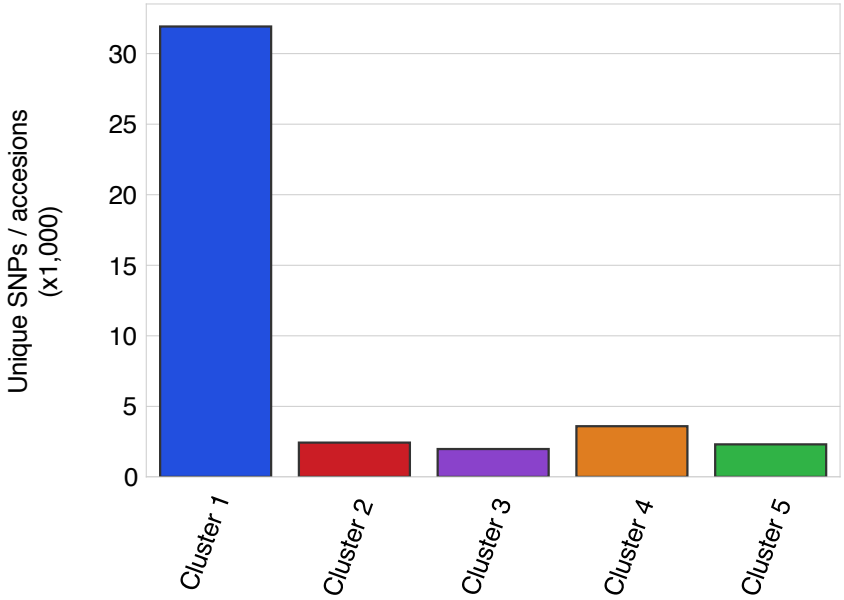

Fig. S2. Number of unique alleles in the five clusters of *D. rotundata*.

Table S2. Population genetics summary statistic in the 308 yam accessions

	After imputation
No. segregating site	5,229,368
No. singleton	1,227,900
θ_W	14.98 x 10^{-4}
θ_π	14.83 x 10^{-4}
Tajima's *D*	-0.0305

Table S3. Likelihood comparison in ∂a∂i

Model	$\log_{10}(L)$	No. parameters	AIC	Illustration of the model
{{A, P}, C} (without migration)	-15289.70	6	30591.40	-
{{C, P}, A} (without migration)	-15765.32	6	31542.64	-
{{C, A}, P} (without migration)	-15765.15	6	31542.29	-
{{A, P}, C} (with migration)	-12739.86	10	25499.72	Fig. 1D
{{A, R}, P} (with migration)	-10149.73	10	20319.47	-
{{P, R}, A} (with migration)	-10385.46	10	20790.92	-
{{A, R}, {P, R}} (with migration)	-10052.96	9	20123.91	Fig. 2C
{{A, R}, {P, R}} - With migration - With population growth - Fix the parameters except for population size	-10046.73	6	20105.47	Fig. 3C

C: Cameroonian *D. praehensilis*
A: *D. abyssinica*
P: (Western) *D. praehensilis*
R: *D. rotundata*

Table S4. Likelihood comparison in fastsimcoal2

Model	$\log_{10}(L)$
{{A, P}, C} (without migration)	-172110.065
{{C, P}, A} (without migration)	-174281.072
{{C, A}, P} (without migration)	-173358.592

Materials and Methods

Table of contents

S1. Reference assembly
- S1.1 Whole genome sequencing by Oxford Nanopore Technology
- S1.2 Quality control
- S1.3 *De novo* assembly
- S1.4 Polishing and removing duplicated contigs
- S1.5 Gene prediction and annotation

S2. Generation of pseudo-chromosomes by anchoring contigs onto a linkage map
- S2.1 Preparing population for mapping
- S2.2 Whole genome re-sequencing
- S2.3 Quality control and alignment
- S2.4 Identification of parental line-specific heterozygous markers
- S2.5 Anchoring and ordering contigs

S3. Genetic diversity analysis
- S3.1 Whole genome re-sequencing of Guinea yam accessions
- S3.2 Quality control, alignment, and SNP calling
- S3.3 Unsupervised clustering analysis
- S3.4 Polymorphism and ploidy of nuclear genomes.

S4. Phylogenomic analysis of African yam
- S4.1 Data preparation
- S4.2 Neighbor-joining tree
- S4.3 Inference of the evolutionary history of wild *Dioscorea* species by ∂a∂i
- S4.4 Inference of the evolutionary history of wild *Dioscorea* species by fastsimcoal2

S5. Test of hybrid origin
- S5.1 Site frequency spectrum polarized by two candidate progenitors of Guinea yam
- S5.2 Inference of the domestication history of Guinea yam by ∂a∂i
- S5.3 Comparison of F_{ST} among three African yams in each chromosome

S6. Haplotype network analysis of whole plastid genome

S7. Inference of the change of population size

S8. Exploration of extensive introgression from wild *Dioscorea* species

S1. Reference assembly

S1.1 Whole genome sequencing by Oxford Nanopore Technology

To generate version 2 of *Dioscorea rotundata* reference genome sequence, we sequenced an F1 individual plant named "TDr96_F1" by PromethION sequencer (Oxford Nanopore Technologies). "TDr96_F1" was the same individual plant used to obtain version 1 of *D. rotundata* reference genome sequence (*1*). The DNA of "TDr96_F1" was extracted from fresh leaves following the proposed method (*1*). The DNA was subjected to size selection and purification with a gel extraction kit (Large Fragment DNA Recovery Kit; ZYMO RESEARCH). The sequencing of purified genome was performed using PromethION at GeneBay, Yokohama, Japan (http://genebay.co.jp).

S1.2 Quality control

As a first step in our pipeline for genome assembly (Fig. SM1), we removed lambda phage genome from raw reads by NanoLyse v1.1 (*2*). Then, we filtered out reads with average read quality score of less than 7 and those that are shorter than 1,000 bases in length by Nanofilt v2.2 (*2*). This was followed by trimming of the first 75 bases to remove low quality bases in all the read that were retained. This generated 3,124,439 reads, corresponding to 20.89 Gbp sequence (Table SM1).

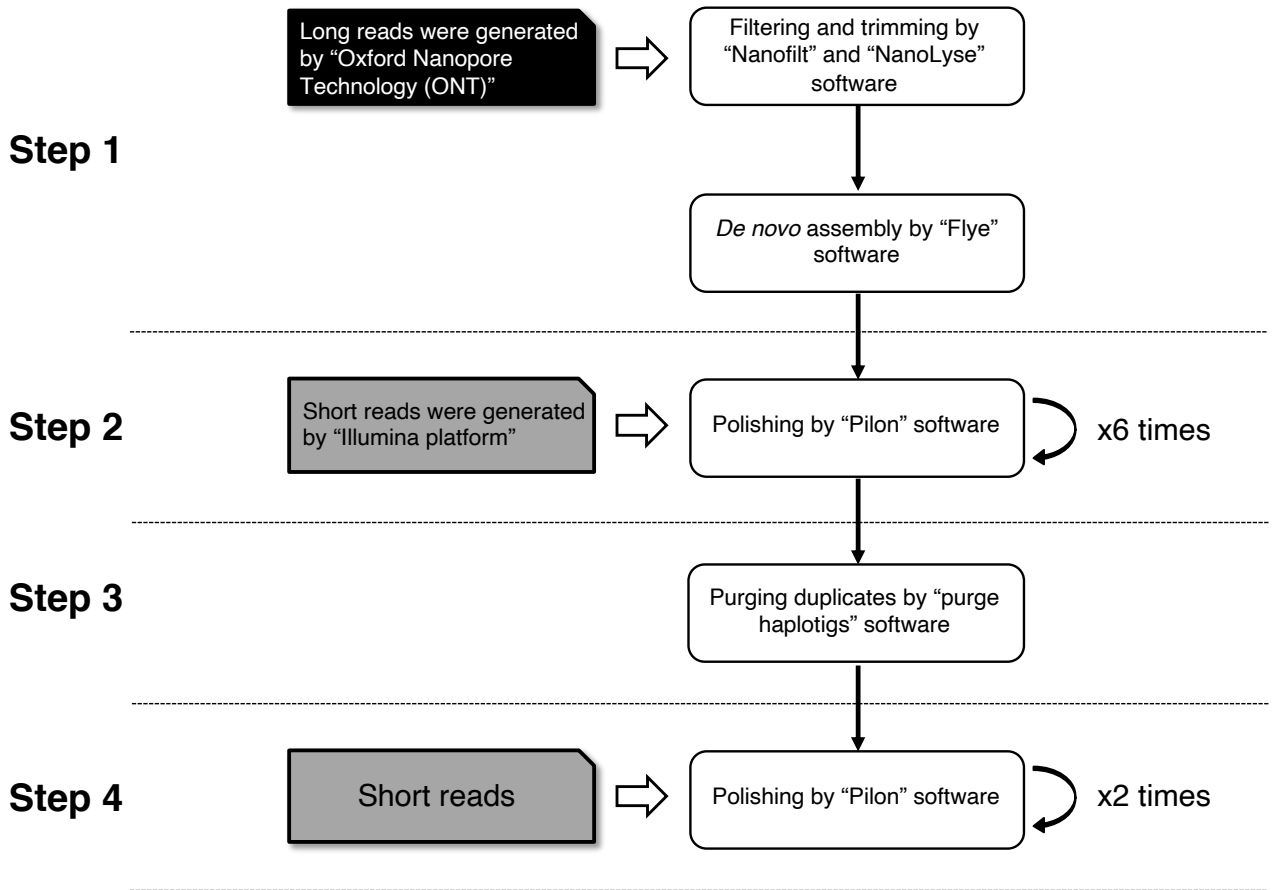

Fig. SM1. Pipeline of genome assembly Ver.2.

Table SM1. Summary of filtered ONT reads.

Summary	
Number of reads	3,124,439
Total base pairs (Gbp)	20.89
Genome coverage	36.6x
Average fragment size (Kbp)	6.7
Longest fragment	211,597
Shortest fragment	1,000
Fragment N50 (Kbp)	8.0

- Raw reads are registered in DRR196916.
- Genome coverage is estimated from the expected genome size of *D. rotundata* (570Mb).

S1.3 *De novo* assembly

We assembled those filtered long DNA sequence reads by Flye v2.4.2 (*3*), using 570 Mbp as the estimated genome size of *D. rotundata* (*1*). This generated 8,721 contigs with N50 of 137,007 base-pairs (Step 1 in Table SM2) and a total size of 636.8Mbp, which is larger than the expected *D. rotundata* genome of 570 Mbp. To evaluate completeness of the gene set in the assembled contigs, we applied BUSCO analysis (Bench-Marking Universal Single Copy) v3.0.2 (*4*). For BUSCO analysis, we set "genome" as the assessment mode and used Embryophyta *odb9* as the database and obtained 40.7% complete BUSCOs (Step 1 in Table SM2).

Table SM2. Summary of reference assembly.

	Step 1	Step 2	Step 3	**Step 4**
Total number of contigs	8,721	8,721	6,513	**6,513**
Total base-pairs (Mbp)	636.8	628.2	579.7	**579.4**
Average contig size (bp)	73,008	72,029	89,004	**88,961**
Longest contig (bp)	2,301,335	2,267,833	2,267,833	**2,267,326**
Shortest contig (bp)	171	171	171	**171**
N50 (bp)	137,007	134,605	152,963	**152,929**
Complete BUSCOs (%)	40.7	89.9	89.3	**90.1**
Complete and single-copy BUSCOs (%)	39.9	83.9	84.9	**85.7**
Complete and duplicated BUSCOs (%)	0.8	6.0	4.4	**4.4**
Fragmented BUSCOs (%)	8.2	3.2	3.2	**3.1**
Missing BUSCOs (%)	51.1	6.9	7.5	**6.8**

S1.4 Polishing and removing duplicated contigs

To correct the assembled contigs, we repeatedly polished them with Illumina short reads (Table SM3) using Pilon v1.23 (*5*) until there is no further change in % of complete BUSCOs. We first aligned illumina jump reads as single reads to the assembled contigs by bwa mem command in BWA v0.7.17 (*6*) and sorted the BAM files by SAMtools v1.9 (*7*). The BAM files were used to run Pilon with the option "--diploid". We then polished the contigs six times. The percentage of complete BUSCOs was

89.9% after the first polishing step (Step 2 in Fig. SM1). To remove duplicated contigs, we used Purge Haplotigs v1.0.2 (*8*), which can remove duplicated contigs based on depth and number of matching bases (Step 3 in Fig. SM1). In Purge Haplotigs, the percent cutoff of aliment coverage was set to 95%. After that, we polished the contigs again. Finally, the percentage of complete BUSCOs was 90.1% after the second polishing process (Step 4 in Fig. SM1). Comparing the features in old reference genome with new reference genome, the number of missing ("N") was drastically reduced (Table SM4).

Table SM3. Sequence list used in polishing.

Name	Sequence Platform	Total size (Gb)	Genome coverage	Accession No.
Fragment (PE)	Illumina "Miseq"	16.77	29.4x	DRR027644
MP jump reads (as Single)				
for 2k	Illumina "Hiseq 2500"	6.43	11.3x	DRR027645
for 3k	Illumina "Hiseq 2500"	7.56	13.3x	DRR027646
for 4k	Illumina "Hiseq 2500"	6.18	10.8x	DRR027647
for 5k	Illumina "Hiseq 2500"	7.20	12.6x	DRR027648
for 6k	Illumina "Hiseq 2500"	7.27	12.8x	DRR027649
for 8k	Illumina "Hiseq 2500"	6.79	11.9x	DRR027650

- All values are calculated after quality control.
- Genome coverage is estimated from the expected genome size of *D. rotundata* (570Mb).
- In terms of jump reads, we only used the reads generated from Illumina "Hiseq 2500".

Table SM4. Comparison of old (*1*) and the new reference assemblies.

Feature	Ver. 1	Ver. 2
Number of scaffolds*	4,723	6,513
Total scaffold* size (Mbp)	594.23	579.41
Longest scaffold* (Mbp)	13.61	2.28
N50 (Mbp)	2.12	0.15
Total 'N' bp	90,097,902	953
Complete BUSCOs (%)	90.7	90.1

*In Version 2, the contigs were used instead of scaffolds.

S1.5 Gene prediction and annotation

For gene prediction, we used 20 RNA-Seq data representing 15 different organs and three different flowering stages in male and female plants (Table SM5). Total RNA was used to construct cDNA libraries using a TruSeq RNA Sample Prep Kit V2 (Illumina) according to the manufacturer's instructions. The extracted RNAs were sequenced by the Illumina platforms NextSeq500 and HiSeq4000. In the quality control step, we filtered the reads and discarded reads shorter than 50 bases and those with average read quality below 20, and trimmed poly A by FaQCs v2.08 (*9*). Quality trimmed reads were aligned to the newly assembled contigs by HISAT2 v2.1 (*10*) with options "--no-mixed --no-discordant --dta". Transcript alignments were assembled by StringTie v1.3.6 (*11*) for each BAM file, separately. Those GFF files were integrated by TACO v0.7.3 (*12*) with the option "-

-filter-min-length 150", generating 26,609 gene models within the new assembly (Table SM6). Additionally, CDSs that were predicted using the previous reference genome (*1*) were aligned to the newly assembled contigs by Spaln2 v2.3.3 (*13*). Consequently, 8,889 CDSs that didn't have any overlap with the new gene models were added to the new gene models (Table SM6). Gene models shorter than 75 bases were removed, and InterProScan v5.36 (*14*) was used to predict ORFs (open reading frames) and strand information for each gene model. Finally, we predicted 35,498 genes including 66,561 transcript variants (Table SM6). For gene annotation, the predicted gene models were searched by Pfam protein family database through InterProScan (*14*) and by blastx command in BLAST+ (*15*) with option "-evalue 1e-10", using the database of Viridiplantae from UniProt as the target database. The resulting gene models and annotations were uploaded to ENSEMBL (http://plants.ensembl.org/Dioscorea_rotundata/Info/Index; for early access http://staging-plants.ensembl.org/Dioscorea_rotundata/Info/Index).

Table SM5. Summary of RNA-seq data for gene prediction.

Sample name	Fastq size		Sequence platform	Comment	Accession No.
	Original (Gbp)	Filtered (Gbp)			
01_Flowers-rachis-top	4.36	4.28	NextSeq500	Top 2 cm of inflorescence	DRR063119
02_Flowers-rachis-lower	4.96	4.87	NextSeq500	Lower 2 cm of inflorescence	DRR063118
03_Flower-bud	3.52	3.46	NextSeq500	Flower bud	DRR063116
04_Axillary-bud	4.31	4.23	NextSeq500	Axillary bud	DRR063115
05_Leaf	3.26	3.18	NextSeq500	Leaf	DRR045127
06_Petiole	4.47	4.38	NextSeq500	Petiole	DRR063121
07_Pulvinus	4.66	4.58	NextSeq500	Pulvinus	DRR063120
08_Rachis	4.59	4.51	NextSeq500	Rachis	DRR063117
09_Stem	3.45	3.36	NextSeq500	Young_stem	DRR045129
10_Spine	4.51	4.43	NextSeq500	Spine	DRR063123
11_Root	3.62	3.54	NextSeq500	Root	DRR063122
12_Tuber-head	4.72	4.65	NextSeq500	Tuber (head)	DRR063126
13_Tuber-middle	4.06	4.00	NextSeq500	Tuber (middle)	DRR063125
14_Tuber-tail	4.48	4.40	NextSeq500	Tuber (tail)	DRR063124
15_fem_Y917-1	4.12	4.08	HiSeq4000	TDr97_00917 female flower early stage 1	DRR208398
16_fem_Y917-2	4.27	4.23	HiSeq4000	TDr97_00917 female flower early stage 2	DRR208399
17_fem_Y917-3	4.43	4.37	HiSeq4000	TDr97_00917 female flower early stage 3	DRR208400
18_mal_Y777-1	4.48	4.42	HiSeq4000	TDr97_00777 male flower early stage 1	DRR208401
19_mal_Y777-2	3.43	3.40	HiSeq4000	TDr97_00777 male flower early stage 2	DRR208402
20_mal_Y777-3	4.13	4.09	HiSeq4000	TDr97_00777 male flower early stage 3	DRR208403

Table SM6. Summary of gene prediction.

	Contigs (6,513)	Pseudo Chrom. (01~20)
No. genes	35,498	30,344
(Total transcript variants)	(66,561)	(57,637)
ORF status		
Complete	22,423	19,502
5' partial	1,225	1,018
3' partial	10,385	8,594
Internal	559	465
No ORF	906	765
Predicted software		
TACO (*12*)	26,609	23,335
Spaln2 (*13*)	8,889	7,009

S2. Generation of pseudo-chromosomes by anchoring contigs onto a linkage map

S2.1 Preparing population for mapping

To develop chromosome-scale "TDr96_F1" genome sequence from the assembled contigs, we generated an F1 progeny containing 156 individuals by crossing two *D. rotundata* breeding lines: "TDr04/219", female parent (P1) and "TDr97/777", male parent (P2).

S2.2 Whole genome re-sequencing

We extracted each DNA sample from the dried leaves of *D. rotundata* following the proposed method (*1*). Libraries for PE short reads were constructed using an Illumina TruSeq DNA LT Sample Prep Kit (Illumina). The PE library was sequenced on the Illumina Hiseq4000 platform. Each summary of sequence and alignment is described in Table SM7 (attached at the bottom of this file).

S2.3 Quality control and alignment

We used FaQCs v2.08 (*9*) to remove unpaired reads and adapters. We then filtered out reads shorter than 75 bases or those whose average read quality score is 20 or lower by prinseq-lite v0.20.4 lite (*16*). We also trimmed bases whose average read quality score is below 20 from the 5' end and the 3' end using sliding window (the window size is five bases, and the step size is one base) in prinseq-lite (*16*). Subsequently, we aligned the filtered reads of P1, P2, and F1 progenies to the newly assembled contigs (supplementary text S1) by bwa mem command in BWA (*6*). After sorting BAM files, we only retained proper paired and uniquely mapped reads by SAMtools (*7*).

S2.4 Identification of parental line-specific heterozygous markers

SNP-type heterozygous marker

SNP-based genotypes for P1, P2, and F1 progenies were obtained as VCF file. The VCF file was generated as follows: (i) SAMtools v1.5 (*7*) mpileup command with options "-t DP,AD,SP -B -Q 18 -C 50" (ii) BCFtools v1.5 (*17*) call command with options "-P 0 -v -m -f GQ,GP" (iii) BCFtools (*17*) view command with options "-i 'INFO/MQ>=40 & INFO/MQ0F<=0.1 & AVG(GQ)>=10" (iv)

BCFtools (*17*) norm command with options "-m+any" (Fig. SM2). We rejected the variants having low read depth (<10) or low genotype quality score (<10) in two parents. Regarding variants having low read depth (<8) or low genotype quality score (<5) in F1 progenies as missing, we only retained the variants having low missing rate (<0.3). After that, only bi-allelic SNPs were selected by the BCFtools (*17*) view command with options "-m 2 -M 2 -v snps". Referring to the genotypes in the VCF file, heterozygous genotypes called by unbalanced allele frequency (out of 0.4-0.6 in two parents, and out of 0.2-0.8 in F1 progenies) were regarded as missing, and filtering for missing rate (<0.3) was applied again. Finally, binomial test was applied to reject SNPs affected by segregating distortion in F1 progenies. This binomial test assumes that the probability of success rate is 0.5 on two-side hypothesis, and we regarded variants having *p*-value less than 0.2 as segregating distortion.

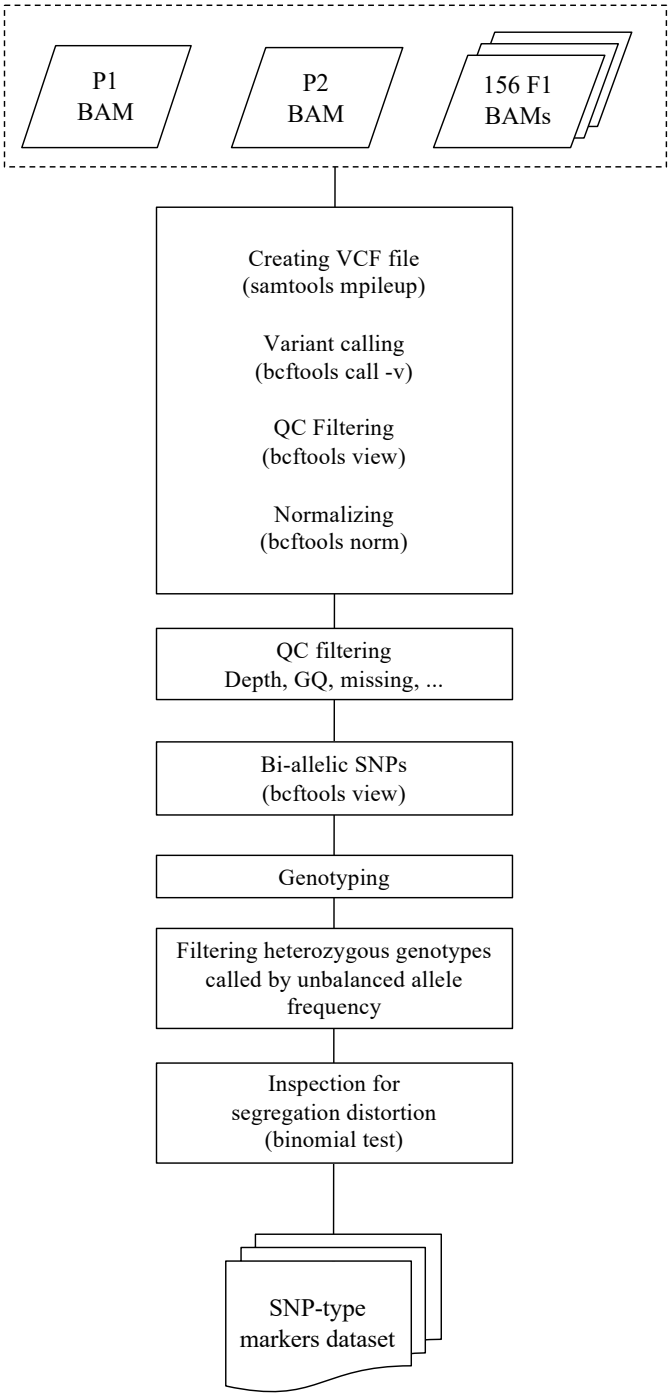

Fig. SM2. Flowchart of SNP-type heterozygous marker selection.

Presence/absence-type heterozygous marker.
First, a VCF file was generated to search for positions having contrasting read depth between the two parental plants P1 and P2 through the following commands: (ⅰ) SAMtools (*7*) mpileup command with options "-B -Q 18 -C 50" (ⅱ) BCFtools (*17*) call command with option "-A" (ⅲ) BCFtools (*17*) view command with options "-i 'MAX(FMT/DP)>=8 & MIN(FMT/DP)<=0' -g miss -V indels". This means that one of the parents (P1 or P2) has enough read depth (>=8) and another parent has no reads aligned on that region (A in Fig. SM3). Subsequently, we converted continuous positions in the VCF file to a feature which indicates start and end coordinate information of a region by BEDTools v.2.26 (*18*) merge command with options "-d 10 -c 1 -o count". After that, we only retained sufficiently wide feature (>=50bp) in the BED file (the 1st BED). To reject false-positives whereby low depth regions are erroneously regarded as absence regions, we focused on both the boundary regions around each feature and features themselves. For boundary regions, the 2nd BED file including expanded (twice-sized) features of each feature given in the 1st BED was generated by BEDTools (*18*) slop command with options "-b 0.5 –pct". Using depth value in each feature given in the 1st BED, presence/absence-based genotypes for parental plants P1, P2, and F1 progenies were determined. For verification to reject the false-positive features, we also referred to the depth values in the boundary regions around each feature. Verified features were only accepted as presence/absence markers. The depth values in each feature were calculated by SAMtools (*7*) bedcov command with option "-Q 0". Also, the depth values in the boundary regions were obtained by subtracting the depth values of the 2nd BED from that of the 1st BED (B in Fig. SM3). For P1 and P2, we regarded genotypes having depth >= 8 as presence genotype meaning the heterozygosity of presence and absence, while those having depth < 2 were classified as absence genotypes meaning the homozygosity of absence. For F1 progenies, we classified markers having depth > 0 and = 0 as presence and absence markers, respectively. Finally, we applied the same binomial test in SNP-type heterozygous markers as in the presence/absence-type heterozygous markers.

A

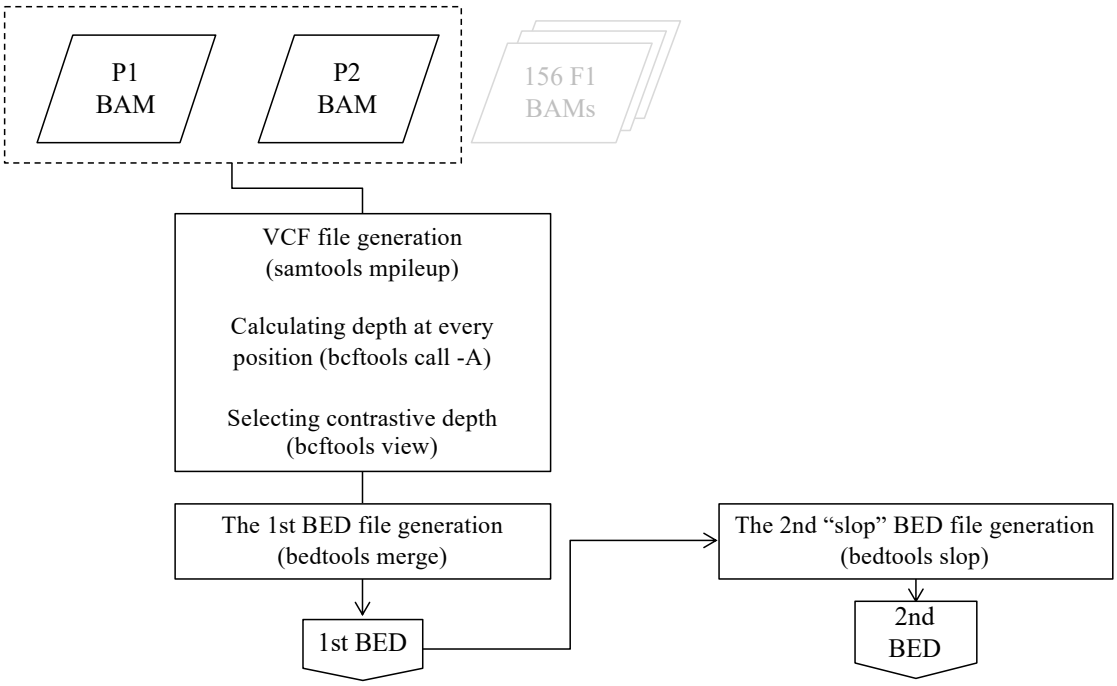

(continued)

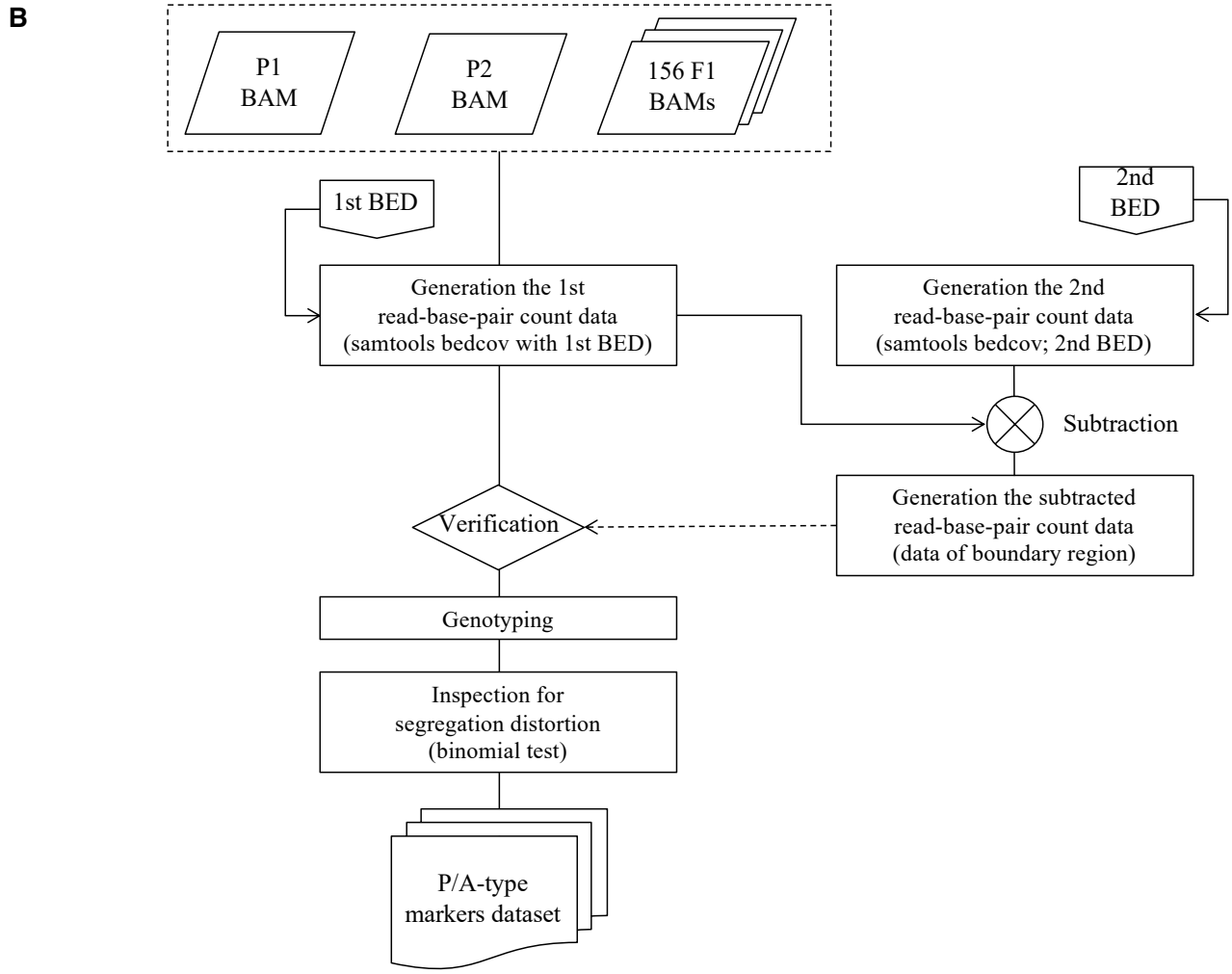

Fig. SM3. Flowchart of presence/absence-type heterozygous marker selection.

Integration of SNP-type and presence/absence-type heterozygous markers. To develop parental line-specific linkage maps, we integrated SNP-type and P/A-type (presence/absence-type) heterozygous makers. Two types of markers, Type-1 markers and Type-2 makers, were defined. If a SNP-type marker is heterozygous in P1 but homozygous in P2 or if a P/A-type maker is present in P1 and absent in P2, it is classified as Type-1 marker (P1-heterozygous marker set). Conversely, if a SNP-type marker is homozygous and heterozygous in P1 and P2, respectively or if a P/A-type maker is absent in P1 but present in P2, it is classified as Type-2 marker (P2-heterozygous marker set).

S2.5 Anchoring and ordering contigs

Pruning and flanking markers by Spearman's correlation coefficients. Distance matrices of Spearman's correlation coefficients (ρ) were calculated for every marker pair in each contig in each marker set (P1-heterozygous marker set and P2-heterozygous marker set). According to the histogram of absolute ρ calculated from each contig, most markers on the same contigs were correlated with each other (Fig. SM4). Therefore, we pruned correlated flanking markers to remove redundant markers (Fig. SM5). Accordingly, we obtained 11,389 markers for linkage mapping (Table SM8).

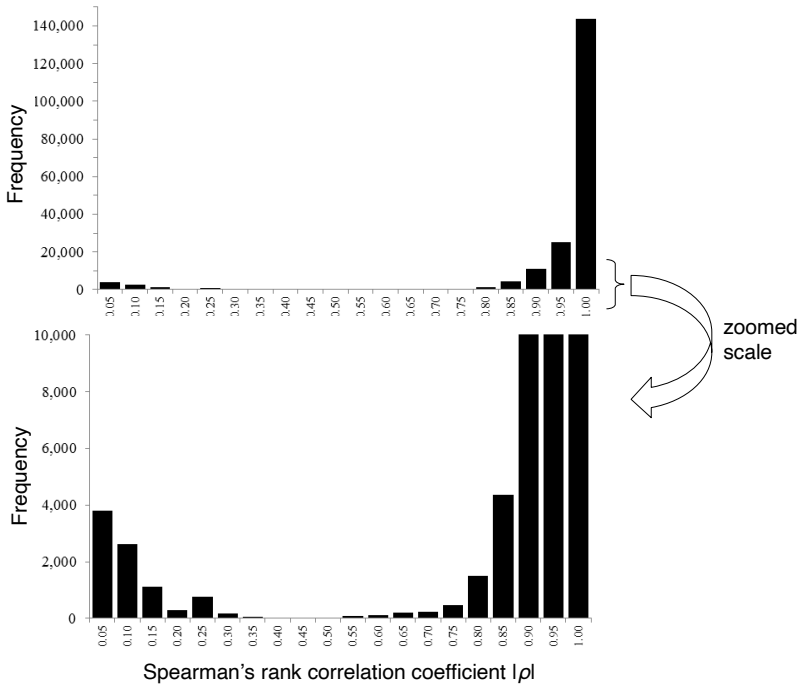

Fig. SM4. Histogram of absolute values of ρ calculated from each contig.

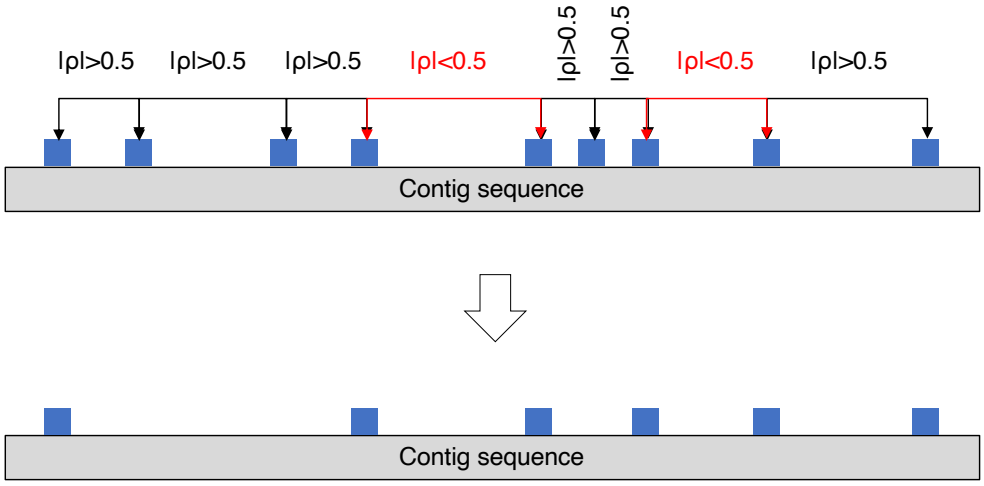

Fig. SM5. A process of pruning correlated flanking markers.

Table SM8. Summary of the anchoring makers.

	Type1	Type2	Type1 + Type2
Total anchoring markers to make linkage group	7,020	4,369	11,389
- SNP	4,607	3,435	8,042
- P/A	2,413	934	3,347
Total base pairs of linkage group having markers (Mbp)	434.7	328.4	495.2
Total anchored base pairs estimated from genome size (%)	75.5	56.7	85.5

Linkage mapping. The markers obtained from the previous section were converted to the genotype-formatted data. Based on that genotype-formatted data, genetic linkage maps were constructed by MSTmap (*19*) with following parameter set: "population_type DH; distance_function kosambi; cut_off_p_value 0.000000000001; no_map_dist 15.0; no_map_size 0; missing_threshold 25.0; estimation_before_clustering no; detect_bad_data no; objective_function ML" for each marker set. After trimming the orphan linkage groups, we solved the complemented-phased duplex linkage groups caused by coupling-type and repulsion-type markers in pseudo-testcross method. Finally, two parental-specific linkage maps were constructed. These two linkage maps were designated as P1-map (which was constructed using Type-1 marker) and P2-map (which was constructed using Type-2 marker) (Fig SM6 and Fig SM7). The linkage groups were visualized by r/qtl (*20*). The numbering of linkage groups is the same as the previous reference genome (*1*).

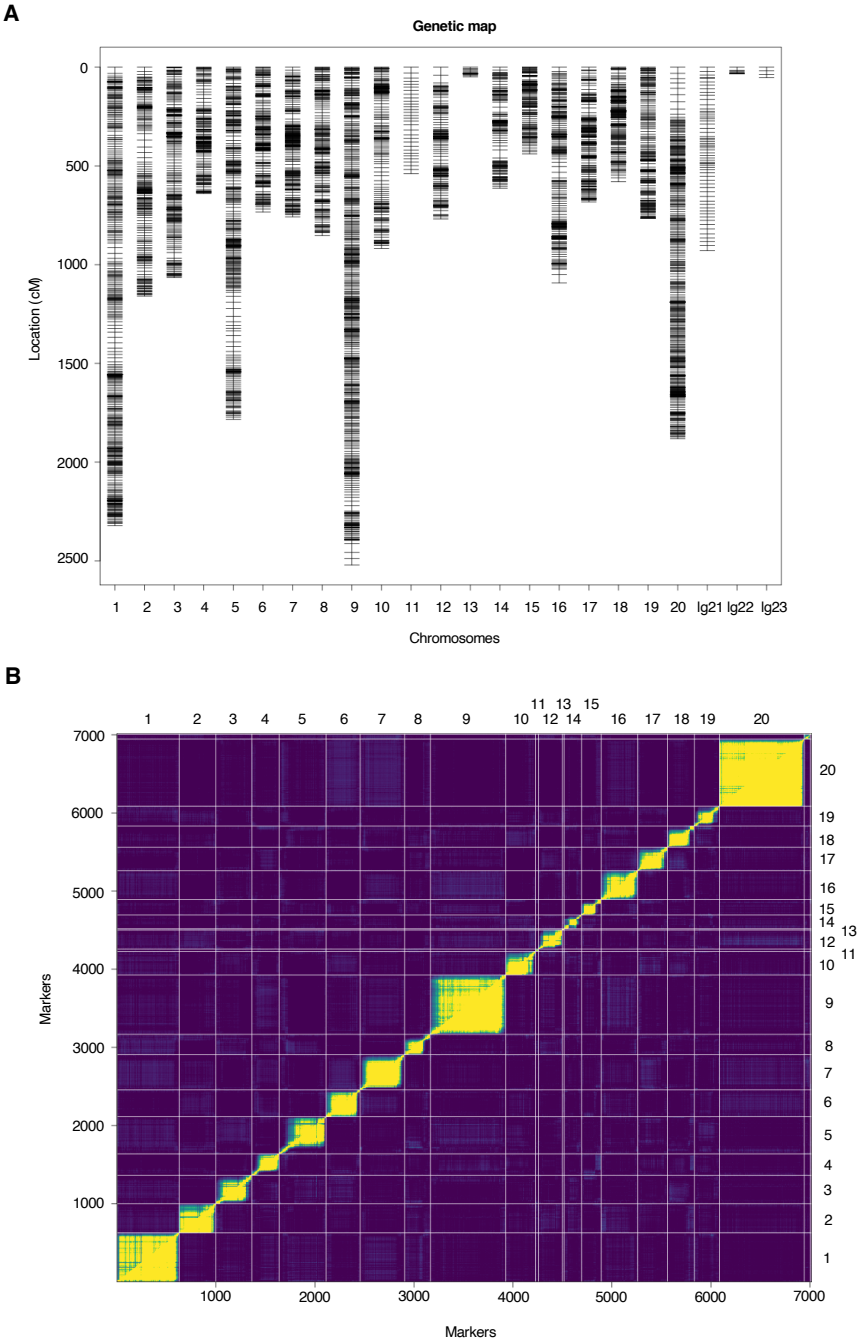

Fig. SM6. P1-map created by P1 heterozygous markers. (A) Contig positions in P1-map. (B) Estimated recombination fractions (upper-left triangle) against LOD score (low-right triangle) plotted by R/qtl (*20*).

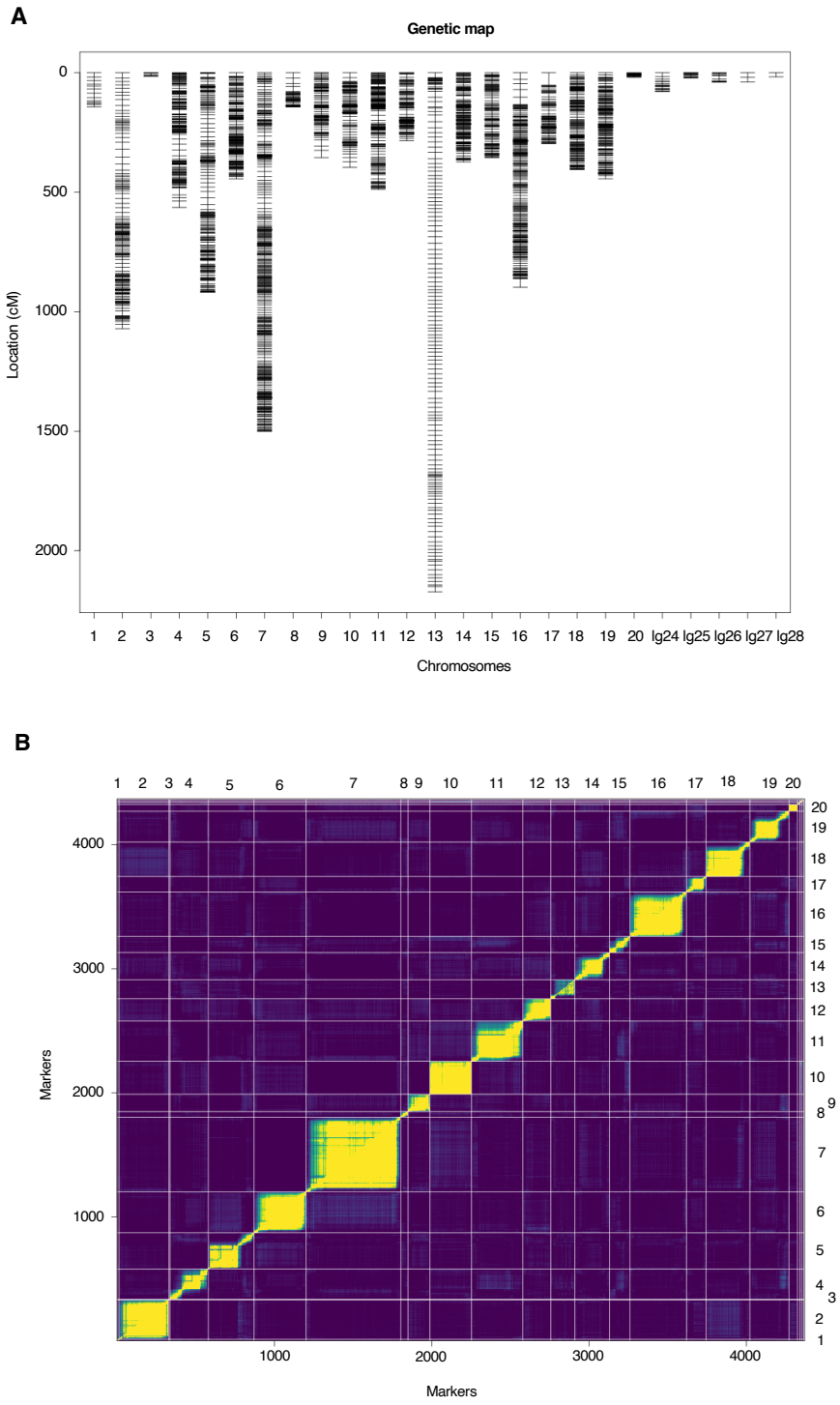

Fig. SM7. P2-map created by P2 heterozygous markers. (A) Contig positions in P2-map. (B) Estimated recombination fractions (upper-left triangle) against LOD score (low-right triangle) plotted by R/qtl (*20*).

Integration of two parental-specific linkage maps to chromosome-scaled physical genome sequence. Based on a matrix derived from those contigs that are shared between P1- and P2-map, linkage groups (Table SM9), the contigs were anchored and linearly ordered as pseudo-chromosomes. During the anchoring and ordering process, we identified contigs whose markers were allocated to different linkage groups. Such contigs were further divided into sub-contigs to ensure that they were

not allocated to different pseudo-chromosomes. To divide the contigs at the proper position, we followed a previously proposed method (*1*). During this procedure, 34 genes including 61 transcript variants were cut and removed. The previously proposed method (*1*) was followed to finally generate the pseudo physical genome sequence composed of 20 pseudo-chromosomes. To compare the newly generated pseudo-chromosomes with the one we constructed previously (*1*), we generated a dot plot by D-Genies (*21*) (Fig. SM8) and counted the anchored base pairs in the new pseudo-chromosomes (Table SM10). The resulting reference genome including unanchored contigs was uploaded to ENSEMBL (http://plants.ensembl.org/Dioscorea_rotundata/Info/Index; for early access http://staging-plants.ensembl.org/Dioscorea_rotundata/Info/Index).

Table SM9. A matrix of the number of the shared contigs between P1-map and P2-map. Linkage group (lg) 21-28 don't have the shared contigs.

		P2-map																								
		1	2	3	4	5	6	7	8	9	10	11	12	13	14	15	16	17	18	19	20	lg24	lg25	lg26	lg27	lg28
P1-map	1	5	2	1	2	0	3	2	0	0	3	2	1	0	1	0	5	0	2	0	1	0	0	0	0	0
	2	0	120	0	1	2	2	3	0	1	1	1	0	0	0	0	1	0	1	2	0	0	0	0	0	0
	3	0	2	3	1	0	3	9	0	1	0	0	0	0	0	0	1	0	1	2	0	0	0	0	2	2
	4	0	0	0	84	2	0	1	0	0	0	0	0	0	3	0	1	0	0	0	0	0	0	0	0	0
	5	0	1	0	3	135	2	3	0	1	1	2	2	0	4	1	0	1	1	2	0	0	0	0	0	0
	6	0	0	0	0	3	128	2	0	1	1	2	0	0	1	0	2	0	0	2	0	0	0	0	0	0
	7	0	2	0	1	2	2	199	0	1	1	3	0	0	0	1	1	0	0	3	0	0	0	0	0	0
	8	0	0	0	1	1	4	1	24	0	0	0	0	0	0	1	4	1	2	1	0	9	0	0	0	0
	9	0	1	0	0	2	4	4	0	71	4	1	0	0	2	1	5	1	0	1	0	0	0	0	0	0
	10	0	1	0	0	0	0	1	0	0	93	1	1	0	1	1	0	1	0	0	0	0	6	0	0	0
	11	0	0	0	0	0	0	1	0	0	0	8	0	0	0	0	0	0	1	0	0	0	0	0	0	0
	12	0	0	0	0	2	0	1	0	0	2	2	75	1	0	1	2	0	5	0	0	0	0	0	0	0
	13	0	0	0	0	0	0	1	0	0	0	0	0	5	0	0	0	0	0	0	0	0	0	0	0	0
	14	0	0	0	2	1	1	1	0	0	2	0	0	1	66	0	0	1	0	1	1	0	0	0	0	0
	15	0	0	0	0	0	0	0	0	1	0	1	0	0	2	42	2	0	0	1	0	0	0	0	0	0
	16	0	1	0	0	2	0	2	0	2	0	1	1	0	0	0	126	1	1	0	0	0	0	0	0	0
	17	0	0	0	1	2	1	1	0	0	0	1	0	1	1	1	2	60	0	0	0	0	0	0	0	0
	18	0	1	0	0	0	2	1	0	0	1	2	1	0	0	0	0	0	118	0	0	0	0	0	0	0
	19	0	1	0	0	0	1	2	0	0	0	2	0	4	0	0	0	0	1	100	0	0	0	0	0	0
	20	1	8	0	0	5	1	4	0	0	5	6	2	3	2	0	4	1	1	0	39	0	0	3	0	0
	lg21	0	0	0	0	0	0	1	0	0	0	0	0	1	0	0	0	0	0	0	0	0	0	0	0	0
	lg22	0	0	0	0	0	0	0	0	0	0	6	0	0	0	0	0	0	0	0	0	0	0	0	0	0
	lg23	0	0	0	0	0	0	0	0	0	0	1	0	0	0	0	0	0	0	0	0	0	0	0	0	0

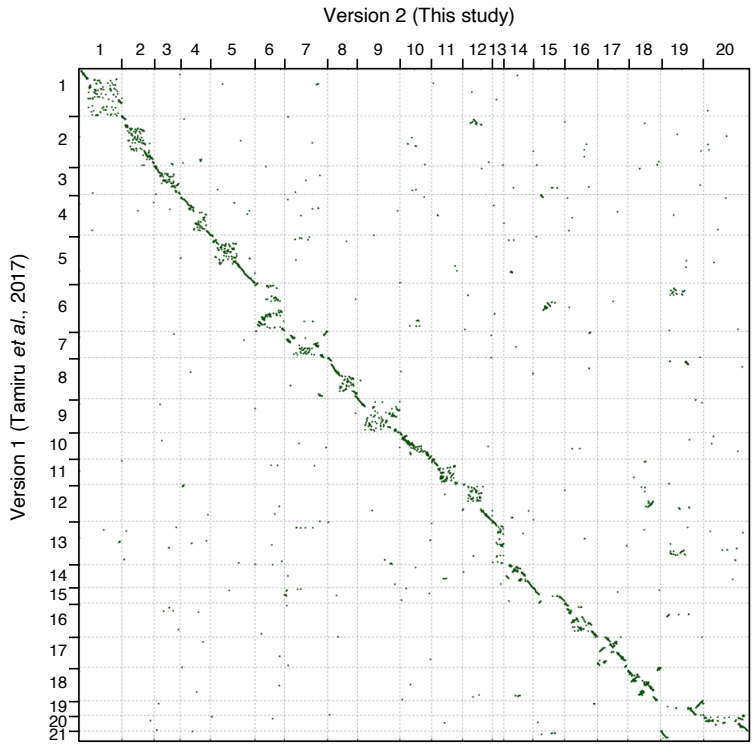

Fig. SM8. Dot plot of the new pseudo-chromosomes (Ver.2) against the previous pseudo-chromosomes (Ver.1) (*1*).

Table SM10. Comparison of old (Ver. 1) (*1*) and new (Ver. 2) pseudo-chromosomes.

Feature	Ver. 1	Ver. 2
Number of Pseudo Chr.	21	20
Total size of Pseudo Chr. (Mbp)	456.67	491.97
Total not 'N' Mbp	406.1	487.31
Total size of Pseudo Chr. / Total scaffold* (%)	76.9	84.9
Complete BUSCOs (%)	82.8%	82.3%

*In version2, the contigs were used instead of scaffolds.

S3. Genetic diversity analysis

S3.1 Whole genome re-sequencing of Guinea yam accessions

For genetic diversity analysis, we selected 333 accessions of *D. rotundata* maintained at IITA, Nigeria, representing the genetic diversity of Guinea yam landraces and improved lines of West Africa. We extracted DNA from the dried leaves of each accession of *D. rotundata* following the proposed method (*1*). Libraries for PE short reads were constructed using an Illumina TruSeq DNA LT Sample Prep Kit (Illumina). The PE library was sequenced on the Illumina Nextseq500 or Hiseq4000 platform. Finally, P1 (TDr04/219) and P2 (TDr97/777) parents used to anchor the contigs and the reference individual "TDr96_F1" were added to 333 accessions. Therefore, we totally used 336 accessions for this analysis. Summary of sequences and alignments are given in Table S1.

S3.2 Quality control, alignment, and SNP calling

We used FaQCs v2.08 (*9*) and prinseq-lite v0.20.4 lite (*16*) for quality control. We used the same parameters provided in supplementary text S2.3, but both of paired and unpaired reads were aligned to the new reference genome by bwa mem command in BWA (*6*) with option "-a". After sorting the BAM files, the VCF file was generated by SAMtools (*7*) mpileup command with options "-t DP,AD,SP -B -Q 18 -C 50", and variants were called by BCFtools (*17*) call command with options "-P 0 -v -m -f GQ,GP". Low quality variants were rejected by BCFtools (*17*) view command with options "-i 'INFO/MQ>=40 & INFO/MQ0F<=0.1 & AVG(GQ)>=5'". Regarding variants having low read depth (<8) or low genotype quality score (<5) as missing, we filtered the SNPs having high missing rate (>=0.3) across all samples and only retained bi-allelic SNPs on the pseudo-chromosomes.

S3.3 Unsupervised clustering analysis

6,124,093 SNPs were retained in 336 Guinea yam accessions through the pipeline of supplementary text S3.2. The VCF file including 336 Guinea yam accessions was converted into GDS file by gdsfmt v1.20 R package implemented in SNPRelate v1.18 (*22*) R package. After that, we ran SNPRelate (*22*), without filtering, for PCA (principal component analysis). Moreover, we used sNMF v1.2 (*23*) for admixture analysis of the 336 Guinea yam accessions. To choose the best value of *K*, we launched sNMF (*23*) for each value of *K* from 2 to 20 (Fig. SM9). We couldn't find the best value of *K* based on cross-entropy criterion, but we defined five cluster for convenience.

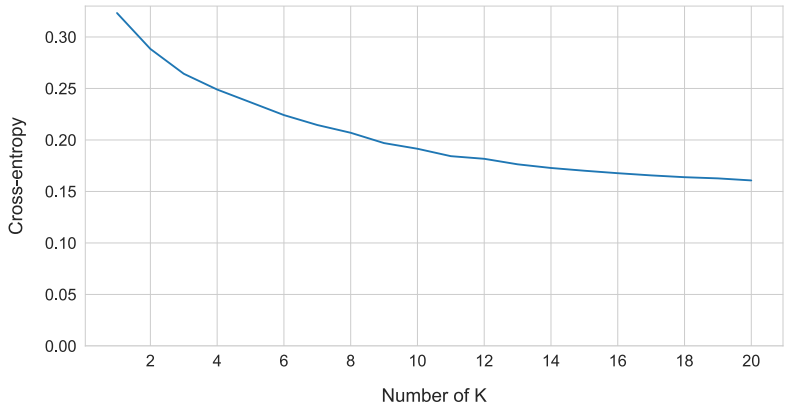

Fig. SM9. Cross-entropy values from *K*=1 to *K*=20 for admixture analysis.

S3.4 Polymorphism and ploidy of nuclear genomes

Heterozygosity ratio and unique alleles. First, we calculated the heterozygosity ratio in each accession (Fig. S1). We defined the heterozygosity ratio as follows:

$$(Heterozygosity\ ratio) = \frac{S}{L}$$

where S is the number of heterozygous SNPs and L is the number of mapped sites in an accession. Second, we counted the unique alleles in each cluster (Fig. S2). An allele is considered unique if it only exits in a cluster even when the allele is a singleton in all accessions.

Flow cytometry.
Ploidy level was estimated by flow cytometry using a Partec Ploidy Analyzer (Sysmex Partec, Gorlitz, Germany). Fully developed fresh young leaves were sampled and chopped (ca. 5mm x 5mm) using a razor blade with 0.4 mL nuclear extraction buffer (solution A of a high-resolution kit; Sysmex Partec, Gorlitz, Germany). The suspension was filtered through a nylon filter (50-μm mesh), and the extracted nuclei were stained with 4′,6-diamino-2-phenylindole solution. After let stand for 5 min at room temperature, the sample was applied for ploidy analyzer at a rate of 5–20 nuclei/s. The DNA index (DI) of each accession was calculated based on the relative amount of DNA in nuclei at the G1 stage compared with that of internal standard. Rice (*Oryza sativa* L.) was used as an internal standard for calibration of the measurements. Flow cytometry was repeated two or three times with different leaf samples to confirm the DI of each accession. The ploidy levels of each accession were determined by comparing their DI with that of the diploid accession, "TDr1673", for which the chromosome number was confirmed microscopically as 2n = 40. (Table S1)

Summary statistics in population genetics. After removing the accessions of cluster 1 due to triploid accessions, we imputed missing genotypes by BEAGLE v4.1 (*24*) with default options. After that, summary statistics in population genetics were calculated (Table S2). Firstly, we counted segregating sites and singletons in 308 Guinea yam accessions. We also estimated Watterson's θ ($\hat{\theta}_W$) (*25*), pairwise nucleotide diversity ($\hat{\theta}_\pi$) (*26*), and Tajima's D (*27*) in the same dataset. We defined $\hat{\theta}_W$ as follows:

$$\hat{\theta}_W = \frac{S}{a * \bar{L}}$$

where a is equal to:

$$a = \sum_{i=1}^{n-1} \frac{1}{i}$$

and $\bar{L}$ is number of average mapped sites in a population and n is a number of sequences.
Also, we defined that $\hat{\theta}_\pi$ is equal to:

$$\hat{\theta}_\pi = \frac{1}{\bar{L}} \frac{n}{n-1} \frac{\sum_{i<j} k_{ij}}{n(n-1)/2}$$

where $\bar{L}$ is the number of average mapped sites in a population, n is the number of sequences, and k_{ij} is number nucleotide differences between the ith and jth sequences.

S4. Phylogenomic analysis of African yam

S4.1 Data preparation

For phylogenomic analysis of African yam, we used 308 Guinea yam accessions sequenced in the present study excluding cluster 1 triploid accessions, as well as 80 *D. rotundata*, 29 *D. abyssinica*, 21 Western *D. praehensilis*, and 18 Cameroonian *D. praehensilis* as sequenced in the previous study (*28*) using two accessions of Asian species *D. alata* as an outgroup (Table SM11). In terms of the samples sequenced in the previous study (*28*), we only used the sequences whose species labels matched a species predicted by the admixture analysis in the previous study (*28*). Also, we removed the sequences which were labeled as hybrid in the previous study *(28*). Two sequences of *D. alata* for outgroup were downloaded from NCBI (Table SM11). Subsequently, read quality control, alignment, and SNP calling of those 458 sequences were conducted through the same pipeline in supplementary text S3.2. Except for the Neighbor-joining (NJ) tree (*29*) (supplementary text S4.2), we only used the SNPs which have the missing rate less than 0.3 in each targeted species. When the markers are polarized by *D. alata*, the SNPs at the positions where the alleles of *D. alata* were not completely fixed or where either of the sequences of *D. alata* was missing were filtered out.

S4.2 Neighbor-joining tree

Before constructing NJ tree (*29*), we only retained SNPs at positions having no missing data across all five species (*D. rotundata*, *D. abyssinica*, Western *D. praehensilis*, Cameroonian *D. praehensilis*, and *D. alata*). When we converted the VCF file including the rest SNPs to multi-FASTA file, heterozygous SNPs were converted to IUPAC code to characterize them as ambiguous markers. To construct the NJ tree (*29*), we ran MEGA X v10.1.8 (*30*) using the rest 463,293 SNPs. In MEGA X (*30*), the bootstrap value was set to 100 and the other parameters were set as default. Finally, the resulting file was drawn by GGTREE v2.0.4 (*31*).

S4.3 Inference of the evolutionary history of wild *Dioscorea* species by ∂a∂i

To elucidate the evolutionary relationships of the three wild *Dioscorea* species, *D. abyssinica* (indicated as A), Western *D. praehensilis* (P). Cameroonian *D. praehensilis* (C) that are closely related to *D. rotundata*, we adopted ∂a∂i analysis (*32*), which allows estimating evolutionary parameters from an unfolded site frequency spectrum. The joint unfolded site frequency spectrum was calculated from the 17,532 polarized SNPs, and it was projected down to 25 chromosomes in each species.

First, three phylogenetic models, {{A, P}, C}, {{C, P}, A}, {{C, A}, P} were tested without considering migration among the species. The parameter bounds of each population size was ranged from 10^{-3} to 100, and those of each divergence time was ranged from 0 to 3, which were suggested

in the manual of ∂a∂i (https://dadi.readthedocs.io/en/latest/). The grid size was set to (40, 50, 60). The maximum iteration for an inference was set to 20. Randomly perturbing the initial values by 'perturb_params' function in ∂a∂i (*32*), the parameters were inferred 100 times. On these conditions, the {{A, P}, C} had the highest likelihood out of the three models (Table. S3).

Based on the assumption that {{A, P}, C} is the true evolutionary relationship among the three wild *Dioscorea* species, the evolutionary parameters were re-estimated by ∂a∂i (*32*) allowing symmetric migration among the species. Then, the parameter bounds of each symmetric migration rate were ranged from 0 to 20, which was also suggested in the manual of ∂a∂i. The parameters were inferred 100 times by ∂a∂i (*32*) with the different initial parameters, and the best parameter set was selected based on Akaike information criterion.

S4.4 Inference of the evolutionary history of wild *Dioscorea* species by fastsimcoal2

To complement our result and to exactly replicate the previous report (*28*), fastsimcoal2 (*33*) used in the previous study (*28*) was also used to test these three models ({{A, P}, C}, {{C, P}, A}, and {{C, A}, P}). Until the step of SNP calling, we basically followed our own pipeline in supplementary text S3.2 based on the reference genome version 1 including the unanchored contigs (*1*) to be consistent with the previous study (*28*). The misclassified samples excluding hybrids were genetically re-classified by the admixture analysis following the previous study (*28*). The threshold of missing rate across all samples was set to 0.25 which was proposed in the previous study (*28*). The resulting SNPs through our pipeline were 87,672, which were less than the number of the analyzed SNPs in the coalescent simulation of the previous study (*28*). Therefore, we skipped the down sampling of the SNPs to 100,000 unlike the previous study (*28*). In other steps and the parameter bounds for the coalescent simulation by fastsimcoal2 (*33*), we exactly followed the method proposed in the previous study (*28*) using the same version of fastsimcoal2 (*33*).

S5. Test of hybrid origin

S5.1 Site frequency spectrum polarized by two candidate progenitors of Guinea yam

We focused on the allele frequencies of 388 *D. rotundata* sequences including 80 in the previous study (*28*) at the SNPs positioned over the entire genome and are oppositely fixed in the two candidate progenitors. The SNP set was generated by following supplementary text S4.1. Based on this SNP set, 144 SNPs were oppositely fixed in the two candidate progenitors across all pseudo-chromosomes, and allele frequencies of these 144 SNPs were calculated and plotted.

S5.2 Inference of the domestication history of Guinea yam by ∂a∂i

To infer the domestication history of Guinea yam, ∂a∂i (*32*) was adopted. Using the 15,461 polarized SNPs generated by following supplementary text S4.1, three phylogenetic models, {{A, R}, P}, {{P, R}, A}, {{A, R}, {P, R}} (hypothesis 1, 2, and 3 in Fig. 2A, respectively) were tested with considering symmetric migration among the species. The parameter bound for the admixed proportion from *D. abyssinica* was ranged from 0 to 1. The other parameter bounds were same to supplementary text S4.3. The maximum iteration for an inference was set to 20. The parameters were inferred 100 times by ∂a∂i (32).

S5.3 Comparison of F_{ST} among three African yams in each chromosome

F_{ST} (*34*) among the three species (*D. abyssinica*, (Western) *D. praehensilis*, and *D. rotundata*) was calculated in each chromosome. We estimated the F_{ST} from:

$$F_{ST} = \frac{H_T - H_S}{H_T}$$

where H_T and H_S are the expected heterozygosity in total population and sub-divided population, respectively, and are equal to:

$$H_T = 2\frac{f_{A1} + f_{A2}}{2}(1 - \frac{f_{A1} + f_{A2}}{2})$$
$$H_S = \frac{2f_{A1}(1 - f_{A1}) + 2f_{A2}(1 - f_{A2})}{2} = f_{A1}(1 - f_{A1}) + f_{A2}(1 - f_{A2})$$

where f_{A1} and f_{A2} are the allele frequencies in each population (*34*). Finally, the calculated F_{ST} were averaged in each chromosome.

S6. Haplotype network analysis of whole plastid genome

The sample set used to construct the haplotype network of the whole plastid genome was same to that in NJ tree (supplementary text S4.2). We aligned the 458 whole genome sequences, together with the whole plastid genome of *D. rotundata* (*1*), to the newly improved reference genome of *D. rotundata*. We basically followed the pipeline described in supplementary text S3.2 for quality control and alignment. Because plastid genome is haploid, "--ploidy" option was set to 1 in BCFtools call command (*17*) when SNPs were called. Singleton SNPs were removed as unreliable markers. Also, SNPs having more than one low quality genotype (GQ<127) across the samples were also removed as unreliable markers. We didn't allow any missing. Finally, haplotype network was constructed by median joining network algorithm (*35*) implemented in PopART (*36*).

S7. Inference of the change of population size

To understand the change of population sizes, demographic history of African yams was re-inferred by ∂a∂i (*32*) allowing migration. By fixing the parameters predicted in supplementary text S5.2 except for the population sizes, we re-estimated each population size at the start and end points after the emergence of those species assuming an exponential increase/decrease of the population sizes. The parameter bounds of population sizes were ranged from 10^{-3} to 100, and the maximum iteration for an inference was set to 20. The parameters were inferred 100 times by ∂a∂i (*32*).

S8. Exploration of extensive introgression from *Dioscorea* species

To explore the possibility of multiple introgression from both parental wild yams, f_4 statistic (*37*, *38*) was applied to the four clusters of *D. rotundata* excluding cluster 1 triploid accessions. Here, f_4 statistic needs four populations; P_{R1} is the first cluster of *D. rotundata*; P_{R2} is the second cluster of *D. rotundata*; P_P is a population of (Western) *D. praehensilis*; P_A is a population of *D. abyssinica*. We estimated $\hat{f}_4(P_{R1}, P_{R2}, P_P, P_A)$ from the following formula using a sliding window analysis with window size of 250Kbp and step size of 25Kbp:

$$\hat{f}_4(P_{R1}, P_{R2}, P_P, P_A) = (\hat{p}_{R1} - \hat{p}_{R2})(\hat{p}_P - \hat{p}_A)$$

where $\hat{p}_j$ is the observed allele frequency in a window in population P_j.

In most windows, $\hat{f}_4$ is close to zero, which means that the window has a concordant genealogy because the two clusters of *D. rotundata* have a small genetic distance (B in Fig. SM10). However, if these two clusters of *D. rotundata* have a large genetic distance and if one of or both populations have a small genetic distance from a wild *Dioscorea* species, then $\hat{f}_4$ skews from 0. Therefore, a locus having a skewed $\hat{f}_4$ has a discordant genealogy (C or D in Fig. SM10). For P_P (the population of *D. praehensilis*) and P_A (the population of *D. abyssinica*), the samples sequenced in the previous study (*28*) were used (Table SM11), and the dataset was prepared by following supplementary text S4.1. As the first screening, all possible combinations of the clusters of *D. rotundata*, excluding accessions in cluster 1, were used for P_{R1} and P_{R2} (Fig. S11). In this analysis, we identified an extensive introgression around the *SWEETIE* gene (4.00Mbp ~ 4.15Mbp on chromosome 17). Because cluster 2 and 5 have the same genealogy pattern around the *SWEETIE* gene, we merged them into one population (P_{25}) and we used this as P_{R1}. Because cluster 4 has the opposite genealogy pattern

to P_{25} around the *SWEETIE* gene, we used P_4 as P_{R2}. As a result, $\hat{f}_4(P_{25}, P_4, P_P, P_A)$ was calculated for the second screening (Fig. 4). If a locus has $|Z(f_4)|>5$, we regarded it as an outlier (red dots in Fig. 4B). To reveal relationship of the *D. rotundata* accessions around the *SWEETIE* gene, Neighbor-Net was constructed by SplitsTree v5.1.4 (*39*) using 308 *D. rotundata* accessions excluding the accessions in cluster 1, 29 *D. abyssinica,* and 21 *D. praehensilis*. A total 458 variants from 4.00Mbp to 4.15Mbp region on chromosome 17 were converted to multi-FASTA. At that time, heterozygous genotypes were converted to IUPAC code.

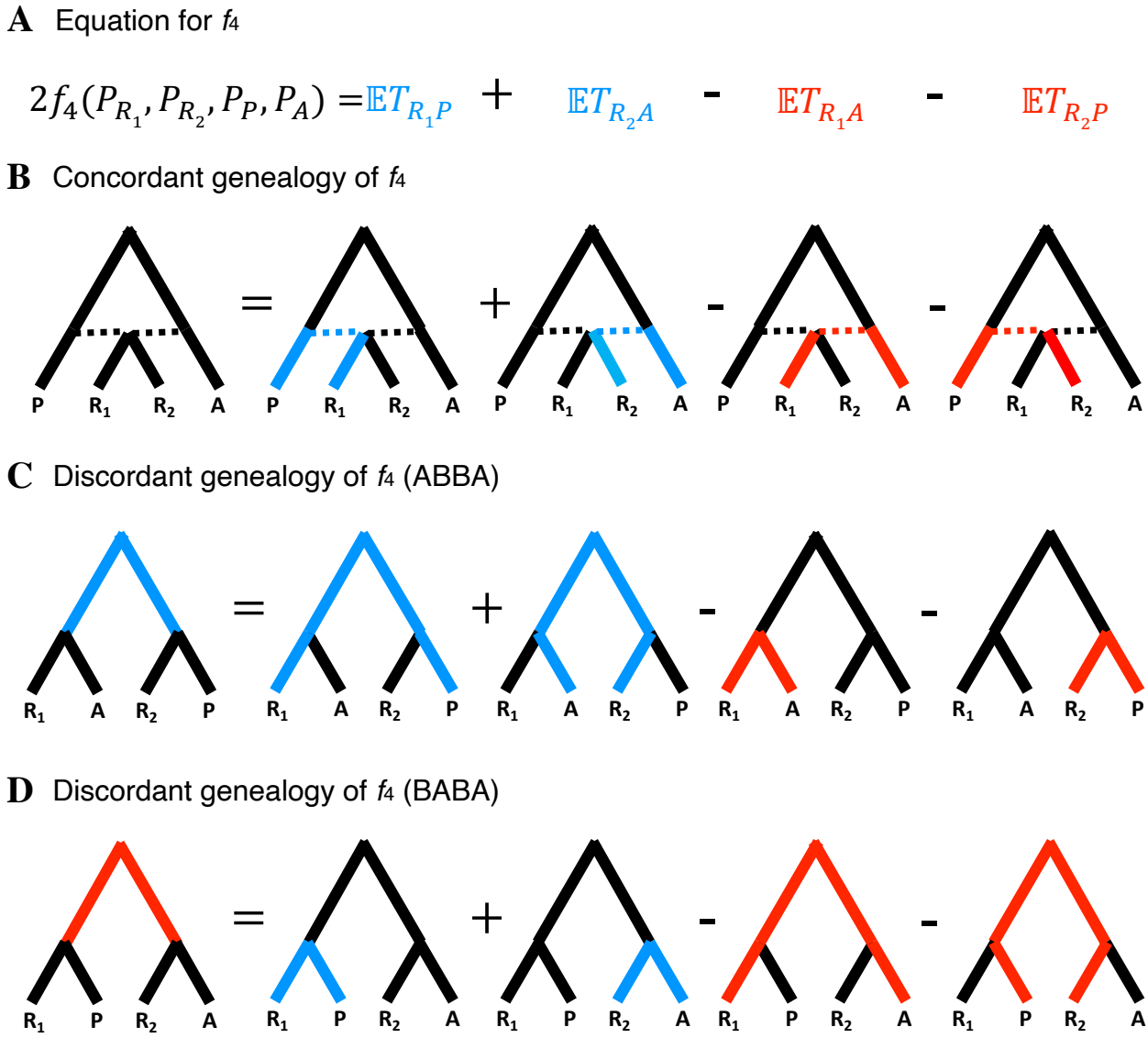

Fig. SM10. Schematic explanation how f_4 behaves in this study adapted from (*38*). "A" represents the population of *D. abyssinica*. "P" represents the population of *D. praehensilis*. "R1" represents the first populations of *D. rotundata*. "R2" represents the second populations of *D. rotundata*.

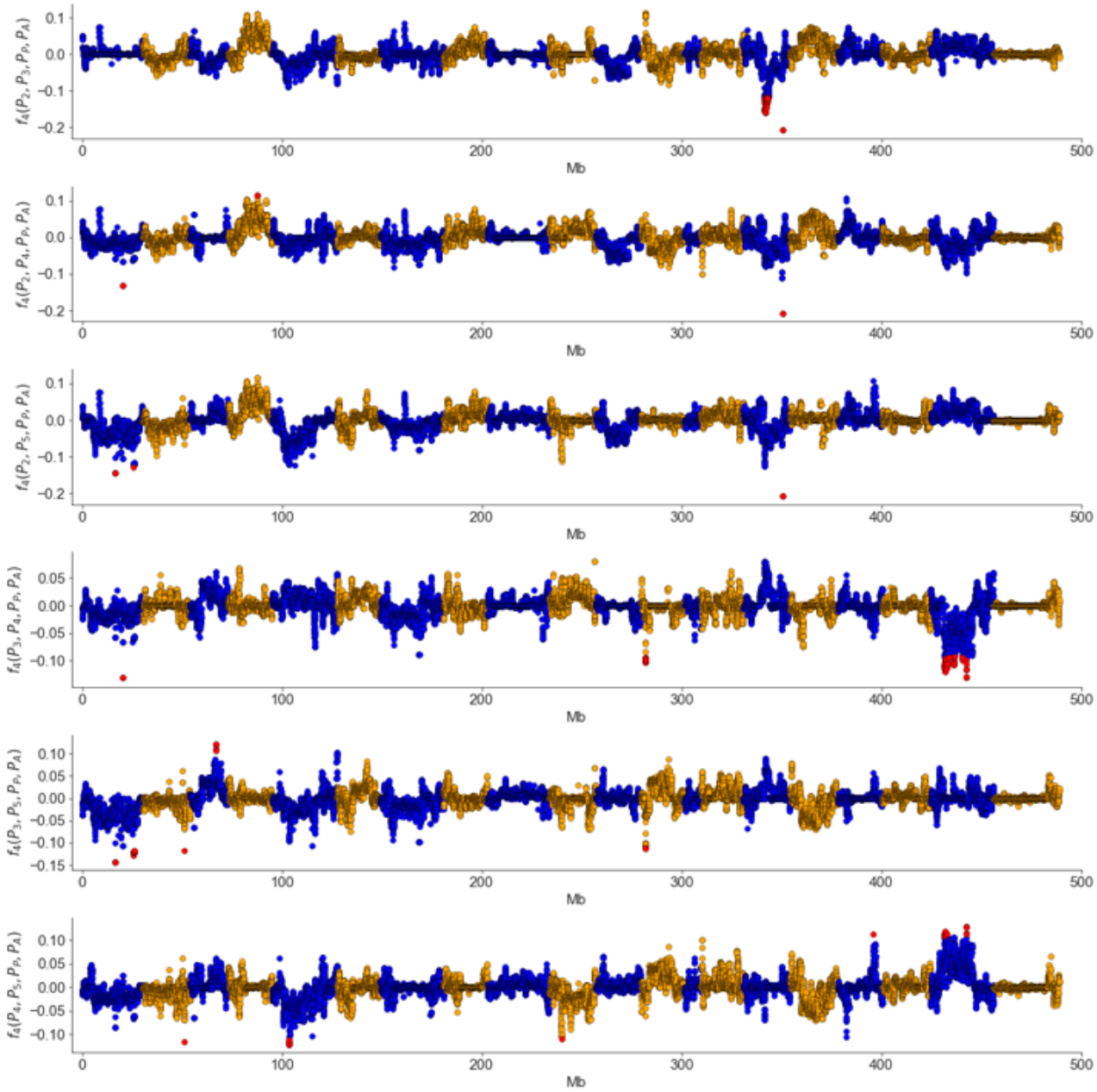

Fig. S11. f_4 in all possible combinations of clusters excluding cluster1. Population P*i* means a population of the cluster *i*.

1. M. Tamiru, S. Natsume, H. Takagi, B. White, H. Yaegashi, M. Shimizu, K. Yoshida, A. Uemura, K. Oikawa, A. Abe, N. Urasaki, H. Matsumura, P. Babil, S. Yamanaka, R. Matsumoto, S. Muranaka, G. Girma, A. Lopez-Montes, M. Gedil, R. Bhattacharjee, M. Abberton, P. L. Kumar, I. Rabbi, M. Tsujimura, T. Terachi, W. Haerty, M. Corpas, S. Kamoun, G. Kahl, H. Takagi, R. Asiedu, R. Terauchi, Genome sequencing of the staple food crop white Guinea yam enables the development of a molecular marker for sex determination. *BMC Biol.* **15**, 86 (2017).
2. W. De Coster, S. D'Hert, D. T. Schultz, M. Cruts, C. Van Broeckhoven, NanoPack: visualizing and processing long-read sequencing data. *Bioinformatics.* **34**, 2666–2669 (2018).
3. M. Kolmogorov, J. Yuan, Y. Lin, P. A. Pevzner, Assembly of long, error-prone reads using repeat graphs. *Nat. Biotechnol.* **37**, 540–546 (2019).

4. F. A. Simão, R. M. Waterhouse, P. Ioannidis, E. V. Kriventseva, E. M. Zdobnov, BUSCO: assessing genome assembly and annotation completeness with single-copy orthologs. *Bioinformatics*. **31**, 3210–3212 (2015).
5. B. J. Walker, T. Abeel, T. Shea, M. Priest, A. Abouelliel, S. Sakthikumar, C. A. Cuomo, Q. Zeng, J. Wortman, S. K. Young, A. M. Earl, Pilon: An Integrated Tool for Comprehensive Microbial Variant Detection and Genome Assembly Improvement. *PLoS ONE.* **9**, e112963 (2014).
6. H. Li, R. Durbin, Fast and accurate short read alignment with Burrows-Wheeler transform. *Bioinformatics*. **25**, 1754–1760 (2009).
7. H. Li, B. Handsaker, A. Wysoker, T. Fennell, J. Ruan, N. Homer, G. Marth, G. Abecasis, R. Durbin, The Sequence Alignment/Map format and SAMtools. *Bioinformatics*. **25**, 2078–2079 (2009).
8. M. J. Roach, S. A. Schmidt, A. R. Borneman, Purge Haplotigs: allelic contig reassignment for third-gen diploid genome assemblies. *BMC Bioinform.* **19**, 460 (2018).
9. C.-C. Lo, P. S. G. Chain, Rapid evaluation and quality control of next generation sequencing data with FaQCs. *BMC Bioinform.* **15**, 366 (2014).
10. D. Kim, B. Langmead, S. L. Salzberg, HISAT: a fast spliced aligner with low memory requirements. *Nat. Methods*. **12**, 357–360 (2015).
11. M. Pertea, G. M. Pertea, C. M. Antonescu, T.-C. Chang, J. T. Mendell, S. L. Salzberg, StringTie enables improved reconstruction of a transcriptome from RNA-seq reads. *Nat. Biotechnol.* **33**, 290–295 (2015).
12. Y. S. Niknafs, B. Pandian, H. K. Iyer, A. M. Chinnaiyan, M. K. Iyer, TACO produces robust multisample transcriptome assemblies from RNA-seq. *Nat. Methods.* **14**, 68–70 (2017).
13. H. Iwata, O. Gotoh, Benchmarking spliced alignment programs including Spaln2, an extended version of Spaln that incorporates additional species-specific features. *Nucleic Acids Res.* **40**, e161 (2012).
14. P. Jones, D. Binns, H.-Y. Chang, M. Fraser, W. Li, C. McAnulla, H. McWilliam, J. Maslen, A. Mitchell, G. Nuka, S. Pesseat, A. F. Quinn, A. Sangrador-Vegas, M. Scheremetjew, S.-Y. Yong, R. Lopez, S. Hunter, InterProScan 5: genome-scale protein function classification. *Bioinformatics*. **30**, 1236–1240 (2014).
15. C. Camacho, G. Coulouris, V. Avagyan, N. Ma, J. Papadopoulos, K. Bealer, T. L. Madden, BLAST+: architecture and applications. *BMC Bioinformatics*. **10**, 421 (2009).
16. R. Schmieder, R. Edwards, Quality control and preprocessing of metagenomic datasets. *Bioinformatics*. **27**, 863–864 (2011).
17. H. Li, A statistical framework for SNP calling, mutation discovery, association mapping and population genetical parameter estimation from sequencing data. *Bioinformatics*. **27**, 2987–2993 (2011).
18. A. R. Quinlan, I. M. Hall, BEDTools: a flexible suite of utilities for comparing genomic features. *Bioinformatics*. **26**, 841–842 (2010).
19. Y. Wu, P. R. Bhat, T. J. Close, S. Lonardi, Efficient and Accurate Construction of Genetic Linkage Maps from the Minimum Spanning Tree of a Graph. *PLoS Genet.* **4**, e1000212 (2008).
20. K. W. Broman, H. Wu, S. Sen, G. A. Churchill, R/qtl: QTL mapping in experimental crosses. *Bioinformatics*. **19**, 889–890 (2003).
21. F. Cabanettes, C. Klopp, D-GENIES: dot plot large genomes in an interactive, efficient and simple way. *PeerJ*. **6**, e4958 (2018).
22. X. Zheng, D. Levine, J. Shen, S. M. Gogarten, C. Laurie, B. S. Weir, A high-performance computing toolset for relatedness and principal component analysis of SNP data. *Bioinformatics*. **28**, 3326–3328 (2012).
23. E. Frichot, F. Mathieu, T. Trouillon, G. Bouchard, O. François, Fast and Efficient Estimation of Individual Ancestry Coefficients. *Genetics*. **196**, 973–983 (2014).

24. S. R. Browning, B. L. Browning, Rapid and Accurate Haplotype Phasing and Missing-Data Inference for Whole-Genome Association Studies By Use of Localized Haplotype Clustering. *Am. J. Hum. Genet.* **81**, 1084–1097 (2007).
25. G. A. Watterson, On the number of segregating sites in genetical models without recombination. *Theor. Popul. Biol.* **7**, 256–276 (1975).
26. M. Nei, F. Tajima, DNA polymorphism detectable by restriction endonucleases. *Genetics*. **97**, 145–167 (1981).
27. F. Tajima, Statistical method for testing the neutral mutation hypothesis by DNA polymorphism. *Genetics*. **123**, 585–595 (1989).
28. N. Scarcelli, P. Cubry, R. Akakpo, A. C. Thuillet, J. Obidiegwu, M. N. Baco, E. Otoo, B. Sonké, A. Dansi, G. Djedatin, C. Mariac, M. Couderc, S. Causse, K. Alix, H. Chaïr, O. François, Y. Vigouroux, Yam genomics supports West Africa as a major cradle of crop domestication. *Sci. Adv.* **5**, eaaw1947 (2019).
29. N. Saitou, M Nei, The neighbor-joining method: a new method for reconstructing phylogenetic trees. *Mol. Biol. Evol.* **4**, 406–425 (1987).
30. S. Kumar, G. Stecher, M. Li, C. Knyaz, K. Tamura, MEGA X: Molecular Evolutionary Genetics Analysis across Computing Platforms. *Mol. Biol. Evol.* **35**, 1547–1549 (2018).
31. G. Yu, D. K. Smith, H. Zhu, Y. Guan, T. T. Lam, GGTREE: an R package for visualization and annotation of phylogenetic trees with their covariates and other associated data. *Methods Ecol. Evol.* **8**, 28–36 (2017).
32. R. N. Gutenkunst, R. D. Hernandez, S. H. Williamson, C. D. Bustamante, Inferring the Joint Demographic History of Multiple Populations from Multidimensional SNP Frequency Data. *PLoS Genet*. **5**, e1000695 (2009).
33. L. Excoffier, I. Dupanloup, E. Huerta-Sánchez, V. C. Sousa, M. Foll, Robust demographic Inference from genomic and SNP data. *PLoS Genet*. **9**, e1003905 (2013).
34. S. Wright, The genetical structure of populations. *Ann. Eugen.* **15**, 323–354 (1951).
35. H. J. Bandelt, P. Forster, A. Röhl, Median-joining networks for inferring intraspecific phylogenies. *Mol. Biol. Evol*. **16**, 37–48 (1999).
36. J. W. Leigh, D. Bryant, popart: full-feature software for haplotype network construction. *Methods Ecol. Evol.* **6**, 1110–1116 (2015).
37. D. Reich, K. Thangaraj, N. Patterson, A. L. Price, L. Singh, Reconstructing Indian population history. *Nature.* **461**, 489–494 (2009).
38. B. M. Peter, Admixture, Population Structure, and F-Statistics. *Genetics.* **202**, 1485–1501 (2016).
39. D. H. Huson, D. Bryant, Application of Phylogenetic Networks in Evolutionary Studies. *Mol. Biol. Evol.* **23**, 254–267 (2006).

Table S1. All sequence information of Guinea yam accessions

Sample			Fastq size		Aligned bam information				Sequence platform	Cluster	Accession No.
Name	IITA name	Ploidy level	Original (Gbp)	Filtered (Gbp)	Aligned (Gbp)	Unmapped (Gbp)	Coverage (%)	Depth			
TDr04_219	TDr04_219	-	38.26	33.10	25.95	0.32	89.7	49.93	MiSeq, HiSeq4000, GAIIx	-	DRR208404,DRR208405,DRR063085
TDr97_777	TDr97_777	-	50.20	43.48	32.72	0.94	89.8	62.90	MiSeq,HiSeq4000,NextSeq500,GAIIx	-	DRR063127,DRR208406,DRR045130-7,DRR063111
TDr96_F1	TDr96_F1	-	16.77	21.34	17.66	0.04	90.3	33.74	MiSeq	-	DRR027644
DRS_001	TDr2946A	2	12.70	11.32	9.28	0.12	86.4	18.53	HiSeq4000	-	DRR208876
DRS_002	TDr1489A	2	8.09	7.02	5.27	0.05	79.0	11.51	HiSeq4000	-	DRR208761
DRS_003	TDr2284A	2	15.28	13.18	9.50	0.16	87.3	18.78	HiSeq4000,NextSeq500	-	DRR208762,DRR208884
DRS_004	TDr1499A	2	13.65	11.70	8.55	0.13	86.9	16.99	HiSeq4000,NextSeq500	cluster2	DRR208763,DRR208885
DRS_006	TDr1509A	2	13.47	11.10	8.13	0.16	86.6	16.19	HiSeq4000,NextSeq500	-	DRR208764,DRR208886
DRS_007	TDr1510A	2	12.30	10.19	7.81	0.14	87.2	15.46	HiSeq4000,NextSeq500	-	DRR208765,DRR208887
DRS_009	TDr3782A	2	13.23	11.21	7.62	0.14	89.0	14.77	HiSeq4000,NextSeq500	-	DRR208766,DRR208888
DRS_010	TDr1533A	2	13.31	11.18	8.32	0.17	86.6	16.58	HiSeq4000,NextSeq500	cluster3	DRR208767,DRR208889
DRS_011	TDr1543A	2	13.22	11.17	7.33	0.18	86.7	14.59	HiSeq4000,NextSeq500	cluster3	DRR208768,DRR208890
DRS_012	TDr1858C	2	14.22	12.56	9.99	0.11	85.6	20.14	HiSeq4000	-	DRR208877
DRS_013	TDr1576A	2	12.81	11.47	9.91	0.15	87.4	19.57	HiSeq4000,NextSeq500	cluster3	DRR208769,DRR208891
DRS_014	TDr1585A	2	14.01	11.78	7.58	0.15	87.1	15.02	HiSeq4000,NextSeq500	-	DRR208770,DRR208892
DRS_015	TDr1585C	2	15.02	12.78	8.02	0.16	87.0	15.92	HiSeq4000,NextSeq500	cluster2	DRR208771,DRR208893
DRS_016	TDr1598A	3	13.80	11.74	7.54	0.43	86.6	15.02	HiSeq4000,NextSeq500	cluster1	DRR208772,DRR208894
DRS_017	TDr1622A	2	12.71	10.81	7.02	0.15	86.8	13.96	HiSeq4000,NextSeq500	cluster2	DRR208773,DRR208895
DRS_018	TDr1628A	2	8.08	7.00	5.24	0.05	77.7	11.65	HiSeq4000	-	DRR208774
DRS_019	TDr1631C	2	15.29	13.62	11.34	0.17	87.8	22.31	HiSeq4000,NextSeq500	-	DRR208775,DRR208896
DRS_020	TDr1649A	2	12.64	10.83	7.22	0.15	86.4	14.42	HiSeq4000,NextSeq500	cluster3	DRR208776,DRR208897
DRS_021	TDr1650B	2	12.42	10.56	8.18	0.15	87.0	16.23	HiSeq4000,NextSeq500	cluster2	DRR208777,DRR208898
DRS_022	TDr1653A	2	12.68	10.86	6.92	0.13	86.5	13.80	HiSeq4000,NextSeq500	-	DRR208778,DRR208899
DRS_023	TDr1655A	2	12.24	10.36	6.42	0.16	86.0	12.89	HiSeq4000,NextSeq500	cluster5	DRR208779,DRR208900
DRS_024	TDr1663A	2	13.69	11.55	8.68	0.17	86.9	17.22	HiSeq4000,NextSeq500	-	DRR208780,DRR208901
DRS_025	TDr1686A	2	12.58	11.14	8.11	0.12	88.2	15.87	HiSeq4000,NextSeq500	cluster4	DRR208781,DRR208902
DRS_026	TDr1707A	2	13.51	11.93	9.04	0.15	88.7	17.58	HiSeq4000,NextSeq500	-	DRR208782,DRR208903
DRS_027	TDr1709A	2	16.91	15.10	12.04	0.22	86.1	24.13	HiSeq4000	-	DRR208878
DRS_028	TDr1711A	2	7.64	6.65	5.15	0.04	80.3	11.06	HiSeq4000	-	DRR208783
DRS_029	TDr3872A	2	12.61	11.23	8.95	0.15	87.1	17.73	HiSeq4000,NextSeq500	-	DRR208784,DRR208904
DRS_030	TDr1732A	2	13.95	12.38	9.83	0.16	88.2	19.23	HiSeq4000,NextSeq500	cluster4	DRR208785,DRR208905
DRS_031	TDr1735A	2	13.02	11.59	7.48	0.15	86.5	14.93	HiSeq4000,NextSeq500	-	DRR208786,DRR208906
DRS_032	TDr2029A	2	11.77	10.51	7.03	0.14	85.7	14.16	HiSeq4000,NextSeq500	-	DRR208787,DRR208907
DRS_033	TDr1760A	2	11.42	9.96	8.19	0.08	87.9	16.09	HiSeq4000,NextSeq500	cluster4	DRR208788,DRR208908
DRS_034	TDr1763C	2	16.32	14.06	11.22	0.09	87.7	22.07	HiSeq4000,NextSeq500	cluster4	DRR208789,DRR208909
DRS_035	TDr1804A	2	12.63	10.98	8.56	0.10	87.7	16.85	HiSeq4000,NextSeq500	cluster4	DRR208790,DRR208910
DRS_036	TDr1775A	3	11.44	9.96	7.52	0.27	87.5	14.82	HiSeq4000,NextSeq500	cluster1	DRR208791,DRR208911
DRS_037	TDr1798A	2	8.14	7.02	5.25	0.05	79.8	11.35	HiSeq4000	-	DRR208792
DRS_038	TDr1805A	2	12.60	11.14	9.16	0.08	86.7	18.22	HiSeq4000,NextSeq500	-	DRR208793,DRR208912
DRS_039	TDr1807A	3	11.35	10.05	7.67	0.26	87.6	15.11	HiSeq4000,NextSeq500	cluster1	DRR208794,DRR208913
DRS_040	TDr1829A	2	11.26	9.77	7.35	0.10	85.9	14.77	HiSeq4000,NextSeq500	cluster3	DRR208795,DRR208914
DRS_041	TDr1850A	2	11.35	10.03	8.20	0.09	86.5	16.36	HiSeq4000,NextSeq500	cluster5	DRR208796,DRR208915
DRS_042	TDr1899A	2	13.90	12.01	7.89	0.15	86.8	15.68	HiSeq4000,NextSeq500	-	DRR208797,DRR208916
DRS_043	TDr1922C	2	7.43	6.29	4.76	0.05	79.7	10.31	HiSeq4000	-	DRR208798
DRS_044	TDr1935A	2	11.67	10.14	7.65	0.14	86.7	15.23	HiSeq4000,NextSeq500	-	DRR208799,DRR208917
DRS_045	TDr2608A	2	12.53	10.86	7.99	0.18	86.7	15.91	HiSeq4000,NextSeq500	-	DRR208800,DRR208918
DRS_046	TDr2041B	2	14.19	12.52	10.16	0.16	86.6	20.26	HiSeq4000,NextSeq500	-	DRR208801,DRR208919

DRS_047	TDr2121A	2	11.61	10.17	7.98	0.10	86.5	15.93	HiSeq4000,NextSeq500	cluster3	DRR208802,DRR208920
DRS_048	TDr2155A	3	13.17	11.47	7.84	0.41	87.6	15.44	HiSeq4000,NextSeq500	cluster1	DRR208803,DRR208921
DRS_049	TDr2159A	2	11.28	9.93	7.79	0.20	86.9	15.46	HiSeq4000,NextSeq500	-	DRR208804,DRR208922
DRS_050	TDr2161C	3	12.97	11.43	7.79	0.42	87.7	15.33	HiSeq4000,NextSeq500	cluster1	DRR208805,DRR208923
DRS_051	TDr2167A	3	11.86	10.44	7.60	0.36	87.6	14.98	HiSeq4000,NextSeq500	cluster1	DRR208806,DRR208924
DRS_053	TDr2207A	2	11.41	9.81	7.75	0.08	86.2	15.51	HiSeq4000,NextSeq500	-	DRR208807,DRR208925
DRS_054	TDr2210A	2	10.71	9.52	7.15	0.14	85.5	14.42	HiSeq4000	cluster2	DRR208879
DRS_055	TDr3311B	2	13.88	12.29	9.69	0.18	88.2	18.96	HiSeq4000,NextSeq500	cluster4	DRR208808,DRR208926
DRS_056	TDr2262C	2	11.63	10.36	8.70	0.19	86.5	17.36	HiSeq4000,NextSeq500	-	DRR208809,DRR208927
DRS_057	TDr2320A	2	8.95	7.70	6.41	0.08	82.2	13.46	HiSeq4000,NextSeq500	cluster3	DRR208928
DRS_058	TDr2484A	2	12.62	11.21	9.03	0.13	86.8	17.96	HiSeq4000,NextSeq500	-	DRR208810,DRR208929
DRS_059	TDr2973A	2	11.15	9.46	7.31	0.10	83.6	15.11	HiSeq4000,NextSeq500	-	DRR208930
DRS_060	TDr2425B	2	10.38	8.92	7.47	0.07	86.5	14.89	HiSeq4000,NextSeq500	-	DRR208931
DRS_061	TDr2427B	3	12.28	11.17	8.47	0.38	87.9	16.63	HiSeq4000,NextSeq500	cluster1	DRR208811,DRR208932
DRS_062	TDr2435A	2	7.61	6.72	5.79	0.05	83.2	12.01	HiSeq4000	cluster3	DRR208812
DRS_063	TDr2439A	2	10.11	9.03	7.64	0.06	86.7	15.22	HiSeq4000,NextSeq500	-	DRR208813,DRR208933
DRS_064	TDr2453A	2	13.41	12.08	9.89	0.16	87.3	19.56	HiSeq4000,NextSeq500	-	DRR208814,DRR208934
DRS_065	TDr2491A	2	13.74	12.46	10.23	0.15	87.1	20.28	HiSeq4000,NextSeq500	-	DRR208815,DRR208935
DRS_066	TDr3569A	2	15.47	14.08	10.11	0.15	88.6	19.70	HiSeq4000,NextSeq500	cluster4	DRR208816,DRR208936
DRS_067	TDr2533C	2	11.24	10.03	7.83	0.12	85.5	15.80	HiSeq4000	cluster3	DRR208880
DRS_068	TDr2554A	3	16.37	14.91	9.73	0.57	88.7	18.93	HiSeq4000,NextSeq500	cluster1	DRR208817,DRR208937
DRS_069	TDr2575A	2	8.89	8.03	7.04	0.09	87.2	13.94	HiSeq4000,NextSeq500	-	DRR208938
DRS_070	TDr2636B	2	8.88	7.89	6.48	0.09	85.9	13.02	HiSeq4000,NextSeq500	-	DRR208939
DRS_071	TDr2674A	2	8.56	7.72	6.81	0.07	86.7	13.56	HiSeq4000,NextSeq500	cluster5	DRR208940
DRS_072	TDr2713A	2	13.04	11.77	9.86	0.13	86.9	19.57	HiSeq4000,NextSeq500	-	DRR208818,DRR208941
DRS_073	TDr1684A	2	15.55	13.87	11.48	0.08	87.0	22.79	HiSeq4000,NextSeq500	-	DRR208819,DRR208942
DRS_074	TDr2948A	2	11.67	10.50	8.98	0.07	87.6	17.69	HiSeq4000,NextSeq500	-	DRR208820,DRR208943
DRS_075	TDr2965A	2	12.16	10.98	9.64	0.10	88.4	18.83	HiSeq4000,NextSeq500	-	DRR208944
DRS_076	TDr2968A	2	9.19	8.21	6.80	0.09	84.5	13.88	HiSeq4000	-	DRR208881
DRS_077	TDr2975A	2	11.13	9.98	8.47	0.08	87.6	16.69	HiSeq4000,NextSeq500	cluster4	DRR208945
DRS_078	TDr4067A	3	12.84	11.59	8.41	0.43	87.9	16.52	HiSeq4000,NextSeq500	cluster1	DRR208821,DRR208946
DRS_079	TDr2577A	2	13.00	11.79	8.57	0.14	88.8	16.65	HiSeq4000,NextSeq500	cluster2	DRR208822,DRR208947
DRS_080	TDr3325A	2	13.81	12.10	10.14	0.19	87.3	20.05	HiSeq4000,NextSeq500	cluster3	DRR208823,DRR208948
DRS_081	TDr3470A	2	9.57	8.49	6.66	0.11	84.7	13.58	HiSeq4000	-	DRR208882
DRS_082	TDr3436A	2	9.71	6.42	5.15	0.05	80.8	11.01	HiSeq4000,NextSeq500	-	DRR208824,DRR208949
DRS_083	TDr3447B	2	12.45	9.46	6.69	0.11	85.7	13.47	HiSeq4000,NextSeq500	-	DRR208825,DRR208950
DRS_084	TDr3519A	3	16.08	14.55	9.55	0.49	88.7	18.59	HiSeq4000,NextSeq500	cluster1	DRR208826,DRR208951
DRS_085	TDr3527A	2	7.58	6.63	5.61	0.05	82.7	11.71	HiSeq4000	cluster5	DRR208827
DRS_086	TDr2276A	2	15.07	13.13	9.37	0.16	87.8	18.43	HiSeq4000,NextSeq500	-	DRR208828,DRR208952
DRS_087	TDr3576A	2	17.05	13.22	10.14	0.16	85.7	20.42	HiSeq4000,NextSeq500	-	DRR208953
DRS_088	TDr3624B	2	9.68	7.84	6.21	0.09	83.3	12.86	HiSeq4000,NextSeq500	cluster5	DRR208954
DRS_089	TDr2503A	2	10.12	9.07	7.50	0.09	85.6	15.11	HiSeq4000	-	DRR208883
DRS_090	TDr3678A	2	15.57	13.52	9.08	0.16	87.4	17.93	HiSeq4000,NextSeq500	-	DRR208829,DRR208955
DRS_091	TDr3719A	2	10.51	8.83	7.13	0.12	85.5	14.39	HiSeq4000,NextSeq500	-	DRR208956
DRS_092	TDr3828B	2	14.56	13.01	9.32	0.14	88.0	18.29	HiSeq4000,NextSeq500	-	DRR208830,DRR208957
DRS_093	TDr3842A	2	16.92	14.92	12.90	0.15	88.5	25.16	HiSeq4000,NextSeq500	-	DRR208958
DRS_094	TDr3863A	2	12.26	10.95	9.22	0.08	87.0	18.29	HiSeq4000,NextSeq500	-	DRR208831,DRR208959
DRS_095	TDr3955C	2	12.58	11.25	9.49	0.13	86.8	18.86	HiSeq4000,NextSeq500	-	DRR208832,DRR208960
DRS_096	TDr2090B	2	11.97	10.73	8.40	0.14	86.5	16.77	HiSeq4000,NextSeq500	cluster5	DRR208833,DRR208961
DRS_097	TDr1772A	2	11.77	10.45	7.60	0.17	86.4	15.17	HiSeq4000,NextSeq500	-	DRR208834,DRR208962
DRS_098	TDr3357A	2	12.18	10.91	9.10	0.14	87.1	18.02	HiSeq4000,NextSeq500	cluster2	DRR208835,DRR208963

DRS_099	TDr4017A	2	13.05	11.46	8.35	0.21	86.8	16.59	HiSeq4000,NextSeq500	cluster3	DRR208836,DRR208964
DRS_100	TDr3623C	2	13.73	11.91	8.88	0.19	87.8	17.45	HiSeq4000,NextSeq500	cluster4	DRR208837,DRR208965
DRS_101	TDr4100A	2	13.31	11.67	9.37	0.18	87.1	18.57	HiSeq4000,NextSeq500	cluster5	DRR208838,DRR208966
DRS_102	TDr2826A	2	8.63	7.53	6.33	0.05	83.7	13.06	HiSeq4000	-	DRR208839
DRS_103	TDr4155A	2	10.98	9.61	7.67	0.15	87.4	15.14	HiSeq4000,NextSeq500	-	DRR208840,DRR208967
DRS_104	TDr4180A	2	11.13	9.80	7.41	0.17	86.1	14.87	HiSeq4000,NextSeq500	cluster5	DRR208841,DRR208968
DRS_106	TDr2042A	2	11.49	10.05	7.77	0.14	86.4	15.53	HiSeq4000,NextSeq500	-	DRR208842,DRR208969
DRS_165	TDr608	-	10.92	9.99	7.98	0.04	86.1	15.99	HiSeq4000	-	DRR208843
DRS_169	TDrFaketsa	-	13.01	11.98	9.39	0.07	85.2	19.00	HiSeq4000	-	DRR208844
DRS_177	TDrGbangu	-	11.57	10.54	8.17	0.05	84.2	16.74	HiSeq4000	-	DRR208845
DRS_208	TDr09/00362	-	9.01	8.25	6.58	0.04	83.7	13.57	HiSeq4000	-	DRR208846
DRS_211	TDr09/00799	-	10.73	9.84	7.82	0.04	85.3	15.83	HiSeq4000	-	DRR208847
DRS_212	TDrMeccakusa	-	8.41	7.64	6.18	0.03	84.4	12.64	HiSeq4000	-	DRR208848
DRS_213	TDr09/09132	-	9.97	9.14	7.40	0.04	85.3	14.98	HiSeq4000	-	DRR208849
DRS_220	TDrOjuiyawo	-	7.58	6.97	5.80	0.04	85.7	11.69	HiSeq4000	-	DRR208850
DRS_253	TDr2119	-	9.33	8.57	7.03	0.05	84.6	14.34	HiSeq4000	cluster2	DRR208851
DRS_259	TDr2347	-	9.94	9.10	6.98	0.05	85.1	14.16	HiSeq4000	cluster4	DRR208852
DRS_282	TDrOgoja	-	12.34	11.27	8.64	0.06	85.0	17.54	HiSeq4000	-	DRR208853
DRS_293	TDr10/00077	-	10.65	9.72	7.73	0.05	83.1	16.05	HiSeq4000	-	DRR208854
DRS_297	TDrGbongi	-	9.56	8.63	6.51	0.06	84.2	13.35	HiSeq4000	-	DRR208855
DRS_307	TDr10/00125	-	8.97	8.23	6.41	0.04	83.3	13.27	HiSeq4000	-	DRR208856
DRS_312	TDrLagos	-	7.85	7.13	5.63	0.05	82.8	11.73	HiSeq4000	-	DRR208857
DRS_318	TDrHembakwase	-	9.25	8.48	6.86	0.05	85.6	13.84	HiSeq4000	-	DRR208858
DRS_320	TDr89/02157	-	11.44	10.42	8.06	0.05	85.4	16.30	HiSeq4000	-	DRR208859
DRS_322	TDr97/00632	-	8.64	7.92	6.19	0.05	82.3	12.98	HiSeq4000	-	DRR208860
DRS_324	TDr00/02405	-	11.07	10.00	7.70	0.05	84.4	15.74	HiSeq4000	-	DRR208861
DRS_325	TDr10/00013	-	10.25	9.28	7.26	0.06	84.0	14.90	HiSeq4000	-	DRR208862
DRS_326	TDr10/00048	-	8.99	8.28	6.81	0.04	84.6	13.90	HiSeq4000	-	DRR208863
DRS_327	TDr10/00179	-	9.13	8.29	6.55	0.05	83.5	13.53	HiSeq4000	-	DRR208864
DRS_328	TDr10/00344	-	10.16	9.27	7.49	0.04	84.8	15.25	HiSeq4000	-	DRR208865
DRS_329	TDr10/00360	-	11.47	10.35	8.04	0.05	84.6	16.41	HiSeq4000	-	DRR208866
DRS_330	TDr10/00459	-	11.39	10.42	8.27	0.05	84.3	16.93	HiSeq4000	-	DRR208867
DRS_331	TDr10/00021	-	10.88	9.96	8.05	0.05	85.6	16.24	HiSeq4000	-	DRR208868
DRS_332	TDr89/02475	-	7.70	7.05	5.97	0.04	85.5	12.05	HiSeq4000	-	DRR208869
DRS_333	TDr89/02677	-	9.64	8.89	7.41	0.05	85.9	14.89	HiSeq4000	-	DRR208870
DRS_334	TDr96/00629	-	9.43	8.64	6.94	0.04	86.3	13.88	HiSeq4000	-	DRR208871
DRS_335	TDr96/01818	-	10.27	9.39	7.53	0.05	86.3	15.07	HiSeq4000	-	DRR208872
DRS_336	TDr99/02562	-	10.56	9.66	7.89	0.05	85.9	15.84	HiSeq4000	-	DRR208873
DRS_337	TDrAkwuchi	-	9.43	8.65	7.11	0.04	86.0	14.28	HiSeq4000	-	DRR208874
DRS_338	TDrDanacha	-	10.57	9.54	7.64	0.06	84.6	15.59	HiSeq4000	-	DRR208875
TDr_001	TDr1492	-	8.93	7.47	6.00	0.05	81.8	12.66	HiSeq4000	cluster3	DRR208563
TDr_002	TDr2262	-	6.84	5.83	4.90	0.04	82.5	10.24	HiSeq4000	-	DRR208564
TDr_003	TDr1533	-	7.61	6.25	5.00	0.05	78.6	10.98	HiSeq4000	cluster3	DRR208565
TDr_004	TDr1559	-	8.65	7.51	5.75	0.07	84.1	11.81	HiSeq4000	cluster4	DRR208566
TDr_005	TDr1577	-	8.77	7.73	6.22	0.22	81.6	13.14	HiSeq4000	cluster3	DRR208567
TDr_006	TDr1598	-	9.47	8.18	5.96	0.07	82.6	12.44	HiSeq4000	cluster2	DRR208568
TDr_007	TDr1615	-	8.48	7.14	5.27	0.16	81.3	11.17	HiSeq4000	cluster1	DRR208569
TDr_008	TDr1628	-	7.36	6.27	5.35	0.05	84.4	10.94	HiSeq4000	-	DRR208570
TDr_009	TDr1669	-	7.41	6.53	4.90	0.03	81.0	10.44	HiSeq4000	cluster2	DRR208571
TDr_010	TDr1707	-	9.48	8.20	6.20	0.06	84.4	12.68	HiSeq4000	-	DRR208572
TDr_011	TDr1717	-	8.85	7.98	6.13	0.05	82.2	12.88	HiSeq4000	-	DRR208573

TDr_012	TDr1763	-	8.62	7.76	6.09	0.05	82.2	12.79	HiSeq4000	-	DRR208574
TDr_013	TDr1769	-	10.00	8.55	6.64	0.23	85.9	13.34	HiSeq4000	cluster1	DRR208575
TDr_014	TDr1799	-	7.81	6.87	4.65	0.03	80.1	10.02	HiSeq4000	-	DRR208576
TDr_015	TDr1825	-	8.01	6.33	5.14	0.05	82.8	10.71	HiSeq4000	cluster4	DRR208577
TDr_016	TDr1876	-	9.56	8.32	6.48	0.21	85.7	13.06	HiSeq4000	cluster1	DRR208578
TDr_017	TDr1937	-	10.02	8.61	6.82	0.06	82.5	14.27	HiSeq4000	cluster3	DRR208579
TDr_018	TDr1939	-	9.87	8.09	6.57	0.05	83.1	13.64	HiSeq4000	cluster2	DRR208580
TDr_019	TDr1949	-	8.22	7.20	6.01	0.05	82.3	12.60	HiSeq4000	cluster2	DRR208581
TDr_020	TDr2015	-	8.50	7.36	5.69	0.17	84.8	11.58	HiSeq4000	cluster1	DRR208582
TDr_021	TDr2028	-	9.44	8.27	6.56	0.21	86.1	13.16	HiSeq4000	cluster1	DRR208583
TDr_022	TDr2038	-	7.88	6.63	5.50	0.03	83.7	11.35	HiSeq4000	-	DRR208584
TDr_023	TDr2050	-	10.79	8.75	6.75	0.08	81.8	14.23	HiSeq4000	-	DRR208585
TDr_024	TDr2059	-	10.16	8.59	6.95	0.06	85.6	14.03	HiSeq4000	cluster4	DRR208586
TDr_025	TDr2090	-	7.64	6.44	4.68	0.05	80.0	10.10	HiSeq4000	-	DRR208587
TDr_026	TDr2104	-	8.55	7.51	5.58	0.06	82.4	11.69	HiSeq4000	cluster4	DRR208588
TDr_027	TDr2110	-	9.84	8.65	6.78	0.21	85.7	13.66	HiSeq4000	cluster1	DRR208589
TDr_028	TDr2211	-	9.65	8.28	6.96	0.05	84.9	14.16	HiSeq4000	-	DRR208590
TDr_029	TDr2080	-	9.78	8.47	7.43	0.07	86.4	14.86	HiSeq4000	-	DRR208591
TDr_030	TDr2349	-	9.61	8.37	7.24	0.12	87.1	14.36	HiSeq4000	-	DRR208592
TDr_031	TDr2363	-	7.70	6.26	4.78	0.04	79.6	10.37	HiSeq4000	cluster2	DRR208593
TDr_032	TDr2406	-	10.33	9.01	7.83	0.06	85.2	15.86	HiSeq4000	cluster2	DRR208594
TDr_033	TDr2432	-	6.70	5.57	4.63	0.04	81.6	9.80	HiSeq4000	cluster2	DRR208595
TDr_034	TDr2439	-	9.57	7.96	6.11	0.06	82.3	12.80	HiSeq4000	-	DRR208596
TDr_035	TDr2458	-	6.94	5.83	5.02	0.04	84.7	10.24	HiSeq4000	cluster4	DRR208597
TDr_036	TDr2502	-	6.51	5.58	4.40	0.04	80.6	9.43	HiSeq4000	cluster5	DRR208598
TDr_037	TDr2581	-	9.62	8.34	7.10	0.10	86.3	14.20	HiSeq4000	cluster4	DRR208599
TDr_038	TDr2645	-	9.37	8.43	6.38	0.05	82.1	13.41	HiSeq4000	cluster3	DRR208600
TDr_039	TDr2674	-	7.65	6.59	5.29	0.04	82.2	11.10	HiSeq4000	cluster5	DRR208601
TDr_040	TDr2681	-	10.16	8.00	5.62	0.18	82.6	11.74	HiSeq4000	cluster1	DRR208602
TDr_041	TDr2683	-	9.63	6.47	4.97	0.09	78.7	10.89	HiSeq4000	cluster3	DRR208603
TDr_042	TDr2687	-	14.48	12.64	11.02	0.10	85.8	22.16	HiSeq4000	cluster3	DRR208604
TDr_043	TDr2701	-	9.63	7.79	6.41	0.06	84.9	13.03	HiSeq4000	-	DRR208605
TDr_044	TDr2724	-	10.14	6.15	4.76	0.10	81.4	10.10	HiSeq4000	-	DRR208606
TDr_045	TDr2694	-	8.06	7.00	6.09	0.05	84.8	12.40	HiSeq4000	cluster2	DRR208607
TDr_046	TDr2770	-	9.33	7.46	5.42	0.07	82.0	11.40	HiSeq4000	cluster4	DRR208608
TDr_047	TDr2936	-	10.09	8.13	5.54	0.09	80.8	11.83	HiSeq4000	-	DRR208609
TDr_048	TDr2965	-	10.01	8.76	7.15	0.06	82.9	14.90	HiSeq4000	-	DRR208610
TDr_049	TDr2973	-	13.14	11.33	8.88	0.28	86.9	17.64	HiSeq4000	cluster1	DRR208611
TDr_050	TDr3002	-	9.89	7.16	5.32	0.08	79.7	11.52	HiSeq4000	cluster3	DRR208612
TDr_051	TDr09/00064	-	8.52	5.64	4.47	0.07	78.5	9.82	HiSeq4000	-	DRR208613
TDr_052	TDr00/00362	-	8.13	7.27	6.03	0.05	84.4	12.32	HiSeq4000	-	DRR208614
TDr_053	TDr05/00589	-	12.86	11.09	9.63	0.08	85.1	19.53	HiSeq4000	-	DRR208615
TDr_054	TDr05/00632	-	7.87	6.74	5.29	0.06	80.3	11.37	HiSeq4000	-	DRR208616
TDr_055	TDr07/00157	-	8.49	7.10	6.10	0.05	83.8	12.57	HiSeq4000	-	DRR208617
TDr_056	TDr09/01932	-	8.47	7.64	6.48	0.05	84.9	13.16	HiSeq4000	-	DRR208618
TDr_057	TDr08/00092	-	8.19	6.98	5.69	0.08	81.2	12.08	HiSeq4000	-	DRR208619
TDr_058	TDr08/00108	-	9.46	8.61	7.02	0.06	85.2	14.21	HiSeq4000	-	DRR208620
TDr_059	TDr08/00122	-	8.98	8.09	6.63	0.09	85.1	13.44	HiSeq4000	-	DRR208621
TDr_061	TDr07/00732	-	10.10	9.16	7.79	0.06	85.1	15.80	HiSeq4000	-	DRR208622
TDr_062	TDr08/00207	-	8.83	7.27	6.13	0.07	84.7	12.49	HiSeq4000	-	DRR208623
TDr_063	TDr08/00617	-	9.35	8.46	7.02	0.06	84.6	14.32	HiSeq4000	-	DRR208624

TDr_064	TDr08/00799	-	11.50	10.44	8.23	0.55	85.7	16.58	HiSeq4000	-	DRR208625
TDr_065	TDr09/00325	-	14.08	12.80	10.42	0.09	85.9	20.96	HiSeq4000	-	DRR208626
TDr_066	TDr96/02433	-	14.54	13.18	10.40	0.15	85.7	20.95	HiSeq4000	-	DRR208627
TDr_067	TDr08/01344	-	15.31	14.04	11.58	0.10	86.3	23.16	HiSeq4000	-	DRR208628
TDr_068	TDr08/01024	-	6.51	5.79	4.89	0.04	84.5	9.99	HiSeq4000	-	DRR208629
TDr_069	TDr09/00023	-	7.32	6.64	5.55	0.05	83.3	11.51	HiSeq4000	-	DRR208630
TDr_070	TDr09/00028	-	9.46	8.59	6.94	0.08	83.9	14.26	HiSeq4000	-	DRR208631
TDr_071	TDr09/00056	-	6.89	5.97	5.12	0.07	84.2	10.49	HiSeq4000	-	DRR208632
TDr_072	TDr09/00070	-	8.13	7.31	6.06	0.05	84.1	12.44	HiSeq4000	-	DRR208633
TDr_073	TDr09/00091	-	7.81	7.01	5.93	0.05	83.7	12.23	HiSeq4000	-	DRR208634
TDr_074	TDr09/00104	-	8.88	8.12	6.80	0.05	85.6	13.71	HiSeq4000	-	DRR208635
TDr_075	TDr09/00108	-	8.73	7.55	6.06	0.06	83.7	12.50	HiSeq4000	-	DRR208636
TDr_076	TDr09/00114	-	7.66	6.38	5.28	0.04	82.9	11.01	HiSeq4000	-	DRR208637
TDr_077	TDr09/00125	-	8.29	7.12	5.83	0.05	82.8	12.16	HiSeq4000	-	DRR208638
TDr_078	TDr09/00134	-	5.53	4.51	3.74	0.03	79.3	8.14	HiSeq4000	-	DRR208639
TDr_079	TDr09/00248	-	9.28	8.19	6.26	0.04	82.5	13.09	HiSeq4000	-	DRR208640
TDr_080	TDr09/00350	-	8.54	7.59	6.36	0.03	83.2	13.18	HiSeq4000	-	DRR208641
TDr_081	TDr99/02789	-	5.88	4.71	3.79	0.02	78.9	8.29	HiSeq4000	-	DRR208642
TDr_082	TDr11/00263.1	-	5.02	4.25	3.73	0.04	82.3	7.81	HiSeq4000	-	DRR208643
TDr_083	TDr08/00161	-	7.23	6.40	5.24	0.06	82.7	10.93	HiSeq4000	-	DRR208644
TDr_084	TDr11/00799	-	13.32	11.78	9.92	0.07	88.2	19.40	HiSeq4000	-	DRR208645
TDr_085	TDr11/01041	-	8.72	7.87	6.55	0.06	86.2	13.12	HiSeq4000	-	DRR208646
TDr_086	TDr12/00474	-	8.47	7.56	5.81	0.06	83.1	12.07	HiSeq4000	-	DRR208647
TDr_087	TDr08/00146	-	8.96	7.98	6.64	0.04	86.6	13.23	HiSeq4000	-	DRR208648
TDr_088	TDrAlumaco	-	10.90	9.16	7.27	0.08	82.2	15.26	HiSeq4000	-	DRR208649
TDr_089	TDrHembakoase	-	6.40	5.79	5.03	0.04	84.8	10.23	HiSeq4000	-	DRR208650
TDr_090	TDr89/02665	-	11.01	9.62	8.24	0.08	86.3	16.48	HiSeq4000	-	DRR208651
TDr_091	TDr05/00046	-	8.32	7.32	5.35	0.06	80.9	11.41	HiSeq4000	-	DRR208652
TDr_092	TDr05/00432	-	8.65	7.33	6.39	0.08	83.8	13.16	HiSeq4000	-	DRR208653
TDr_093	TDr05/00389	-	5.53	4.60	3.74	0.03	79.4	8.14	HiSeq4000	-	DRR208654
TDr_094	TDr08/00023	-	7.24	6.10	5.23	0.05	82.7	10.93	HiSeq4000	-	DRR208655
TDr_095	TDr08/00115	-	7.82	6.64	5.84	0.08	85.6	11.78	HiSeq4000	-	DRR208656
TDr_096	TDr08/00197	-	9.05	7.81	6.66	0.04	85.4	13.45	HiSeq4000	-	DRR208657
TDr_097	TDr08/00974	-	6.68	5.61	4.93	0.04	85.2	9.99	HiSeq4000	-	DRR208658
TDr_098	TDr08/00896	-	8.32	7.54	6.41	0.04	85.1	12.99	HiSeq4000	-	DRR208659
TDr_099	TDr08/00841	-	11.21	9.83	7.43	0.09	85.0	15.09	HiSeq4000	-	DRR208660
TDr_100	TDr0836	-	7.49	6.51	4.97	0.06	79.3	10.82	HiSeq4000	-	DRR208661
TDr_101	TDr1686	-	10.98	9.61	8.03	0.18	86.9	15.96	HiSeq4000	cluster4	DRR208662
TDr_102	TDr3010	-	12.57	11.02	9.10	0.20	85.5	18.36	HiSeq4000	-	DRR208663
TDr_103	TDr3357	-	11.48	10.24	8.63	0.13	85.5	17.41	HiSeq4000	cluster2	DRR208664
TDr_104	TDr3408	-	11.17	9.98	8.39	0.13	86.1	16.81	HiSeq4000	-	DRR208665
TDr_105	TDr3430	-	9.58	8.42	7.19	0.14	86.3	14.38	HiSeq4000	-	DRR208666
TDr_106	TDr3519	-	9.88	8.82	6.71	0.29	85.9	13.48	HiSeq4000	cluster1	DRR208667
TDr_107	TDr3567	-	10.00	8.74	7.24	0.21	85.4	14.63	HiSeq4000	-	DRR208668
TDr_108	TDr3569	-	10.02	8.88	7.43	0.15	86.6	14.81	HiSeq4000	cluster4	DRR208669
TDr_109	TDr3579	-	8.82	7.71	5.91	0.30	85.8	11.88	HiSeq4000	cluster1	DRR208670
TDr_110	TDr3592	-	8.67	7.71	5.90	0.25	85.7	11.89	HiSeq4000	cluster1	DRR208671
TDr_111	TDr3610	-	10.20	9.02	7.46	0.17	86.6	14.86	HiSeq4000	cluster4	DRR208672
TDr_112	TDr3663	-	10.92	9.65	8.10	0.15	86.3	16.21	HiSeq4000	-	DRR208673
TDr_113	TDr3814	-	11.07	9.68	8.13	0.13	86.7	16.19	HiSeq4000	-	DRR208674
TDr_114	TDr3881	-	11.82	10.57	9.07	0.14	86.6	18.07	HiSeq4000	-	DRR208675

TDr_115	TDr4028	-	11.29	9.98	8.31	0.15	86.9	16.51	HiSeq4000	cluster4	DRR208676
TDr_116	TDr08/00641	-	11.86	10.49	8.78	0.18	85.5	17.72	HiSeq4000	-	DRR208677
TDr_117	TDr08/00756	-	9.84	8.60	7.29	0.18	85.4	14.73	HiSeq4000	-	DRR208678
TDr_118	TDr09/00131	-	9.12	7.95	6.77	0.12	84.9	13.76	HiSeq4000	-	DRR208679
TDr_119	TDr1569	-	8.97	7.66	6.44	0.10	85.2	13.05	HiSeq4000	-	DRR208680
TDr_120	TDr2931	-	9.01	7.86	6.83	0.10	85.1	13.84	HiSeq4000	cluster2	DRR208681
TDr_121	TDr2331.1	-	10.29	9.05	7.64	0.11	84.7	15.57	HiSeq4000	-	DRR208682
TDr_122	TDr1958	-	8.66	7.55	5.85	0.22	85.6	11.80	HiSeq4000	cluster1	DRR208683
TDr_123	TDr1905	-	11.62	10.34	8.58	0.18	85.2	17.37	HiSeq4000	cluster5	DRR208684
TDr_124	TDr1928	-	10.93	9.73	8.29	0.11	86.1	16.61	HiSeq4000	-	DRR208685
TDr_125	TDr3322	-	9.48	8.20	6.69	0.17	86.0	13.43	HiSeq4000	cluster4	DRR208686
TDr_126	TDr2048	-	9.82	8.67	7.23	0.15	85.5	14.59	HiSeq4000	-	DRR208687
TDr_127	TDr2126	-	10.08	8.85	7.33	0.14	85.8	14.75	HiSeq4000	-	DRR208688
TDr_128	TDr2249	-	9.38	8.29	6.23	0.23	85.5	12.59	HiSeq4000	cluster1	DRR208689
TDr_129	TDr2297	-	9.97	8.72	6.53	0.30	85.7	13.16	HiSeq4000	cluster1	DRR208690
TDr_130	TDr2342	-	11.08	9.61	7.73	0.16	86.2	15.48	HiSeq4000	cluster4	DRR208691
TDr_131	TDr2355	-	10.27	9.06	6.82	0.29	85.8	13.72	HiSeq4000	cluster1	DRR208692
TDr_132	TDr2564	-	8.75	7.63	6.49	0.13	85.7	13.07	HiSeq4000	-	DRR208693
TDr_133	TDr2698	-	10.55	9.12	7.30	0.16	85.7	14.72	HiSeq4000	cluster4	DRR208694
TDr_134	TDr2974	-	12.48	11.01	8.18	0.32	86.5	16.33	HiSeq4000	cluster1	DRR208695
TDr_135	TDr2975	-	9.23	8.17	6.20	0.24	85.6	12.50	HiSeq4000	cluster1	DRR208696
TDr_136	TDr3507	-	10.29	9.05	7.67	0.11	85.3	15.52	HiSeq4000	cluster2	DRR208697
TDr_137	TDr3006	-	10.03	8.85	7.68	0.12	85.1	15.59	HiSeq4000	cluster5	DRR208698
TDr_138	TDr08/00091	-	7.14	6.30	5.43	0.08	83.8	11.18	HiSeq4000	-	DRR208699
TDr_139	TDr08/01464	-	7.29	6.42	5.59	0.06	84.4	11.44	HiSeq4000	-	DRR208700
TDr_140	TDr08/00989	-	6.96	6.07	5.18	0.09	83.3	10.72	HiSeq4000	-	DRR208701
TDr_141	TDr09/00050	-	7.43	6.50	5.51	0.07	84.3	11.29	HiSeq4000	-	DRR208702
TDr_142	TDr09/00055	-	9.41	8.24	6.96	0.12	84.1	14.28	HiSeq4000	-	DRR208703
TDr_144	TDr09/00061	-	9.15	7.96	6.85	0.09	85.6	13.80	HiSeq4000	-	DRR208704
TDr_145	TDr09/00123	-	8.34	7.28	6.13	0.10	83.9	12.62	HiSeq4000	-	DRR208705
TDr_146	TDr09/00124	-	8.76	7.72	6.59	0.12	85.0	13.39	HiSeq4000	-	DRR208706
TDr_147	TDr09/00220	-	13.21	11.50	9.30	0.15	85.8	18.70	HiSeq4000	-	DRR208707
TDr_148	TDr09/00280.1	-	8.31	7.30	6.22	0.08	84.4	12.73	HiSeq4000	-	DRR208708
TDr_149	TDr09/00324	-	7.26	6.27	5.39	0.09	83.0	11.20	HiSeq4000	-	DRR208709
TDr_150	TDr08/01046	-	12.03	10.56	8.82	0.17	86.2	17.65	HiSeq4000	-	DRR208710
TDr_151	TDrAme	-	14.49	12.87	10.65	0.26	85.9	21.39	HiSeq4000	-	DRR208711
TDr_152	TDrUfenyi	-	12.72	11.18	9.11	0.33	86.6	18.15	HiSeq4000	-	DRR208712
TDr_153	TDr2365	-	12.77	11.26	9.52	0.21	85.4	19.25	HiSeq4000	cluster3	DRR208713
TDr_154	TDr1956	-	10.78	9.74	8.42	0.14	86.0	16.91	HiSeq4000	-	DRR208714
TDr_155	TDr2859	-	11.25	10.13	7.87	0.26	86.3	15.73	HiSeq4000	cluster1	DRR208715
TDr_156	TDr07/000732	-	9.98	8.91	7.72	0.06	85.1	15.66	HiSeq4000	-	DRR208716
TDr_157	TDr08/00764	-	10.88	9.73	8.33	0.09	85.7	16.77	HiSeq4000	-	DRR208717
TDr_158	TDr09/00155	-	9.60	8.63	7.45	0.08	86.5	14.86	HiSeq4000	-	DRR208718
TDr_159	TDr96/01724	-	8.68	7.74	6.72	0.08	84.9	13.65	HiSeq4000	-	DRR208719
TDr_160	TDr08/01287	-	8.54	7.67	6.68	0.06	85.6	13.47	HiSeq4000	-	DRR208720
TDr_161	TDr08/01090	-	9.38	8.41	7.29	0.05	84.9	14.82	HiSeq4000	cluster5	DRR208721
TDr_162	TDr2366	-	9.63	8.50	7.08	0.06	83.8	14.58	HiSeq4000	-	DRR208722
TDr_163	TDr2467	-	9.49	8.55	7.44	0.04	85.2	15.08	HiSeq4000	cluster2	DRR208723
TDr_164	TDr3003	-	9.10	8.14	7.08	0.09	85.2	14.35	HiSeq4000	-	DRR208724
TDr_165	TDr3294	-	8.55	7.66	6.69	0.06	85.9	13.44	HiSeq4000	-	DRR208725
TDr_166	TDr3338	-	11.19	10.03	8.66	0.11	85.2	17.54	HiSeq4000	cluster5	DRR208726

TDr_167	TDr3327	-	10.46	9.35	8.01	0.09	85.3	16.20	HiSeq4000	cluster2	DRR208727
TDr_168	TDr3647	-	10.31	9.19	7.90	0.09	87.4	15.61	HiSeq4000	-	DRR208728
TDr_169	TDr3965	-	11.68	10.48	9.05	0.08	85.5	18.26	HiSeq4000	cluster2	DRR208729
TDr_170	TDr3643	-	10.61	9.47	7.98	0.11	85.0	16.19	HiSeq4000	cluster5	DRR208730
TDr_171	TDr2630	-	8.74	7.71	6.49	0.06	85.7	13.08	HiSeq4000	-	DRR208731
TDr_172	TDr2984	-	11.08	9.72	7.93	0.13	83.2	16.44	HiSeq4000	-	DRR208732
TDr_173	TDr3682	-	9.72	8.74	7.58	0.05	85.1	15.38	HiSeq4000	cluster2	DRR208733
TDr_174	TDr3447	-	8.74	7.75	6.54	0.05	85.1	13.27	HiSeq4000	-	DRR208734
TDr_175	TDr4100	-	8.01	7.17	6.20	0.05	84.6	12.66	HiSeq4000	cluster5	DRR208735
TDr_176	TDr2009	-	10.11	9.05	7.88	0.07	85.2	15.95	HiSeq4000	cluster3	DRR208736
TDr_177	TDr2331.2	-	9.39	8.36	7.18	0.05	84.5	14.66	HiSeq4000	-	DRR208737
TDr_178	TDr3882	-	10.82	9.66	8.22	0.06	85.2	16.65	HiSeq4000	-	DRR208738
TDr_179	TDr2032	-	11.31	10.02	8.45	0.08	85.3	17.09	HiSeq4000	-	DRR208739
TDr_180	TDr11/01036	-	10.84	9.62	8.16	0.07	86.9	16.22	HiSeq4000	-	DRR208740
TDr_181	TDr09/00082	-	9.89	8.79	7.55	0.06	85.5	15.24	HiSeq4000	-	DRR208741
TDr_182	TDr09/00043	-	9.02	7.98	6.81	0.04	85.6	13.74	HiSeq4000	-	DRR208742
TDr_183	TDr09/00364	-	9.62	8.61	7.45	0.07	85.0	15.12	HiSeq4000	-	DRR208743
TDr_184	TDr08/00083	-	9.46	8.39	7.06	0.10	85.0	14.33	HiSeq4000	-	DRR208744
TDr_185	TDr08/01919	-	8.24	7.36	6.40	0.06	85.7	12.89	HiSeq4000	-	DRR208745
TDr_186	TDr09/00216	-	8.75	7.80	6.69	0.05	84.9	13.61	HiSeq4000	-	DRR208746
TDr_187	TDr11/00271	-	8.66	7.68	6.52	0.04	86.5	13.01	HiSeq4000	-	DRR208747
TDr_188	TDr95/18544	-	8.96	8.02	6.90	0.08	85.8	13.87	HiSeq4000	-	DRR208748
TDr_189	TDr11/00263.2	-	9.07	8.09	6.90	0.04	86.1	13.83	HiSeq4000	-	DRR208749
TDr_190	TDr11/00787	-	10.80	9.63	8.38	0.07	87.3	16.56	HiSeq4000	-	DRR208750
TDr_191	TDr09/00385	-	10.35	9.20	7.93	0.05	85.8	15.94	HiSeq4000	-	DRR208751
TDr_192	TDr08/00001	-	11.28	9.96	8.37	0.15	86.8	16.65	HiSeq4000	-	DRR208752
TDr_193	TDr09/00107	-	10.73	9.54	8.19	0.06	85.0	16.63	HiSeq4000	-	DRR208753
TDr_194	TDr08/00882	-	10.05	8.98	7.78	0.07	85.9	15.65	HiSeq4000	-	DRR208754
TDr_195	TDr08/010161	-	8.65	7.60	6.51	0.08	85.9	13.08	HiSeq4000	-	DRR208755
TDr_196	TDr08/01051	-	9.79	8.74	7.58	0.05	85.0	15.38	HiSeq4000	-	DRR208756
TDr_197	TDr08/00292	-	10.60	9.48	8.21	0.10	88.3	16.04	HiSeq4000	-	DRR208757
TDr_198	TDr94/01108	-	10.10	9.00	7.72	0.08	85.4	15.60	HiSeq4000	-	DRR208758
TDr_199	TDr09/00280.1	-	11.04	9.73	8.31	0.09	85.2	16.83	HiSeq4000	-	DRR208708
TDr_200	TDr87/00211	-	9.64	8.60	7.46	0.06	86.5	14.88	HiSeq4000	-	DRR208760

Table SM7. Summary of sequence alignment of mapping population

Sample		Fastq size		Aligned bam information				Sequence platform	Comment	Accession No.
Name	IITA name	Original (Gbp)	Filtered (Gbp)	Aligned (Gbp)	Unmapped (Gbp)	Coverage (%)	Depth			
TDr04_219	TDr04_219	38.26	33.10	17.15	0.32	82.8	35.73	MiSeq, HiSeq4000, GAIIx	MP2 family Mono parent	DRR208404,DRR208405,DRR063085
TDr97_777	TDr97_777	25.47	22.71	11.20	0.29	79.4	24.35	MiSeq,HiSeq4000,NextSeq500,GAIIx	MP2 family Male parent	DRR063127,DRR208406,DRR045130-7,DRR063111
MP2_001	MP2_001	8.20	7.14	4.20	1.00	76.9	9.43	HiSeq4000	-	DRR208407
MP2_002	MP2_002	6.42	5.61	3.45	0.64	73.2	8.13	HiSeq4000	-	DRR208408
MP2_003	MP2_003	5.95	5.11	2.92	0.87	71.6	7.03	HiSeq4000	-	DRR208409
MP2_004	MP2_004	7.13	6.24	3.90	0.70	74.8	8.99	HiSeq4000	-	DRR208410
MP2_005	MP2_005	9.75	8.49	4.59	1.56	75.2	10.53	HiSeq4000	-	DRR208411
MP2_006	MP2_006	7.90	7.01	4.39	0.76	77.2	9.80	HiSeq4000	-	DRR208412
MP2_007	MP2_007	7.50	6.57	4.11	0.75	75.8	9.35	HiSeq4000	-	DRR208413
MP2_008	MP2_008	7.52	6.60	3.93	0.81	74.3	9.13	HiSeq4000	-	DRR208414
MP2_009	MP2_009	7.36	6.48	4.12	0.62	76.3	9.33	HiSeq4000	-	DRR208415
MP2_010	MP2_010	6.49	5.72	3.66	0.55	75.2	8.39	HiSeq4000	-	DRR208416
MP2_011	MP2_011	5.98	5.28	3.41	0.49	77.1	7.63	HiSeq4000	-	DRR208417
MP2_012	MP2_012	8.25	7.31	4.69	0.77	76.9	10.53	HiSeq4000	-	DRR208418
MP2_013	MP2_013	9.33	8.05	4.81	1.00	76.2	10.89	HiSeq4000	-	DRR208419
MP2_014	MP2_014	9.84	8.65	5.56	0.81	78.0	12.32	HiSeq4000	-	DRR208420
MP2_015	MP2_015	11.21	9.80	6.29	0.93	78.5	13.82	HiSeq4000	-	DRR208421
MP2_016	MP2_016	12.97	11.36	6.86	1.18	78.1	15.15	HiSeq4000	-	DRR208422
MP2_017	MP2_017	3.89	2.96	1.48	0.36	67.0	3.83	HiSeq4000	-	DRR208423
MP2_018	MP2_018	12.70	11.17	7.04	1.10	78.3	15.53	HiSeq4000	-	DRR208424
MP2_019	MP2_019	5.00	4.31	2.32	0.41	74.2	5.38	HiSeq4000	-	DRR208425
MP2_020	MP2_020	10.13	9.04	6.04	0.78	78.1	13.34	HiSeq4000	-	DRR208426
MP2_023	MP2_023	4.98	3.90	2.10	0.35	71.4	5.08	HiSeq4000	-	DRR208427
MP2_024	MP2_024	10.08	8.74	5.10	1.27	75.4	11.68	HiSeq4000	-	DRR208428
MP2_025	MP2_025	4.80	3.53	1.91	0.38	70.2	4.70	HiSeq4000	-	DRR208429
MP2_026	MP2_026	8.36	7.38	4.88	0.66	77.5	10.86	HiSeq4000	-	DRR208430
MP2_027	MP2_027	5.35	3.86	2.05	0.37	71.6	4.93	HiSeq4000	-	DRR208431
MP2_028	MP2_028	8.11	7.08	4.45	0.72	76.4	10.05	HiSeq4000	-	DRR208432
MP2_029	MP2_029	9.89	8.61	5.03	1.08	75.4	11.52	HiSeq4000	-	DRR208433
MP2_031	MP2_031	10.33	9.08	6.04	0.79	78.5	13.30	HiSeq4000	-	DRR208434
MP2_032	MP2_032	16.56	12.57	6.45	1.21	78.9	14.12	HiSeq4000	-	DRR208435
MP2_033	MP2_033	7.32	6.41	4.19	0.62	77.5	9.34	HiSeq4000	-	DRR208436
MP2_034	MP2_034	8.05	6.99	4.40	0.79	75.0	10.12	HiSeq4000	-	DRR208437
MP2_035	MP2_035	9.06	7.95	4.96	0.83	77.3	11.07	HiSeq4000	-	DRR208438
MP2_037	MP2_037	9.70	8.41	5.16	0.99	77.3	11.53	HiSeq4000	-	DRR208439
MP2_039	MP2_039	7.54	6.58	4.00	0.82	75.4	9.17	HiSeq4000	-	DRR208440
MP2_043	MP2_043	9.15	7.93	4.24	0.71	77.3	9.46	HiSeq4000	-	DRR208441
MP2_044	MP2_044	9.75	8.60	5.28	0.95	76.9	11.85	HiSeq4000	-	DRR208442
MP2_047	MP2_047	8.95	7.64	4.04	0.76	77.1	9.03	HiSeq4000	-	DRR208443
MP2_048	MP2_048	8.27	7.24	3.94	0.69	77.4	8.80	HiSeq4000	-	DRR208444
MP2_050	MP2_050	11.17	9.77	5.67	1.35	76.2	12.85	HiSeq4000	-	DRR208445
MP2_052	MP2_052	9.98	8.75	5.18	1.13	75.1	11.90	HiSeq4000	-	DRR208446
MP2_053	MP2_053	11.85	9.88	4.74	2.21	72.0	11.37	HiSeq4000	-	DRR208447
MP2_054	MP2_054	10.38	6.95	3.67	0.70	77.1	8.21	HiSeq4000	-	DRR208448
MP2_055	MP2_055	12.74	10.66	5.55	1.85	74.8	12.81	HiSeq4000	-	DRR208449

MP2_057	MP2_057	8.68	7.41	4.06	1.24	72.2	9.72	HiSeq4000	-	DRR208450
MP2_058	MP2_058	11.14	9.54	6.10	0.89	78.2	13.47	HiSeq4000	-	DRR208451
MP2_060	MP2_060	8.31	7.05	3.51	0.79	76.0	7.97	HiSeq4000	-	DRR208452
MP2_061	MP2_061	12.07	10.38	6.88	0.95	79.0	15.04	HiSeq4000	-	DRR208453
MP2_063	MP2_063	7.03	5.43	2.96	0.51	76.3	6.71	HiSeq4000	-	DRR208454
MP2_064	MP2_064	11.23	9.50	5.46	1.28	76.0	12.39	HiSeq4000	-	DRR208455
MP2_113	MP2_113	6.79	5.71	3.29	0.79	75.0	7.57	HiSeq4000	-	DRR208456
MP2_114	MP2_114	7.80	6.62	3.60	0.94	70.9	8.75	HiSeq4000	-	DRR208457
MP2_116	MP2_116	7.17	6.14	3.78	0.66	75.5	8.64	HiSeq4000	-	DRR208458
MP2_117	MP2_117	6.52	5.53	3.38	0.55	75.9	7.69	HiSeq4000	-	DRR208459
MP2_121	MP2_121	11.64	10.04	5.72	1.45	76.1	12.96	HiSeq4000	-	DRR208460
MP2_122	MP2_122	9.07	7.65	4.33	1.15	75.5	9.89	HiSeq4000	-	DRR208461
MP2_125	MP2_125	9.25	8.04	4.87	0.86	77.7	10.82	HiSeq4000	-	DRR208462
MP2_126	MP2_126	8.65	7.46	4.36	1.00	76.1	9.89	HiSeq4000	-	DRR208463
MP2_127	MP2_127	11.45	9.94	6.22	0.99	78.0	13.76	HiSeq4000	-	DRR208464
MP2_128	MP2_128	10.17	8.91	5.41	1.01	77.1	12.11	HiSeq4000	-	DRR208465
MP2_129	MP2_129	11.75	10.05	5.97	1.32	77.4	13.30	HiSeq4000	-	DRR208466
MP2_130	MP2_130	9.04	7.78	4.94	0.75	76.8	11.10	HiSeq4000	-	DRR208467
MP2_131	MP2_131	10.02	8.69	5.59	0.85	78.2	12.34	HiSeq4000	-	DRR208468
MP2_132	MP2_132	9.93	8.56	5.23	0.99	77.2	11.69	HiSeq4000	-	DRR208469
MP2_133	MP2_133	7.97	6.87	4.29	0.71	77.0	9.63	HiSeq4000	-	DRR208470
MP2_136	MP2_136	9.56	8.20	4.48	1.48	76.2	10.14	HiSeq4000	-	DRR208471
MP2_137	MP2_137	10.99	9.51	5.70	1.15	76.5	12.86	HiSeq4000	-	DRR208472
MP2_138	MP2_138	8.51	7.42	4.61	0.76	77.3	10.28	HiSeq4000	-	DRR208473
MP2_139	MP2_139	9.41	8.27	5.12	0.83	75.9	11.65	HiSeq4000	-	DRR208474
MP2_140	MP2_140	8.91	7.74	4.74	0.90	76.9	10.65	HiSeq4000	-	DRR208475
MP2_141	MP2_141	9.22	7.61	4.05	1.22	72.2	9.69	HiSeq4000	-	DRR208476
MP2_142	MP2_142	10.72	9.12	4.11	2.49	73.3	9.67	HiSeq4000	-	DRR208477
MP2_143	MP2_143	7.99	6.94	4.03	0.91	75.3	9.24	HiSeq4000	-	DRR208478
MP2_144	MP2_144	9.30	8.14	5.31	0.79	77.5	11.83	HiSeq4000	-	DRR208479
MP2_145	MP2_145	10.35	8.99	5.13	1.17	76.5	11.56	HiSeq4000	-	DRR208480
MP2_146	MP2_146	10.87	9.44	5.39	1.41	77.1	12.07	HiSeq4000	-	DRR208481
MP2_147	MP2_147	9.96	8.80	5.79	0.76	78.4	12.75	HiSeq4000	-	DRR208482
MP2_149	MP2_149	9.80	8.64	5.74	0.78	78.0	12.71	HiSeq4000	-	DRR208483
MP2_150	MP2_150	7.47	6.31	3.17	1.22	71.5	7.65	HiSeq4000	-	DRR208484
MP2_151	MP2_151	8.96	7.85	4.80	0.90	78.0	10.63	HiSeq4000	-	DRR208485
MP2_152	MP2_152	12.30	10.66	6.41	1.29	78.8	14.02	HiSeq4000	-	DRR208486
MP2_154	MP2_154	9.78	8.41	4.56	1.42	75.8	10.38	HiSeq4000	-	DRR208487
MP2_155	MP2_155	10.40	9.01	5.31	1.23	77.5	11.82	HiSeq4000	-	DRR208488
MP2_156	MP2_156	8.67	7.49	4.32	1.00	76.2	9.79	HiSeq4000	-	DRR208489
MP2_157	MP2_157	7.64	6.64	4.00	0.84	76.0	9.08	HiSeq4000	-	DRR208490
MP2_158	MP2_158	8.84	7.67	4.85	0.79	77.8	10.77	HiSeq4000	-	DRR208491
MP2_159	MP2_159	9.82	8.47	4.97	1.16	77.2	11.10	HiSeq4000	-	DRR208492
MP2_160	MP2_160	8.43	7.33	4.57	0.73	77.2	10.23	HiSeq4000	-	DRR208493
MP2_161	MP2_161	8.93	7.71	4.46	1.10	77.1	9.99	HiSeq4000	-	DRR208494
MP2_162	MP2_162	12.11	10.46	5.71	1.62	77.4	12.73	HiSeq4000	-	DRR208495
MP2_166	MP2_166	12.03	10.49	6.27	1.21	76.7	14.09	HiSeq4000	-	DRR208496
MP2_167	MP2_167	9.67	8.39	4.63	1.31	74.7	10.70	HiSeq4000	-	DRR208497
MP2_168	MP2_168	15.43	13.47	8.68	1.28	79.0	18.96	HiSeq4000	-	DRR208498

MP2_169	MP2_169	12.87	11.15	6.58	1.40	77.7	14.62	HiSeq4000	-	DRR208499
MP2_170	MP2_170	13.20	11.31	6.24	1.83	77.3	13.94	HiSeq4000	-	DRR208500
MP2_172	MP2_172	11.50	9.60	5.68	1.08	75.6	12.97	HiSeq4000	-	DRR208501
MP2_173	MP2_173	10.20	8.86	4.90	1.31	74.9	11.28	HiSeq4000	-	DRR208502
MP2_174	MP2_174	10.70	9.28	5.37	1.26	77.7	11.95	HiSeq4000	-	DRR208503
MP2_175	MP2_175	13.09	11.51	7.00	1.21	77.4	15.60	HiSeq4000	-	DRR208504
MP2_177	MP2_177	6.33	5.38	2.88	1.00	71.7	6.93	HiSeq4000	-	DRR208505
MP2_178	MP2_178	5.89	5.10	3.00	0.66	73.2	7.07	HiSeq4000	-	DRR208506
MP2_179	MP2_179	4.55	3.89	2.47	0.42	73.5	5.79	HiSeq4000	-	DRR208507
MP2_180	MP2_180	7.09	6.10	3.54	0.86	74.8	8.17	HiSeq4000	-	DRR208508
MP2_181	MP2_181	6.41	5.45	3.05	0.91	72.6	7.26	HiSeq4000	-	DRR208509
MP2_182	MP2_182	8.34	7.16	4.72	0.71	78.2	10.42	HiSeq4000	-	DRR208510
MP2_183	MP2_183	8.89	7.74	5.12	0.74	77.0	11.47	HiSeq4000	-	DRR208511
MP2_185	MP2_185	6.46	5.49	3.06	0.97	72.4	7.30	HiSeq4000	-	DRR208512
MP2_186	MP2_186	6.37	5.37	3.39	0.59	76.0	7.70	HiSeq4000	-	DRR208513
MP2_187	MP2_187	5.86	4.97	2.86	0.72	72.4	6.83	HiSeq4000	-	DRR208514
MP2_188	MP2_188	8.36	7.11	4.48	0.83	76.4	10.12	HiSeq4000	-	DRR208515
MP2_189	MP2_189	6.63	5.69	3.34	0.75	73.9	7.80	HiSeq4000	-	DRR208516
MP2_190	MP2_190	6.41	5.35	3.44	0.58	77.4	7.67	HiSeq4000	-	DRR208517
MP2_191	MP2_191	7.46	6.22	3.76	0.85	74.9	8.67	HiSeq4000	-	DRR208518
MP2_192	MP2_192	6.76	5.71	3.54	0.64	74.8	8.16	HiSeq4000	-	DRR208519
MP2_193	MP2_193	9.63	8.56	5.41	0.86	77.5	12.06	HiSeq4000	-	DRR208520
MP2_196	MP2_196	11.11	9.85	6.23	0.96	78.2	13.76	HiSeq4000	-	DRR208521
MP2_197	MP2_197	7.35	6.22	3.96	0.66	76.6	8.92	HiSeq4000	-	DRR208522
MP2_198	MP2_198	8.72	7.48	4.86	0.74	78.2	10.74	HiSeq4000	-	DRR208523
MP2_199	MP2_199	6.66	5.90	3.58	0.69	74.8	8.25	HiSeq4000	-	DRR208524
MP2_200	MP2_200	7.00	6.22	3.99	0.61	75.8	9.08	HiSeq4000	-	DRR208525
MP2_201	MP2_201	8.36	7.17	4.39	0.86	75.4	10.06	HiSeq4000	-	DRR208526
MP2_202	MP2_202	9.03	7.71	3.83	1.87	74.4	8.88	HiSeq4000	-	DRR208527
MP2_203	MP2_203	7.58	6.73	4.06	0.76	76.8	9.12	HiSeq4000	-	DRR208528
MP2_204	MP2_204	10.55	9.21	5.02	1.48	77.2	11.22	HiSeq4000	-	DRR208529
MP2_205	MP2_205	11.71	10.10	6.18	1.22	77.5	13.76	HiSeq4000	-	DRR208530
MP2_206	MP2_206	8.72	7.29	3.94	1.43	74.1	9.16	HiSeq4000	-	DRR208531
MP2_208	MP2_208	11.54	10.28	6.41	1.12	78.2	14.16	HiSeq4000	-	DRR208532
MP2_211	MP2_211	9.81	8.70	5.44	1.02	78.4	11.98	HiSeq4000	-	DRR208533
MP2_213	MP2_213	10.05	8.77	5.30	1.02	78.0	11.73	HiSeq4000	-	DRR208534
MP2_214	MP2_214	8.64	7.69	4.64	0.96	76.1	10.53	HiSeq4000	-	DRR208535
MP2_215	MP2_215	9.92	8.76	5.62	0.81	78.0	12.43	HiSeq4000	-	DRR208536
MP2_216	MP2_216	9.92	8.64	5.19	1.10	75.4	11.88	HiSeq4000	-	DRR208537
MP2_218	MP2_218	9.62	8.52	5.24	1.10	75.4	11.99	HiSeq4000	-	DRR208538
MP2_219	MP2_219	7.57	6.57	4.15	0.70	74.8	9.57	HiSeq4000	-	DRR208539
MP2_220	MP2_220	7.81	6.90	4.21	0.78	76.1	9.55	HiSeq4000	-	DRR208540
MP2_221	MP2_221	9.33	8.28	5.13	0.92	76.2	11.63	HiSeq4000	-	DRR208541
MP2_222	MP2_222	9.13	7.90	4.79	1.02	75.7	10.93	HiSeq4000	-	DRR208542
MP2_224	MP2_224	11.19	9.85	6.23	1.05	77.1	13.95	HiSeq4000	-	DRR208543
MP2_225	MP2_225	8.97	7.74	4.41	1.09	74.2	10.25	HiSeq4000	-	DRR208544
MP2_227	MP2_227	14.19	12.43	7.97	1.15	78.7	17.48	HiSeq4000	-	DRR208545
MP2_228	MP2_228	9.03	7.86	4.92	0.90	76.8	11.05	HiSeq4000	-	DRR208546
MP2_229	MP2_229	10.39	9.13	5.71	0.97	77.5	12.73	HiSeq4000	-	DRR208547

MP2_231	MP2_231	10.31	8.99	5.62	0.96	77.6	12.50	HiSeq4000	-	DRR208548
MP2_232	MP2_232	11.06	9.64	6.00	1.04	77.1	13.41	HiSeq4000	-	DRR208549
MP2_233	MP2_233	9.57	8.46	5.23	1.07	76.8	11.76	HiSeq4000	-	DRR208550
MP2_234	MP2_234	6.96	6.02	3.42	0.89	73.4	8.05	HiSeq4000	-	DRR208551
MP2_235	MP2_235	8.71	7.54	4.21	1.25	73.9	9.82	HiSeq4000	-	DRR208552
MP2_236	MP2_236	5.82	4.95	3.06	0.56	73.8	7.16	HiSeq4000	-	DRR208553
MP2_237	MP2_237	6.46	5.55	3.27	0.80	74.2	7.61	HiSeq4000	-	DRR208554
MP2_239	MP2_239	7.08	6.14	3.77	0.73	75.0	8.66	HiSeq4000	-	DRR208555
MP2_240	MP2_240	6.92	6.00	3.70	0.78	74.4	8.59	HiSeq4000	-	DRR208556
MP2_241	MP2_241	10.28	8.87	4.73	1.60	74.7	10.92	HiSeq4000	-	DRR208557
MP2_242	MP2_242	8.82	7.65	4.62	0.85	75.3	10.58	HiSeq4000	-	DRR208558
MP2_245	MP2_245	5.90	5.15	3.32	0.51	76.3	7.50	HiSeq4000	-	DRR208559
MP2_246	MP2_246	6.86	5.98	3.77	0.70	76.6	8.50	HiSeq4000	-	DRR208560
MP2_247	MP2_247	6.97	6.01	3.70	0.65	74.3	8.61	HiSeq4000	-	DRR208561
MP2_248	MP2_248	6.45	5.60	3.62	0.57	76.7	8.14	HiSeq4000	-	DRR208562

Table SM11. All sequence information of ourgroups.

Sample		Fastq size		Aligned bam information				Comment	Accession No.
Name	Name in Scarcelli et al. 2019	Original (Gbp)	Filtered (Gbp)	Aligned (Gbp)	Unmapped (Gbp)	Coverage (%)	Depth		
alata1		28.11	23.95	10.73	1.24	48.0	38.59	D.alata	ERR1019033
alata2		11.58	11.15	3.88	1.37	43.1	15.54	D.alata	SRR7062294
ns004_A5689	A5689	4.22	4.19	3.09	0.34	75.2	7.09	D.abyssinica:Nigeria	SRR8451439
ns005_A5690	A5690	5.79	5.72	4.06	0.37	68.5	10.24	D.abyssinica:Nigeria	SRR8451438
ns006_A5691	A5691	5.53	5.49	2.85	1.73	68.4	7.20	D.abyssinica:Nigeria	SRR8451437
ns007_A5693	A5693	5.93	5.89	4.54	0.15	78.3	10.01	D.abyssinica:Nigeria	SRR8451434
ns008_A5694	A5694	4.87	4.84	3.91	0.04	77.3	8.72	D.abyssinica:Nigeria	SRR8451371
ns009_A5695	A5695	4.55	4.52	3.35	0.42	78.4	7.37	D.abyssinica:Nigeria	SRR8451459
ns010_A5696	A5696	4.75	4.61	3.55	0.22	74.9	8.17	D.abyssinica:Nigeria	SRR8451458
ns011_A5697	A5697	5.70	5.66	4.41	0.15	80.2	9.48	D.abyssinica:Nigeria	SRR8451382
ns012_A5699	A5699	3.25	3.22	2.45	0.15	71.8	5.89	D.abyssinica:Nigeria	SRR8451381
ns013_A5700	A5700	4.79	4.76	3.59	0.32	77.0	8.05	D.abyssinica:Nigeria	SRR8451384
ns014_A5701	A5701	5.99	5.95	4.38	0.37	78.6	9.62	D.abyssinica:Nigeria	SRR8451383
ns015_A5702	A5702	3.96	3.93	2.95	0.29	74.9	6.79	D.abyssinica:Nigeria	SRR8451378
ns016_A5703	A5703	4.53	4.49	3.09	0.37	65.3	8.17	D.abyssinica:Nigeria	SRR8451377
ns017_A5704	A5704	4.95	4.91	2.85	1.17	69.6	7.08	D.abyssinica:Nigeria	SRR8451380
ns018_A5705	A5705	5.54	5.49	3.75	0.67	74.5	8.68	D.abyssinica:Nigeria	SRR8451379
ns019_A52	A52	1.66	1.63	1.44	0.02	70.8	3.52	D.abyssinica:Benin	SRR8451376
ns020_A62	A62	2.35	2.31	2.06	0.02	77.3	4.60	D.abyssinica:Benin	SRR8451375
ns021_A67	A67	7.54	7.42	6.12	0.12	85.2	12.40	D.abyssinica:Benin	SRR8451343
ns023_A467	A467	5.72	5.64	5.08	0.06	82.0	10.69	D.abyssinica:Benin	SRR8451345
ns024_A537	A537	6.22	6.13	5.28	0.05	79.3	11.49	D.abyssinica:Benin	SRR8451346
ns025_A3009	A3009	3.33	3.27	2.92	0.03	76.7	6.57	D.abyssinica:Benin	SRR8451347
ns027_A5068	A5068	1.98	1.95	1.67	0.04	65.7	4.38	D.abyssinica:Ghana	SRR8451349
ns028_A5045	A5045	2.61	2.56	2.21	0.04	74.4	5.12	D.abyssinica:Ghana	SRR8451350
ns029_A5047	A5047	3.32	3.27	2.80	0.04	75.0	6.46	D.abyssinica:Ghana	SRR8451351
ns030_A5048	A5048	9.39	9.23	7.75	0.10	82.9	16.14	D.abyssinica:Ghana	SRR8451352
ns031_A5059	A5059	10.28	10.10	7.09	1.66	82.5	14.82	D.abyssinica:Ghana	SRR8451320
ns032_A5061	A5061	2.81	2.77	1.91	0.54	72.4	4.55	D.abyssinica:Ghana	SRR8451319
ns033_A5066	A5066	8.09	7.95	6.74	0.11	80.7	14.41	D.abyssinica:Ghana	SRR8451318
ns034_A5067	A5067	7.67	7.55	6.51	0.06	82.0	13.71	D.abyssinica:Ghana	SRR8451317
ns035_P5344	P5344	3.33	3.30	2.46	0.10	70.6	6.02	D.praehensilis:Cameroon:Cameroonian D.praehensilis	SRR8451316
ns036_P5350	P5350	4.06	4.02	2.77	0.20	63.5	7.52	D.praehensilis:Cameroon:Cameroonian D.praehensilis	SRR8451315
ns037_P5358	P5358	4.21	4.17	3.09	0.15	73.2	7.29	D.praehensilis:Cameroon:Cameroonian D.praehensilis	SRR8451314
ns038_P5369	P5369	3.10	3.08	2.17	0.32	70.2	5.34	D.praehensilis:Cameroon:Cameroonian D.praehensilis	SRR8451313
ns039_P5378	P5378	3.01	2.99	2.31	0.05	70.5	5.66	D.praehensilis:Cameroon:Cameroonian D.praehensilis	SRR8451322
ns040_P5381	P5381	3.90	3.87	2.97	0.11	72.8	7.05	D.praehensilis:Cameroon:Cameroonian D.praehensilis	SRR8451321

ns041_P5404	P5404	4.53	4.49	3.31	0.31	74.3	7.69	D.praehensilis:Cameroon:Cameroonian D.praehensilis	SRR8451462
ns042_P5413	P5413	3.78	3.75	2.82	0.16	73.5	6.62	D.praehensilis:Cameroon:Cameroonian D.praehensilis	SRR8451463
ns043_P5417	P5417	4.61	4.58	3.44	0.19	74.1	8.01	D.praehensilis:Cameroon:Cameroonian D.praehensilis	SRR8451460
ns044_P5420	P5420	2.25	2.23	1.65	0.15	65.9	4.31	D.praehensilis:Cameroon:Cameroonian D.praehensilis	SRR8451461
ns045_P5424	P5424	5.30	5.26	3.74	0.42	74.4	8.68	D.praehensilis:Cameroon:Cameroonian D.praehensilis	SRR8451466
ns046_P5427	P5427	4.25	4.22	3.24	0.05	72.9	7.66	D.praehensilis:Cameroon:Cameroonian D.praehensilis	SRR8451467
ns047_P5430	P5430	3.34	3.31	2.41	0.10	63.5	6.56	D.praehensilis:Cameroon:Cameroonian D.praehensilis	SRR8451464
ns048_P5434	P5434	2.80	2.77	2.10	0.06	61.8	5.86	D.praehensilis:Cameroon:Cameroonian D.praehensilis	SRR8451465
ns049_P5438	P5438	3.64	3.61	2.36	0.62	70.6	5.76	D.praehensilis:Cameroon:Cameroonian D.praehensilis	SRR8451468
ns050_P5441	P5441	4.13	4.09	3.04	0.23	73.7	7.12	D.praehensilis:Cameroon:Cameroonian D.praehensilis	SRR8451469
ns051_P5448	P5448	4.73	4.69	3.66	0.09	73.6	8.58	D.praehensilis:Cameroon:Cameroonian D.praehensilis	SRR8451449
ns054_P5318	P5318	5.04	4.99	3.07	0.62	67.7	7.83	D.praehensilis:Cameroon:Cameroonian D.praehensilis	SRR8451450
ns055_P5746	P5746	3.80	3.77	2.66	0.43	65.3	7.02	D.praehensilis:Nigeria:Western D.praehensilis	SRR8451453
ns056_P5708	P5708	6.19	6.13	4.22	0.39	64.5	11.30	D.praehensilis:Nigeria:Western D.praehensilis	SRR8451452
ns057_P5710	P5710	3.89	3.86	2.61	0.48	70.0	6.42	D.praehensilis:Nigeria:Western D.praehensilis	SRR8451455
ns058_P5713	P5713	3.24	3.21	2.34	0.22	67.2	6.02	D.praehensilis:Nigeria:Western D.praehensilis	SRR8451454
ns059_P5716	P5716	2.56	2.53	1.91	0.03	63.0	5.23	D.praehensilis:Nigeria:Western D.praehensilis	SRR8451457
ns061_P5720	P5720	3.87	3.84	2.99	0.17	73.5	7.02	D.praehensilis:Nigeria:Western D.praehensilis	SRR8451430
ns062_P5723	P5723	3.63	3.61	2.17	0.93	68.9	5.44	D.praehensilis:Nigeria:Western D.praehensilis	SRR8451431
ns063_P5728	P5728	3.75	3.71	2.65	0.34	64.3	7.11	D.praehensilis:Nigeria:Western D.praehensilis	SRR8451432
ns064_P5729	P5729	7.31	7.25	4.58	1.01	72.5	10.89	D.praehensilis:Nigeria:Western D.praehensilis	SRR8451433
ns065_P424	P424	3.46	3.40	3.03	0.04	79.1	6.61	D.praehensilis:Benin:Western D.praehensilis	SRR8451426
ns066_P425	P425	1.63	1.60	1.44	0.02	69.5	3.57	D.praehensilis:Benin:Western D.praehensilis	SRR8451427
ns067_P457	P457	4.21	4.13	3.46	0.12	74.5	8.01	D.praehensilis:Benin:Western D.praehensilis	SRR8451428
ns068_P462	P462	4.33	4.26	3.68	0.08	79.7	7.98	D.praehensilis:Benin:Western D.praehensilis	SRR8451429
ns069_P323	P323	4.22	4.15	3.70	0.05	80.5	7.94	D.praehensilis:Benin:Western D.praehensilis	SRR8451435
ns070_P464	P464	5.29	5.21	4.65	0.05	80.6	9.96	D.praehensilis:Benin:Western D.praehensilis	SRR8451436
ns073_P2990	P2990	2.88	2.84	2.56	0.03	77.6	5.70	D.praehensilis:Benin:Western D.praehensilis	SRR8451409
ns075_P4918	P4918	2.45	2.40	1.82	0.27	72.6	4.33	D.praehensilis:Ghana:Western D.praehensilis	SRR8451415
ns076_P4919	P4919	5.46	5.36	4.04	0.45	79.4	8.79	D.praehensilis:Ghana:Western D.praehensilis	SRR8451414
ns077_P4920	P4920	6.04	5.93	4.63	0.53	80.3	9.95	D.praehensilis:Ghana:Western D.praehensilis	SRR8451413
ns078_P4921	P4921	4.73	4.65	3.73	0.31	79.5	8.11	D.praehensilis:Ghana:Western D.praehensilis	SRR8451412
ns079_P4928	P4928	3.77	3.71	2.99	0.24	78.4	6.57	D.praehensilis:Ghana :Western D.praehensilis	SRR8451407